Department of Precision and Microsystems Engineering

Design of a Snap Acting Pneumatic Relay to Reduce Air Loss in a Wafer Floating Air Film Conveyor

S.J. Brilstra

Report no. : 2017.062
Supervisor : Dr.ir. R.A.J. van Ostayen
Professor : Prof.dr.ir. J.L. Herder
Specialisation : Mechatronic System Design
Type of report : MSc. Thesis
Date : 18 December 2017

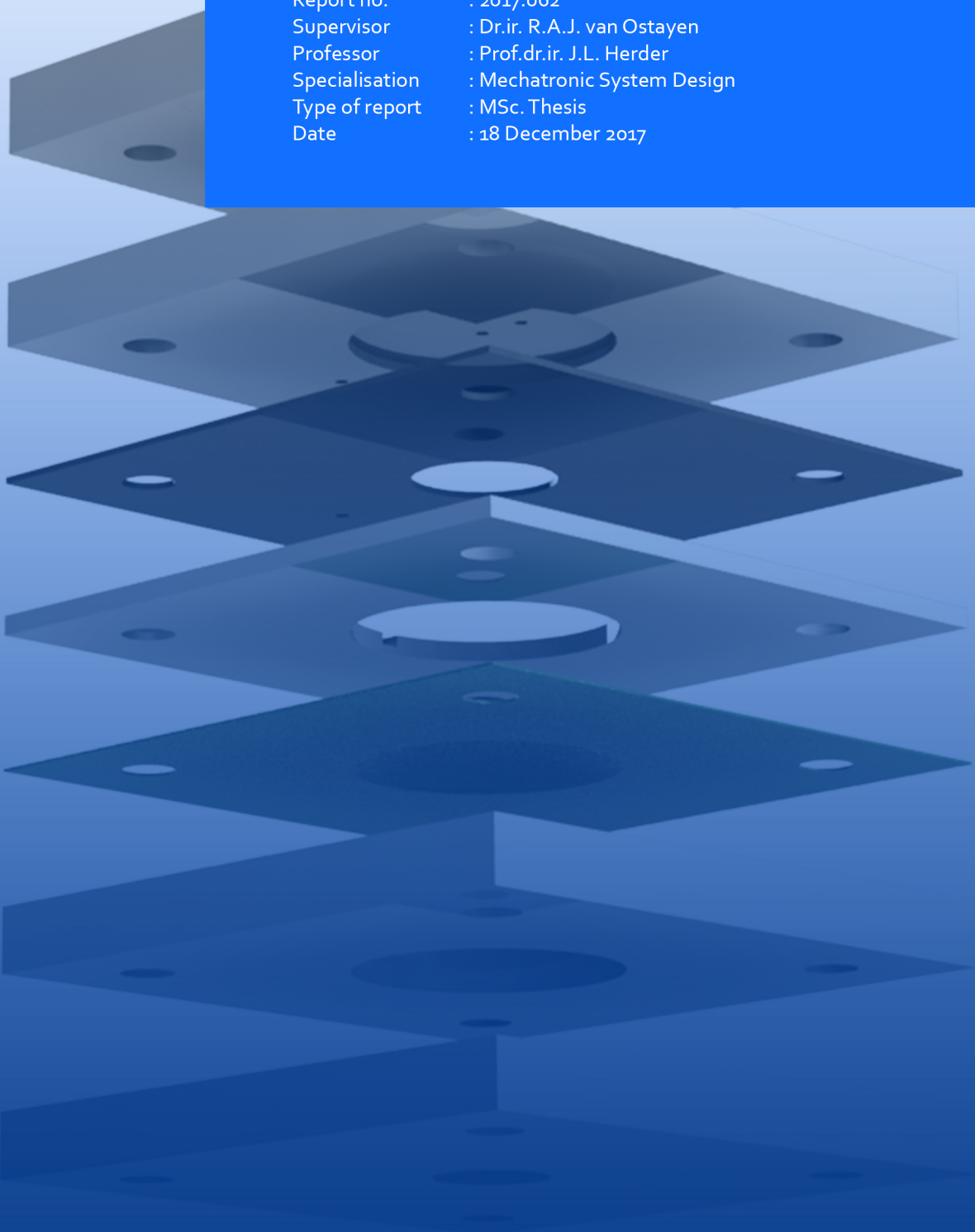

TU Delft

Design of a Snap Acting Pneumatic Relay to Reduce Air Loss in a Wafer Floating Air Film Conveyor

by

S.J. Brilstra

to obtain the degree of Master of Science
at the Delft University of Technology,

Student number: 4012518

TU Delft

Abstract

In the high-tech semiconductor industry floating air conveyors are used to transport and position silicon substrates. An interesting point for improvement is to limit the loss of pressurized air as conveyors are only effective at the position of the substrate.

The goal of this research is to develop a local pneumatic valve, that is implemented underneath the surface of a floating air conveyor. Depending on the position of a substrate, the valve is actuated using a pressure signal.

A conceptual design is conceived with information found in a literature study. With the use of the nozzle-flapper principle, a pneumatic relay is actuated. This relay has a circular waved membrane that snaps to its inverse shape, to open or close a channel. The nozzle is embedded in the surface of the conveyor. On the opposite side it is connected to a pressure source and the relay. The flapper is represented by a floating substrate. As a wafer floats above the nozzle, the pressure will increase in the nozzle and a connected relay will be actuated.

The proposed nozzle-wafer concept is modelled to investigate its characteristics. It is found that a desired nozzle back pressure can be achieved by setting the appropriate nozzle restriction and supply pressure. However, at higher pressures the fly-height will be influenced by the nozzles. Therefore, a minimal switching pressure for the relay is key.

The arrangement of nozzles and relays in a conveyor is examined. In this research a black box is used for the valve in order for multiple relay concepts to be applicable. With the current function two inputs are needed to fully operate the relay. It is possible to make a grid where substrates move in one direction and an extra array of outlets are active around it, to make a smoother air film. No arrangement is found that can be used in different directions.

Simulations of the snap acting relay showed unreliable membrane behaviour. An adjustment is made in the design for the prototype. A design using a circular single curved membrane is introduced, because the models are consistent in converging to a solution of its snapping behaviour.

A layered design approach is used for the prototype, where lasercut PMMA plates are glued together. Plastic membranes are created with a vacuum form method. Initial testing of these membranes showed unexpected behaviour like flipping in other shapes and breaking. Also the switching pressure to snap back to the starting position is considerable lower. A prototype is built using the only properly snapping membrane that is found. In a static experiment it proved that the relay functions as it is intended.

This concludes the first iteration of the design process. A working snap acting membrane is fabricated and tested. Because of the behaviour of the other tested membranes it is taken into account that this prototype might not have a lifespan higher than switching a hundreds times. Simulations showed that a nozzle-wafer system can provide a back pressure to switch a valve. However, this pressure must be minimal, in order that it does not affect the fly-height of the wafer.

Lastly an alternative design is introduced. Using an elastic membrane with different size surfaces, lower pressures can close off air channels with a higher supply pressure. This combined by a nozzle-wafer conveyor with a resistor network underneath is recommended to investigate in the second iteration of the design process.

Contents

1 Introduction

In the high-tech semiconductor industry, chips are produced from thin substrates. During the different processes used in manufacture, a high precision positioning system is needed. J. Wesselingh developed such a system using an thin air film to float and transport the substrate on.

An interesting point for improvement is to limit the loss of pressurized air used by such a system. This is less of a problem in the high-tech semiconductor industry, as the used air is only a small fraction of the costs. It is however more relevant in the floating air conveyors used in the solar cell industry. Conveyors are only effective at the position of the substrate. At the other positions this air is directly send to the atmosphere.

The goal of this research is to develop a local pneumatic valve, that is implemented underneath the surface of a floating air conveyor. It is actuated depending on the position of the substrate, using a pressure signal and a nozzle-flapper system.

Different concepts are discussed based on literature. One concept is further investigated using simulations and experimental testing of a prototype.

To better understand the air conveyor a literature study is performed and described in chapter 2. This includes a part devoted to explain some standard pneumatic proportional control valve principles, such as the nozzle-flapper system. It concludes the chapter by presenting different pneumatic control valves and relays found in academic literature.

In chapter 3, the information from the literature study is used to pick a conceptual design that will be the focus of this research. A pneumatic relay using a snap acting membrane is chosen to be investigated. With the use of the nozzle flapper principle the relay will be actuated. The nozzle is embedded in the surface of the conveyor and the flapper is represented by the floating substrate. The chapter concludes with an analysis of this nozzle-wafer system.

The implementation of a pneumatic relay and nozzle-wafer in an air conveyor is analysed in chapter 4. Different configurations are investigated by using a black box for the relay. This is done in order for different designs to be applicable.

The switching behaviour of the snap acting relay is examined using different models in chapter 5. The results were unsatisfactory. Therefore an alternative snap acting concept is presented. It has the same function, but uses a simpler single curved membrane.

This single curve concept is fabricated and tested in chapter 6. First the fabrication method is briefly explained. The creation of reliable membranes proved difficult, the use and failing of membranes is investigated further.

Chapter 7 concludes this report and development for of an snap acting relay implemented in an air conveyor. It also gives recommendations for future studies.

2
Literature Review

An overview is given of an existing floating wafer system. The working principle together with points of improvement are presented. Next, the proposed development of a valve is described.

After that, a short section is devoted to explain some standard pneumatic proportional control valve principles. Subsequently an overview is presented of commercial available proportional valves. Next an review is given on academic research of pneumatic control valves and relays.

2.1 Total system

In the high-tech semiconductor industry, chips are produced from thin substrates. During the different processes used during manufacture, a high precision positioning system is essential. Increasing demands from the consumers tend towards miniaturisation and lowering of the cost. The substrates get larger in area and smaller in thickness while the feature size decreases. Thus substrates become more fragile and the features more vulnerable to contamination.

A new potential positioning device has been developed by J. Wesselingh [2]. In this design the substrate is floating on a thin air film. In the figure below the concept of the air actuator is shown fig. 2.1.

Figure 2.1: Air actuator concept with a substrate on it. (Source: [2])

2.1.1 Working Principle

The concept was conceived by van Ostayen [3]. The function of the air actuator is both suspending the substrate in the air and driving it in a direction. This is the so called bearing function and motor function.

Throughout this section the actuator is considered in a large array. This means that periodic boundary conditions are used. Also the density of the air is considered constant, due to the small pressure variations changing around atmospheric pressure. The temperature is also considered constant.

Motor Function

The motor function is derived from the viscous shear of the thin air film under the substrate. The actuator contains a pocket in which air flows (pressure driven) from the inlets to the outlets. At the inlet the pressure is above ambient pressure and at the outlet below. Due to the no-slip condition at the surface of the substrate a shear stress develops at the boundary, the so called motor force. Equations have been derived for the motor force and flow characteristics [2].

With an array of these actuators, more traction force is generated. The different pockets are separated by dams to reduce back flow between bordering pockets. By directing the flow in different directions, enough degrees of freedom are attained to realize the motor function for a planar stage.

Bearing Function

The out of plane bearing function is similar to a vacuum preloaded air bearing. The average air pressure on the actuator surface lifts the substrate to a defined height. Before the air enters the actuator it flows through a restrictor. The pressure difference across this restrictor varies with the fly height of the substrate.

The out of plane stiffness of the system can be very high. At each actuator a restrictor can be added to the inlet, which gives a distributed stiffness. This can even counter deformations in he substrate, provided it is thin enough. No active control is needed.

The bearing function fulfils multiple objectives. It carries the substrate and flattens it into the shape of the base plate. The flattening effect is realised by use of the distributed stiffness.

Pros-cons

The potential advantages of the air actuator are listed below:

1. Compared to more traditional wafer handling systems, that use a carrier stage or gantries, an air actuator system has a smaller moving mass. This results in smaller forces being required and thus a more precise system van be achieved.
2. A single moving mass reduces unwanted system dynamics, that would otherwise be present by stacked motion stages.
3. The in plane stiffness provided by the actuator is zero between the substrate and fixed world. Only some coupling is present due to damping. No external disturbances are transmitted to the substrate.
4. The bearing stiffness can be designed to be very low to decouple the substrate from the fixed world. It can also be made high in order to reduce global substrate deformations.
5. The substrate only has contact with air, which reduces chance of damage and contamination if the gas is clean enough.
6. Thickness variations in silicon wafers could be measured and potentially be counter-acted by the air actuators to create a flat top surface.

Of course there are some potential disadvantages of using such a system:

1. The actuator provides limited amount of lateral force. This is due to the low friction. It can become difficult to generate high enough accelerations for high servo stiffness.

2. Air flow and general fluid dynamics can be difficult to predict accurately, when turbulence and unsteady flow arise.

2.1.2 Control Dynamics

In-plane the system is marginally stable and thus control is needed for the motor function. Different configurations of the pressure control are discussed below. Priority was given to make a linear system, since that is simpler to control.

To control the position via the air actuator, the motor force that is generated has to change continuous in direction and magnitude. This can be done by controlling the pressure drop over the pocket or by controlling the depth of the pocket. Both control methods are possible and have been explored (see Wesselingh [2] and Vuong [4]). In this research the study of the pressure controlled concepts will be continued.

A change in pressure is simply realised with a valve. A valve behaves as a variable non-linear orifice restriction. It changes both the pressure and flow when varied. Pressure regulation was chosen over flow regulation in Wesselinghs design, because generally low-cost pressure valves have a faster response than flow regulator valves.
The fly height of the substrate will fluctuate if the average pressure in the pocket varies.

Valve selection is done with the following points in mind. A proportional valve is chosen instead of a on/off valve. Otherwise PWM techniques or multiple valves would be required to get the desired result. The bandwidth of the valve should be higher than the system dynamics, so it is not limiting the performance.

A single valve is used to control multiple actuators due to cost and also the large size of a valve relative to the rest of the air actuator. The valve can be placed in series or parallel to the system fig. 2.2.

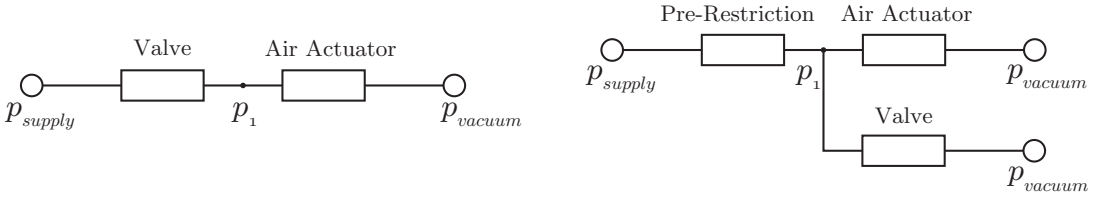

Figure 2.2: Valve placement configurations in series and parallel

The air actuator system itself is considered linear. The non-linear valve resistance before the system will result in a non-linear response at p_1. A linear response is preferred for control and the valve orifice should not add noise to the system.

Series Configuration
A disadvantage of the series placement is that the turbulent flow resulting from that valve can introduce disturbances downstream. An advantage of the series configurations is that the flow path can be completely sealed off. This can be beneficial for subsequent systems where commutation between air actuators in an array is incorporated. Another advantage is that there is leakage of pressurized air, before the air reaches the actuators.

Parallel Configuration
In the parallel placement there is no valve restriction in the main flow path. Thus the problem of introducing noise into the system by an orifice restriction is circumvented. Next to that the full excitation range of the valve is usable, which enhances the dynamic performance. However, the flow path cannot be closed with this configuration. A major disadvantage of the parallel case is that a lot of pressurized air is discarded by the so called bleed-off valve. This costs a lot of energy.

An analysis for a variable number of actuator cells driven by one valve resulted in the following insight. When a few actuator cells are driven by one valve, the configurations are comparable to each other. At a higher number of cells driven by a valve the parallel configuration has a better linearity but needs a higher supply pressure and has a higher power consumption. The number of actuators does not have much influence, it only affects the maximum excitation pressure range.

The series configuration needs an unrealistic supply flow for higher number of actuators driven. In general the series configuration is more desirable when controlling each actuator by one valve. The parallel arrangement is more applicable when controlling more actuators with a valve. The parallel case is applied in the experimental setup of Wesselingh using a commercial valve.

2.1.3 Current System

Some dimensions are given of the system designed by Wesselingh, along with the commercial proportional valve that is implemented. In the table below table 2.1 some characteristics of the current system are listed. In fig. 2.4 the air actuator is shown with some of the before mentioned dimensions. It also shows that one valve provides air for 8 actuators. The system of actuators next to each other is shown in fig. 2.3.

Table 2.1: Dimensions of the Current System

	Symbol	Parameter	Value
Air Actuator			
	L	Actuator Length	10 mm
	l	Pocket Length	8 mm
	h	Dam Height	20 µm
	H	Fly height	10 µm
	D_i	Diameter Inlet	1.6 mm
Restrictions			
	R_p	Pre-restriction	1.7 $\mathrm{Pa\,s\,mm^{-3}}$
	R_i	inlet restriction	3.1 $\mathrm{Pa\,s\,mm^{-3}}$
	R_a	actuator restriction	3.1 $\mathrm{Pa\,s\,mm^{-3}}$
Air Supply			
	Δp_{act}	Δp over actuator	$\geq$ 25 kPa
	p_s	Control Supply	15 kPa
	p_v	Vacuum Supply	-10 kPa
	Δp_{tot}	Total pressure drop system	25 kPa
	Q	Total Flow	10 $\mathrm{L\,min^{-1}}$
Manifold Supply			
	D_{lrg}	Large channel ⌀	6 mm
	D_{ctr}	Control channel diameter ⌀	3 mm
	D_{act}	Actuator channel ⌀	1.6 mm

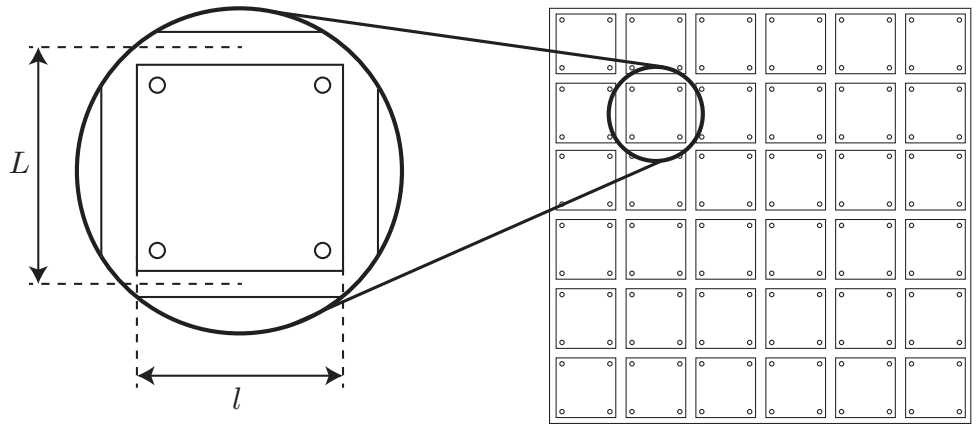

Figure 2.3: Schematic of 6 × 6 actuators

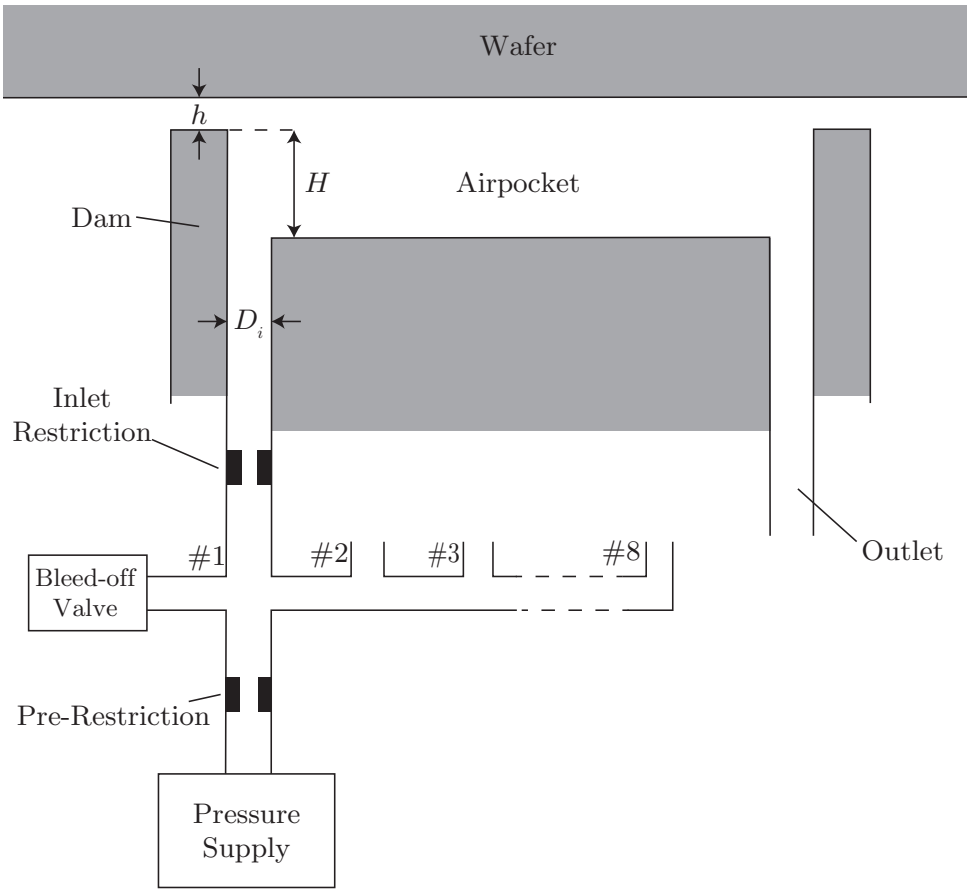

Figure 2.4: Schematic of Current System

Current Valve
The proportional valve that is used in the system is the LFPA8000120H. This valve uses a piezo electric bimorph actuator to seal a tube of 0.8 mm diameter. This bimorph requires a bias voltage of 160 V along with a control voltage. With the chosen amplifier the piezo can be driven with a bandwidth of 10 kHz.

2.1.4 Proposed Development

In short, Wesselinghs design uses large electric valves to control air to several air actuators via a network of supply lines.

This research will focus on a system where valves are implemented close to the surface of the air actuators and are operated on the basis of locally measured data. Specifically, by measuring air pressure inside a pocket. In this way the length of supply lines are minimized and the air conveyor can be switched locally where it is effective.

In the following section the basic principles of pneumatic control valves are explained. Then an overview is presented of different valve and relay concepts that could be useful. This overview is divided in a table of commercially available proportional valves and a survey of academic research on proportional valves and pneumatic relays. In the next chapter this information will be used to propose a concept to develop.

2.2 Pneumatics

In [5] the basic principle of pneumatic control valves is explained. The components of such a controller consist often out of a pneumatic nozzle-flapper as the first stage amplifier and a pneumatic relay as the second stage amplifier. Two types of proportional controllers are extensively used in industry, the force-distance type controller and force-balance type controller. In the following sections these concepts are briefly explained.

2.2.1 Pneumatic Nozzle-Flapper Amplifier

In fig. 2.5 the basic structure of a nozzle-flapper amplifier is illustrated. A constant pressure p_s is being fed into the system and goes through an orifice. The air can then move down to the control valve or to the nozzle on the right.

By a small change in the flapper position the pressure back in the nozzle will differ greatly. When the flapper comes closer to the nozzle, the opposition of the air flow increases. This results in a higher back pressure in the nozzle. If the flapper touches the nozzle the back pressure will be equal to the supply pressure. If the flapper is far away from the nozzle there is no flow restriction and the back pressure will be equal to the ambient pressure. The orifice diameter must be smaller than the nozzle diameter in order for the back pressure to be able to equal atmospheric pressure.

In industry the power amplification of the nozzle-flapper is frequently not sufficient and a pneumatic relay is required.

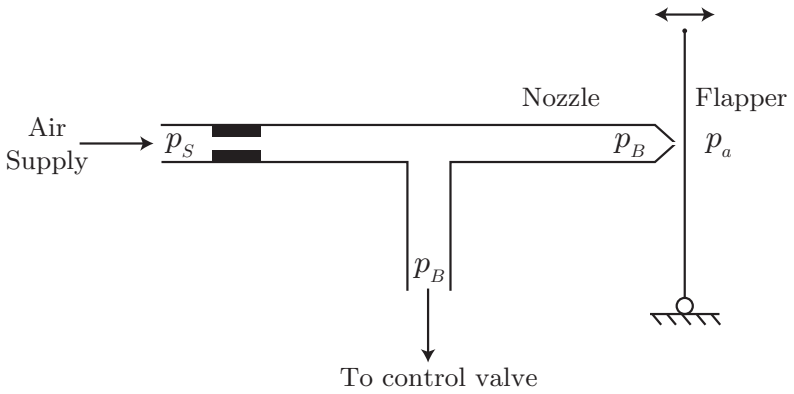

Figure 2.5: Schematic of a nozzle flapper amplifier (Source: [5]).

2.2.2 Pneumatic Relay

In the figures below a simplified model of a pneumatic relay is illustrated (fig. 2.6.a). Four channels are connected to relay. A supply channel, an input channel, an output channel and a vent to the atmosphere.

A membrane separates a chamber with on one side the input pressure and on the other side atmospheric pressure. As the input pressure increases the membrane is deformed downwards. This opens a path to the supply channel (fig. 2.6.b). Both the supply channel and vent are now connected to the output. A portion of the flow is dissipated to the atmosphere.

If the input pressure is further increased, the path to the vent is cut off (fig. 2.6.c). The output pressure is equal to the supply pressure.

The pneumatic relay can handle a much larger flow of air, than the nozzle-flapper amplifier. Often the pneumatic relay is combined with the nozzle-flapper mechanism to create a type of pressure controller described in the next section.

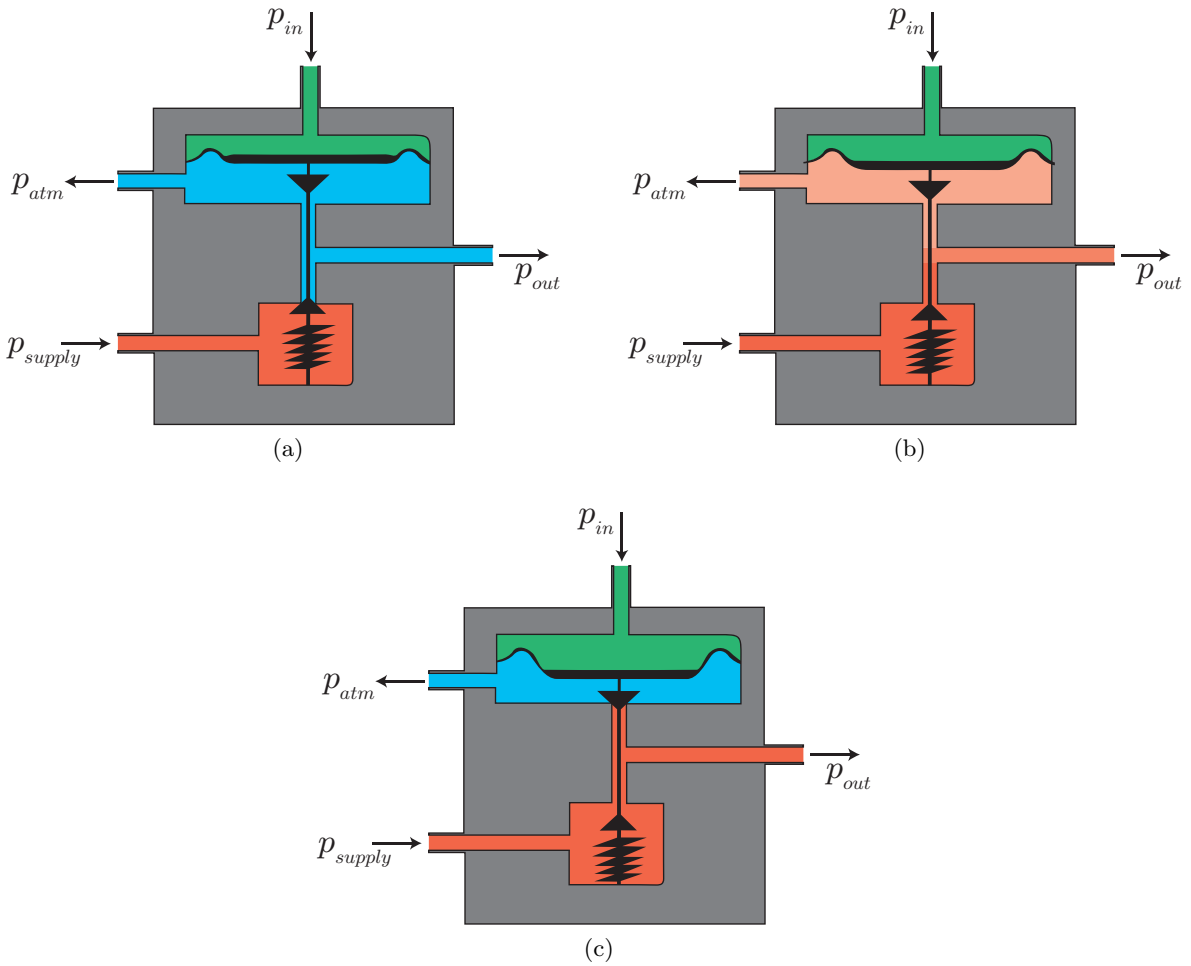

Figure 2.6: Schematics of Nozzle Flapper Amplifiers

2.2.3 Force-Distance Type Controller

The two amplifiers are now combined to make a force-distance type controller (fig. 2.7). The nozzle back pressure regulates the position of the diaphragm in the pneumatic relay. There is a pneumatic feedback implemented to reduce the movement of the flapper. This is realised with a variable linkage between the feedback bellows and flapper. The flapper can be moved by both the error as the feedback signal.

The working principle is as follows. When the error signal becomes too large, the flapper will move to the left, increasing the nozzle back pressure. This will move the diaphragm down, which in turn increases the pressure leading out of the valve (the control pressure). The bellows will expand and the flapper will move to the right (effectively lowering the control pressure). Due to the feedback the change in control pressure can be great while the flapper moves only a small quantity. The feedback bellows should however move the flapper less than the error signal, otherwise the control pressure would not change.

There are pneumatic controllers that do not have this feedback mechanism. They are commonly know as pneumatic on/off controllers and have a very high sensitivity.

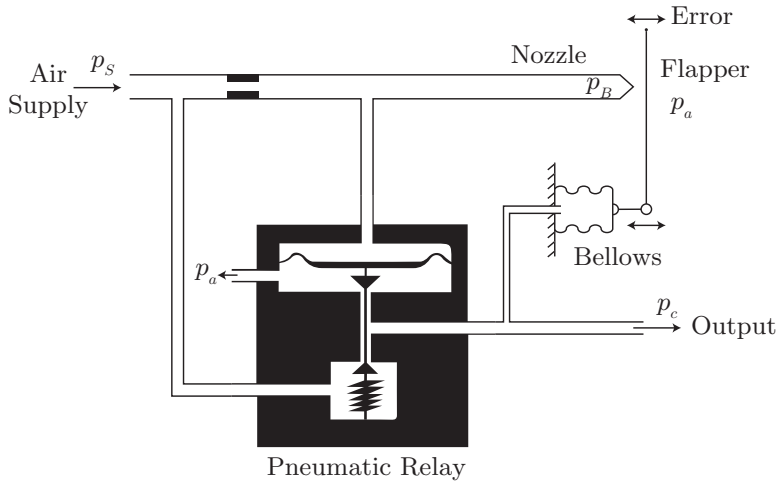

Figure 2.7: Schematic of a force-distance type controller. (Source: [5])

2.2.4 Force-Balance Type Controller

An other type of controller is the force-balance type (fig. 2.8). It is widely used in industry and has a similar working principle as the force-distance type controller. Its main advantage is that suffers from a less friction because it excludes a lot of mechanical joints.

This controller only works with pressure signals. The reference input and output are converted to pressure signals. This controller still has a nozzle flapper at the bottom where the diaphragm acts as the flapper. The nozzle leads to the atmosphere.

The air flows from the supply through an orifice (reduces the pressure) to the nozzle flapper. Depending on the reference and output pressure the diaphragm opens or closes the nozzle, decreasing or increasing the control pressure.

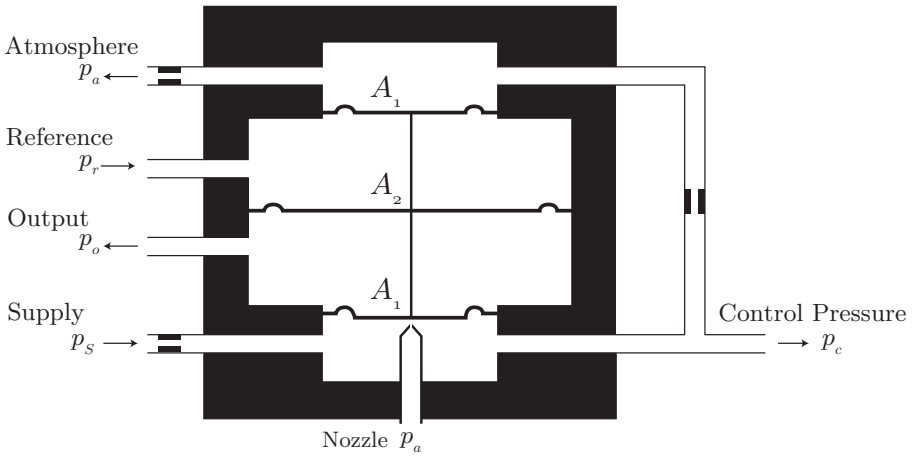

Figure 2.8: Schematic of a force-balance type controller. (Source: [5])

2.2.5 Commercial Valves

As a locally placed valve in the air conveyor is no longer available, a replacement is needed.

In appendix A an overview is given of commercial valves along with their specifications.

2.3 Academic Papers and Journals

The literature search for a pneumatic valve is discussed in this section. A review article was examined as an inspiration for this investigation [6]. The method of conducting such a literature study is described in the following steps.

2.3.1 Method

1. Define keywords and find synonyms for these words relating to the project. These keywords will be used to search for relevant information on the subject. Scopus and Google Scholar are used to find articles and scientific papers and Escapenet for patents.

2. By different combinations of keywords papers are found. The first filter consists of assessing the title and figures of the papers for relevant information. If they appear to be significant, the abstract is read. Should the paper remain interesting, it will be completely read.

3. Formulate constraints according to the design problem. This to filter information that is not relevant.

4. A classification is made of the found information. Summaries of the most interesting papers are written.

5. The results of analysing the papers (and patents) are discussed, referencing the articles.

6. Concluding, the literature study is finished by proposing the manner in which the project will be continued.

The sets of keywords that are used in the initial search are listed in the table below table 2.2. Different combinations of the keywords were entered to get the broadest search results. Proportional valves are considered because they add the possibility to control the airflow and thus the flyheigth of the floating wafer.

Table 2.2: Sets of keywords used to search literature

Set	Keywords
1	Micro, nano , small
2	Piezo valve
3	Pressure control
4	Proportional valve
5	Pneumatics

In the next sections articles are shortly discussed to give insight in the research that has been performed in the field.

2.3.2 Piezo-Electric Valves

An overview is given on tasks that proportional pneumatic valves perform in fluid power systems by Murrenhoff [7]. Recent improvements show a trend into microvalves and low power consumption. The demand for small valves is combined with the need for enhanced dynamics. Some typical valves are illustrated. Valves with integrated control circuits, low power valves

(typically piezovalves) and microvalves. Piezovalves can be used for on/off control and proportional control.

The electro-pneumatic proportional valve converts an electrical input signal into a pneumatic pressure or flow. Traditionally an electromagnet or a torque motor is used as the electromechanical conversion device in a proportional flow control valve. Due to drawbacks of these devices (slow response, large volume etc.) such valves are difficult to improve. Presently there are two types of piezoelectric valves. One type that is driven by a rigid displacement actuator [8] and a type driven by a resonant displacement actuator [9].

Nozzle-Flapper
Gang et al. [10] propose a nozzle-flapper type valve based on a piezoelectric motor. It uses the same working principle as the two stage nozzle flapper described in section 2.2.1 only now the distance between the flapper and nozzle is controlled by the piezoelectric motor's output displacement.

A model of the piezoelectric motor is established using a system identification method and a mathematical model of the valve is described. A testing system was developed for the prototype. Results showed that simulation and experiment are in agreement. This type of valve has a higher stability and control position than traditional electro-pneumatic pressure valves, due to the continuous displacement output of the piezoelectric motor.

The development of an proportional valve with piezoelectric actuators is discussed [11]. To alter the flow in the airstream, the resistive method is used. This is something in the path of the airstream. The goal was to miniaturize the size while at the same time improving the static and dynamic response. The paper focusses on an experimental model. The stroke of the piezoelectric stack is amplified in a hydraulic fashion.

Amplified Piezoactuator
Piezovalves are considered for their quick response. Even though the small displacement by their actuators need to be amplified. Two gas valves were developed and are described [12]. The first is a piezo-actuated gas valve that has a frequency modulation of 400 Hz with a stroke of 100 µm. The second is a proportional piezoelectric valve for precise gas flow.

The valve design has the actuator located in the pressure chamber. Isolation between the pressure chamber and actuator is desirable for clean operations. Another design consideration applies to the poppet's geometry. A flat poppet is suited for on/off control while a pin form is suited for proportional control.

The valves are modelled and tested, they show good behaviour with respect to solenoid valves.

2.3.3 MEMS Microvalves

An overview is given of the primary design considerations of a micro machined proportional control valve [13]. The need for a small-volume, high precision mass flow controller for minute fluid flows has not yet been fulfilled. Such a mass flow controller consists out of a mass flow sensor, a proportional control valve and control electronics connected in a closed loop. The design concepts that are most suitable for the intended microvalve are shown in further detail [14].

For a differential pressure , controlling fluid flow requires control over the flow resistance. The concepts in this paper achieve this by changing the mechanical geometry (low leakage). Basic design consists out of an orifice in a fixed plate that is covered by a translating plunger. A powered actuator is required to achieve precise control.

Many design concepts for MEMS valves are based on a vertically translating plunger to cover an orifice. Hard material is not preferred as the plunger and orifice plate will not deform and make a tight seal. Also when a particle lands between the two plates it will prevent the valve from fully closing.

The rigid plunger can be replaced by a flexible membrane, that deforms precisely over the orifice. This is called a flexible membrane valves, they suffer however from more fragility and are more permeable to moisture and gasses. Another modification is to fix one side of the plunger to the surrounding material. This gives a tilting plate valve.

A bending plate valve relies on material properties such as thermal expansion or piezoelectric strain to deform the plate towards or away from the orifice. A different concept is to horizontal translate (slide) a plate. A micro scale version of a needle valve

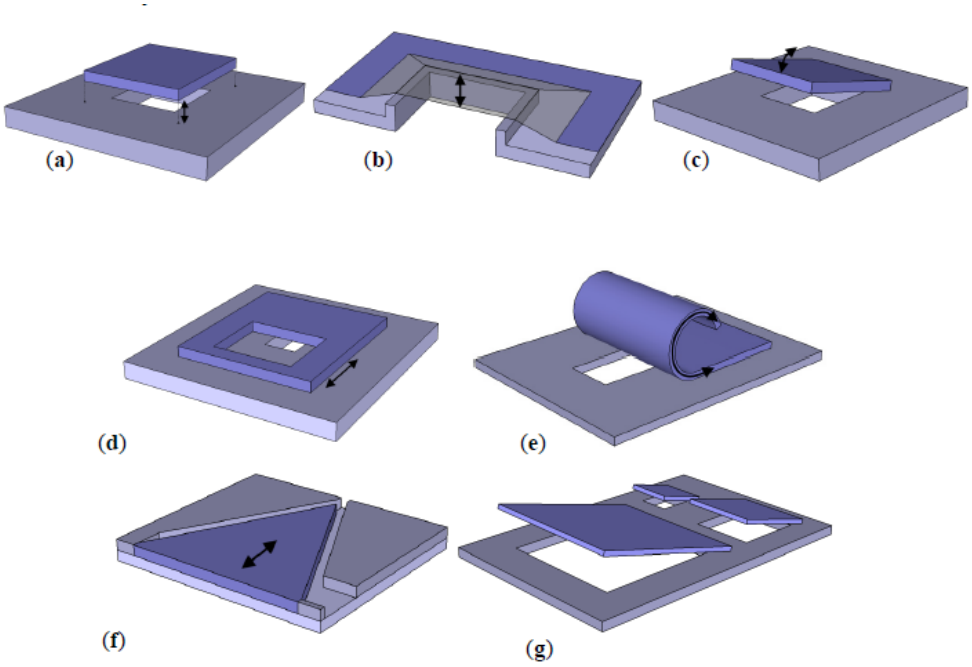

Figure 2.9: Overview concepts (source: [13]): (a) Vertically translating plate, (b) Vertically translating membrame, (c) Tilting plate, (d) Horizontal translating plate, (e) Bending plate, (f) Needle, (g) Scaling

Different actuators are considered such as a thermal expansion actuator, shape alloy actuators, electrostatic actuators, electromagnetic actuators and piezoelectric actuators. A table is presented with all the options and their performances fig. 2.9.

Cantilever Microbeam

The design and operation of a new piezoelectric valve is discussed in this paper [15]. The only moving part next to the piezoelement is a small O-ring. The valve can run in pulsed and continuous mode. This valve was designed for the production of short gas pulses at high backing pressure. The valve was tested at a frequency up to 5 kHz.

In the design considerations the following points are included. A displacement of 30-70 µm is needed for the application of pulsed molecular beams for nozzle diameters of 100-300 µm. A high dynamical response. (10 us or less), variable repetition rate (5 kHz) and sufficient blocking force (1-2 N).

The piezoelectric ceramics can be manufactured as unimorph, bimorph and multilayer stacks.

This valve utilizes a parallel poled bimorph piezoelectric structure to maximize the deflection. Tests were performed and showed that the first eigenfrequenecy was well above 5 kHz, so an even higher repetition rate could be achieved (maybe 10 kHz).

In general these microvalves do not have sufficient maximum flow capabilities to be used for an air actuator. However, they can still be used as a source of inspiration for other concepts.

2.3.4 Pneumatic Mechanical Relays

Another search is done to look for existing designs of pneumatic relays. Combinations of keywords in table 2.3 below where used in Google scholar to search for relevant information.

Table 2.3: Sets of keywords used to search literature

Set	Keywords
1	Pneumatic Relay
2	Small, Micro
3	Diaphragm, Membrane
4	Bellows

In the following part some valve concepts, that where found or conceived, are elaborated upon. They are classified in concepts that use a diaphragm, concept that use bellows or concepts that could use both. A figure along with a description of the concept is given for each type.
It was found that pneumatic relays can be characterized by a number of properties. In table 2.4 these properties are summarised. The leaking effects are classified in bleeding and non-bleeding valves. When a relay is switching between two channels, the output can be connected to the two channels at the same time (bleeding) or closed off so supply flow is not wasted (non-bleeding).

The relay can be proportional, which means that depending on the value of the input the output will change. This can for instance be a linear relationship. With these kind of valves the value of the output can thus be controlled with the input. A on/off acting relay will switch when the input has exceeded a certain level. So these valves only has a on or off function as the name implies.

All of the relays need a mechanism to change a pneumatic pressure into a mechanical displacement in order to close and open certain channels. This is done by using a thin membrane that will deform under pressure. It can also be done by bellows. Which are basically a mechanical spring combined with a membrane. So the difference is not that large because a lot of relays use springs or flexure mechanism along with membranes.

Finally the acting type says something about how the input will change the output. In direct acting valves the output pressure will increase when the input does. And with reverse it is just the other way around.

Table 2.4: Properties of Pneumatic Relays

Leaking Effects	Actuation	Pneum-mechanical transition	Acting type
Bleed	Proportional	Diaphragm/membrane	Direct
Non-Bleed	On/Off	Bellows	Reverse

Plug Diaphragm Type

This type of valve uses a diaphragm to transform the input pressure into an displacement. A plug is attached to the membrane that closes off one channel and opens another and vice versa depending on the input pressure (fig. 2.10).

A. Allen *et al.* [16] patented a design that uses this principle. It is a direct acting proportional valve. It does bleed because the supply and exhaust channel open at the same time when switched. It also uses a flexure mechanism to hold the plug into place.

There are also plug diaphragm concepts [17] that use a channel that runs through the plug. In that way other geometries can be achieved.

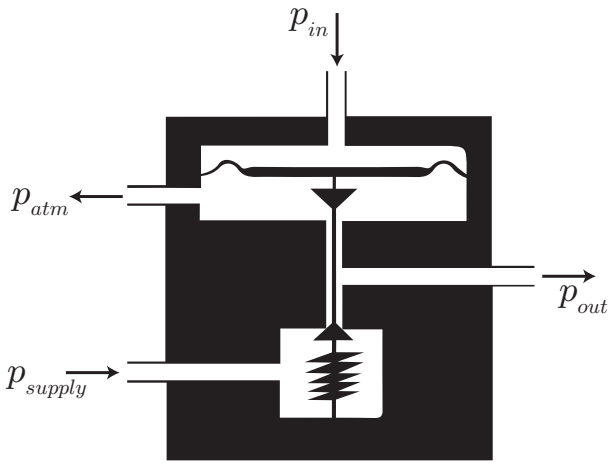

Figure 2.10: The plug diaphragm concept

Lever Flexure Type

As stated before S. Besch *et al.* [18] designed a proportional valve that uses a bimorph to control the beam between an supply and vacuum source. Another concept uses the same sort of lever like structure to increase a small displacement by a bellows or membrane, in a larger displacement at the plug that closes channels off (fig. 2.11).

J.W. Philips [19] made a concept where this was used in combination with a snap acting beam. This means that it has a on/off type behaviour.

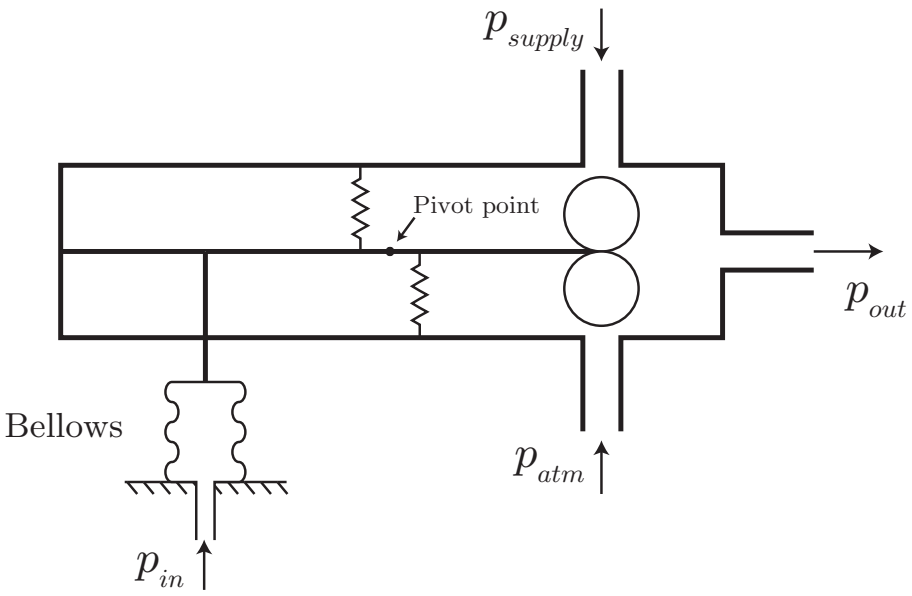

Figure 2.11: Lever Function concept

Membrane closing Type

These concepts use a deforming membrane to close off certain channels. So there does not have to be a plug attached to the membrane which generally makes the design more simple. K.G. Kreuter *et al.* [20] designed a valve using this principle. The chamber in which the membrane is located has certain humps that come into contact with the deformed membrane.

J.E. Hogel [21] designed an valve that uses a snap acting disc to close and open channels fig. 2.12. The membrane is stable in two positions. When the input pressure is higher than the supply pressure, the output channel will be connected with the outside world (vent). When the input pressure drops below the supply pressure, the membrane will snap back and the vent channel will be closed off. The output will then be connected to the supply channel.

This is thus a reverse acting on/off valve. Since no proportional control is established due to the bi-stable behaviour of the diaphragm. And as the input pressure increases the output pressure will decrease, because it will be connected to the atmosphere and vice versa.

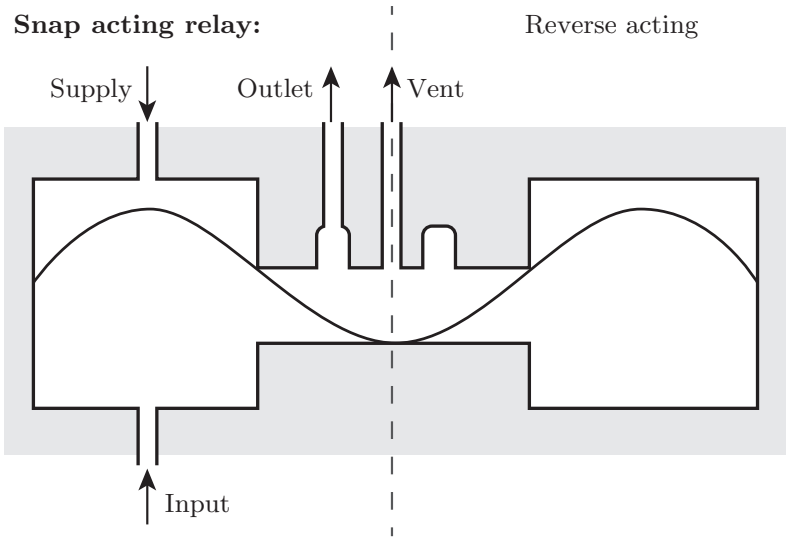

Figure 2.12: The Snapdisc concept

Rotating Type

Another type of relay was inspired by a design by K.L. Tate [22]. The idea is to transfer a pressure signal with a rotating part. This will open certain channels and close others. In fig. 2.13 a rotating cylinder will switch between the channels.

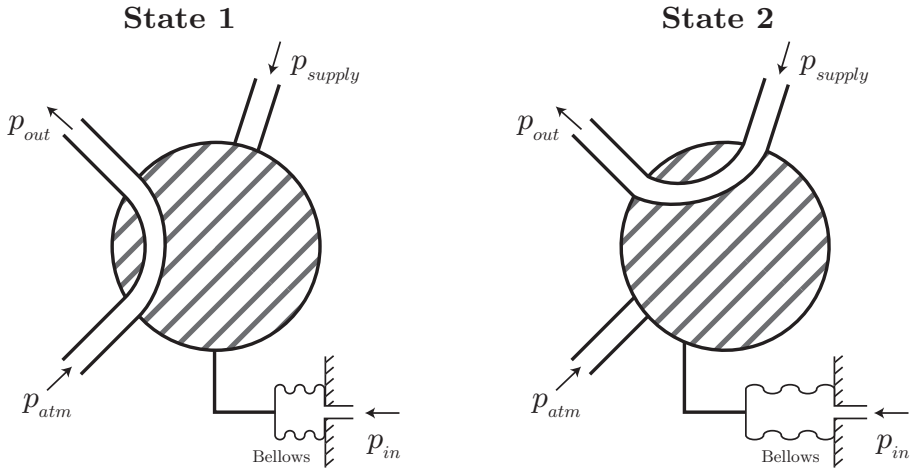

Figure 2.13: Rotating cylinder concept, no bleed

Bellows Type

In the book *Control systems for heating, ventilating, and air conditioning* [17] a chapter is dedicated to pneumatic control devices. One of the control devices described there uses a horizontal beam and two balls that close off channels. With such a configuration different concepts can be created (fig. 2.14).

Here (in this case) a bellows will move the horizontal beam upwards as the input pressure increases. This will close of the vent and open the supply channel. A proportional function is possible with this concept. The 2 switching channels could also lie on the same surface. In that case the beam could rotate to make sure one opening increases as the other decreases.

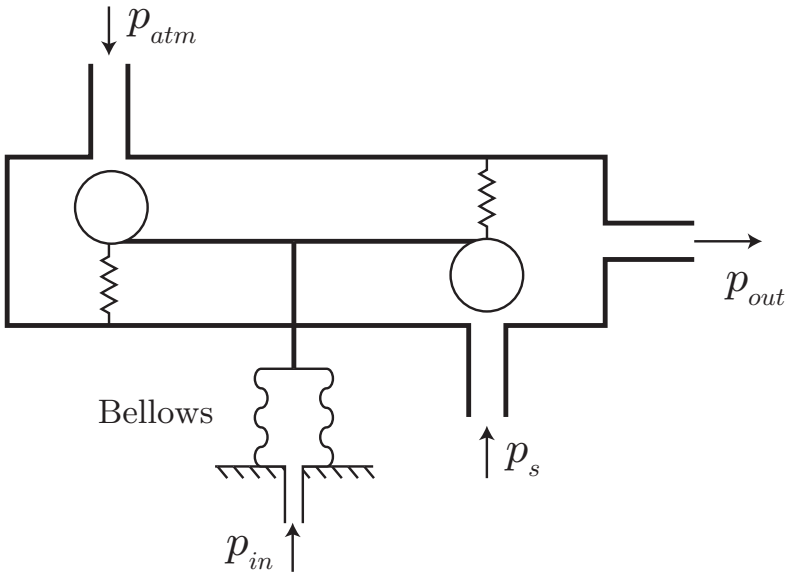

Figure 2.14: Proportional bellows concept

2.3.5 Models and Applications of Pneumatic Valves

In this section different models and applications found in papers and journals are described. This is more general information to give insight in pneumatic advancement and less applicable to the issue of interest.

Three Way Valve
A model is presented of a certain three way proportional pressure valve [23]. This is done by modelling the internal mechatronic devices of the valve to correctly represent the valve's dynamics behaviour for different operating conditions. The physical parameters used in this model were identified by means of experiments.

The pneumatic proportional controller its functions are divided into four blocks: regulation, command, actuation and feedback. The normalized signal of the regulation is compared to the feedback signal (pressure sensor). The reference signal is converted to a mass flow rate by the command block that is send to the actuation block to apply the changes.

Solenoid Valve
The parameters that define the dynamic behaviour of a pressure valve are identified using theoretical models and experiments [24]. One of the main disadvantages of pneumatics are non-linearities due to friction and air compressibility. Mass and energy conservation theory along with least squares method an eighth order black box model with known parameters is identified. It can predict behaviour with errors of less than 10%. Internal parts of pneumatic proportional valves are hardly known which leads to the use of standard (less accurate) models.

The valve analysed uses a plunger along with a spring and spool displacement and internal pressure output. (solenoid valve). If the solenoid provides a force the plunger will move downward and let air run from the supply to the control volume. When the air in the control volume is at the reference pressure, the solenoid voltage drops to let the plunger move upward and close the supply off.

If the control volume pressure is higher than the reference input, the solenoid voltage decreases and the valve diaphragm deforms upwards. The air exits the vale through the exhaust until the control volume pressure and solenoid force are equal. Using the previous mentioned theories, the identified parameters are able to depict the systems dynamic behaviour at an accuracy of 91,6%.

Blood Pressure Monitoring
One of the options is further developed in a design and characterization of a MEMS microvalve [14]. The valve has a built in capacitive displacement sensing and is fitted with a piezoelectric actuator for active control. The sensor facilitates high bandwidth proportional control. This is crucial for non-invasive blood pressure waveform monitoring using a counter pressure.

Non-invasive real-time monitoring of the blood pressure waveform (BPW) can be used for screening for cardiovascular disease. A proven device to perform such a task, utilises a pressurized finger cuff. The blood pressure can be measured if the cuff pressure is equal to the arterial pressure. Current systems are bulky and downscaling is preferred. To create a portable system, a micro valve for miniaturized gas flow control is developed.

A translating plate design is chosen, for its simple fabrication and large design freedom. The finished valve has been analysed for movement with COMSOL. The fabrication process is explained.

An integrated test setup is made to mechanically characterize the microvalve. The fluidic behaviour is required to implement the capacitive displacement sensor in a control loop. The gas flow is measured as a function of valve separation at different pressures. The results showed that the maximum stroke is 3.5 µm, the measured flow is lower than the predicted value (due to

the pressure drop over the flow meter). The valve cannot fully close, partly due to the piezoactuator and partly due to contamination in the air. The measured capacitance lies in the range of 2844 pF for separations of 0.5-4 µm.

High-Speed Pressure Clamp
The design and system performance of a high-speed pneumatic pressure clamp is described [18]. A new type of differential piezoelectric control valve is the key control element. It controls both the pressure and vacuum. In this design the response time is improved by doubling the resonant frequency of the single ended support of the piezo bimorph, by supporting it at two sides. By minimizing the dead volume and by placing a pressure sensor on the valve. A zero voltage gives zero pressure.

The valve is split in a top and bottom part fig. 2.15. The bimorph is placed between the pressure source (top) and vacuum source (bottom). The outlet of the valve is located at the end of the bimorph. When voltage is applied the bimorph bends towards or away from the pressure sources. This closes or opens a path to the pressure or vacuum source, effectively enabling proportional control. The pressure clamp system has worked reliable for 2 years.

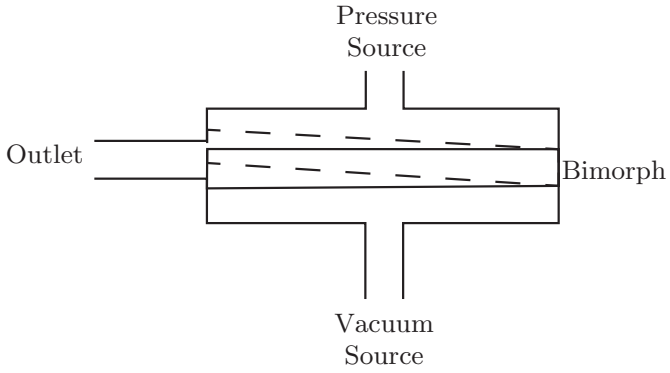

Figure 2.15: Bimorph valve

Vehicle ABS
Jeon et al. presents a system to control wheel slip for ABS of a passenger vehicle [25]. It uses a piezo valve modulator. First the design parameters of the valve and modulator are identified by applying braking pressure variation during ABS activity.

Design simplicity is difficult to realise with solenoid valves. A different actuating method is searched as a replacement. So called smart material actuators, such as electrorheological (ER) fluids, piezoelectric materials and shape memory alloys are looked at. With piezoelectric actuators miniaturization can be achieved for valve systems.

A flapper-nozzle with piezoelectric actuation valve is designed. The valve is connected to the pressure modulator to amplify the controllable pressure range. This system is then applied to an ABS system, using a quarter car model. A model is given of the piezovalve system.

Micropropulsion
Recent developments in micro-propulsion components for microspacecraft are reported on in this paper [26], including a micro piezoelectric valve. First a short overview of microspacecrafts is given along with a section on micropropulsion.

A micro-piezo valve is under development. It moves a circular corrugated diaphragm with a piezoelectric actuator. It rests on a valve seat in the closed position. The valve stroke depends on the voltage applied. This valve can be used for flow control applications. A prototype is completed and initial flow tests are done to determine the required force loading of the piezostack at various feed pressures.

2.3.6 Discussion

In this chapter several different valves have been reviewed. Piezo-electric valves where proportional control is possible and simpler mechanical pneumatic relays that switch on or off with a pressure signal.

In the next chapter a concept is chosen with the use of the presented information for further development.

3

Concept and Analysis of a Nozzle Wafer System

In this section a conceptual design will be described that will be the focus of this research. The information from the literature study from the previous chapter is used to arrive at the concept.

The problem and research statements are presented. Also a first analysis of the nozzle wafer concept is described.

3.1 Nozzle Wafer Concept

Inspired by the nozzle flapper design discussed in section 2.2.1 a concept is conceived (fig. 3.1). In this system a the nozzle flapper mechanism is embedded in the surface of a floating wafer table. In this configuration the wafer acts as a flapper. Thus the pressure will increase inside the nozzle when the wafer is floating over the nozzle and detects the wafer.

The nozzle is connected to a pneumatic relay valve that will open a channel from a pressure source to the surface. This is the channel that provides the thin layer of air on which the wafer floats (the airactuator). The nozzle only provides an airflow to detect the wafer, not to create an airlayer to float on.

If a floating conveyor is equipped with these relays, the air actuators are switched on only on the wafer position. In this manner the use of unnecessary pressurized air can be prevented and costs can be saved. For instance in the production of solar cells [27].

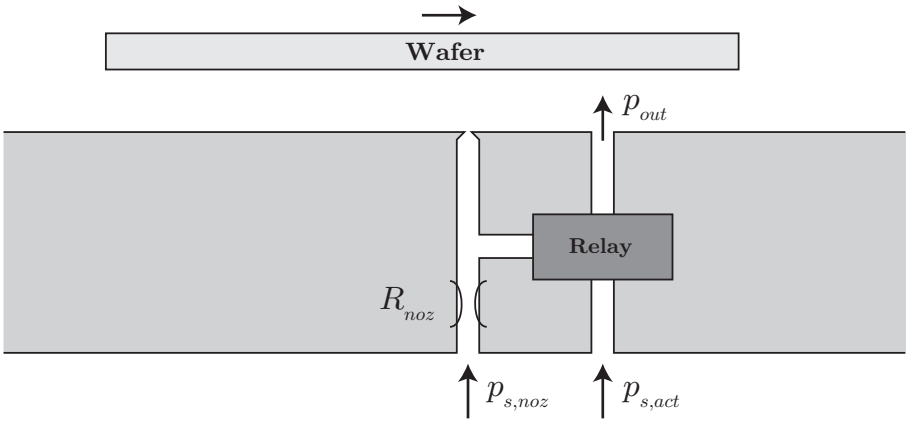

Figure 3.1: Nozzle-wafer model

A system like this has the following advantages. It only uses pneumatic and mechanical parts,

compared to a system that uses electric powered valves in which the complexity rises steeply. For an electric system the nozzle back-pressure has to be converted to an electrical signal in order to communicate with the valve. Alternatively a vision measuring system could be used, but this increases the complexity even more so in terms of calibration. If the proposed system is properly calibrated, it is a plug and play system that only needs pressurized air to function.

3.2 Problem statements

Problem statement
In the high-tech semiconductor industry, chips are produced from thin substrates. During the different processes used during manufacture, a high precision positioning system is needed. A positioning device was developed by J. Wesselingh. In this design the substrate is floating on a thin air film.

An interesting point for improvement is to limit the loss of pressurized air used by such a system. This is less of a problem in the high-tech semiconductor industry, as the used air is only a small fraction of the costs. It is however more relevant in the floating air conveyors used in the solar cell industry. Conveyors are only effective at the position of the substrate. At the other positions this air is directly send to the atmosphere. The longer the transport band the more pressure is wasted.

Research statement
The following points are to be researched or done:

1. Make a model of the nozzle wafer concept, to better investigate the concepts feasibility.
2. Develop a pneumatic relay that can be operated using the nozzle back pressure from the nozzle-wafer concept. First simulate its use in a model of the design. Then validate this model by manufacturing and performing experiments on the valve.
3. Investigate the implementation of a nozzle-wafer system in a conveyor. Focus on the connecting logic.
4. If this fails an alternative design can be proposed or investigated.

3.3 Valve Concept Choice

In section 2.3 different valve concepts were presented. MEMS valves are dismissed, because they do not provide enough flow in order for wafer air layer to float.

Local piezo-electric valves are a viable choice. They are fast and provide more flow. However, a major disadvantage is that they are electrically operated and need a large power source. This means control is necessary and electric pressure sensors are needed locally to operate the valve. In appendix B a new proportional piezo-electric valve from FESTO is tested.

The investigated pneumatic relays do not have this disadvantage. They can be operated directly with a pressure signal. If such a relay is implemented in the nozzle wafer concept, and properly calibrated, a plug and play system can possibly be realised. Here only pressurized air has to be connected for the system to function.

3.3.1 Pneumatic Relay Chosen Concept

The snap disc concept is chosen, because it seems quite simple to manufacture. It does not consist out of a lot of parts and only has the membrane as a moving part. It cannot be used

as a proportional controller, but the focus of this design lies on the on/off behaviour. The difficulties lie in the manufacturing of the bi-stable membrane. A commercial implementation has not been found, its worth investigating if a working snap acting pneumatic relay can be designed and made.

Using the patent as inspiration other concepts can be conceived. The different channels can be attached to the relay in other ways. If the input pressure is originating from the nozzle, it will have a high value when a wafer is on top of the nozzle. Thus closing the relay, and opening it when the wafer is no longer detected.

Another problem is that the input pressure to open the valve needs to be higher than the supply in order to work. This means that the nozzle back pressure need to be higher than the air film pressure, which is impractical. These problems can be diverted by swapping the supply and input channels.

When the channels are connected as in figure 3.2, the closing of the valve can be controlled with an extra input. Now there can be a period where the valve remains open, even when the two nozzles are not detecting the wafer. In the remainder of this chapter different connecting schemes are investigated. In subsequent chapters this concept is further expanded in models and a prototype.

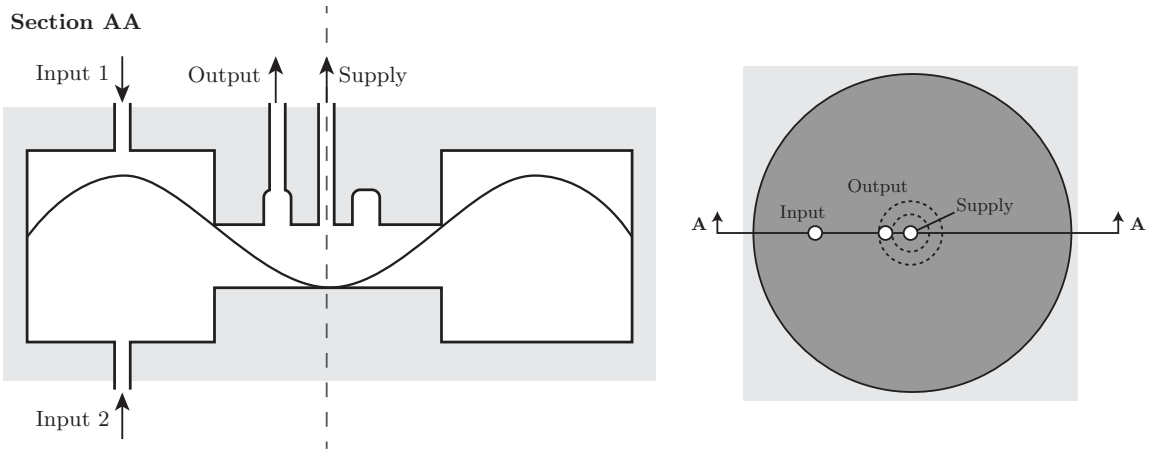

Figure 3.2: Snap Acting Relay with an Extra Input, in open Position

3.4 Analysis of a Floating Wafer System

To research if the proposed system is feasible a model is made of the nozzle-flapper mechanism. As was described in the previous section, the flapper is represented by a floating wafer and the nozzle will be embedded in the surface. First the modelling goals are described and what part of reality it simulates. Next up the models boundary conditions are explained and the results are discussed.

3.4.1 Modelling Goals

In short the goals of this simulation are:

1. To examine the behaviour of a nozzle wafer system.
2. To investigate if this concept is applicable and at what pressures.
3. Perform a parameter study of this model.

3.4.2 Model Setup

In fig. 3.3 the a floating wafer is illustrated. There are two air-inlets under the wafer, a pressure source that provides air for the thin film on which the wafer floats p_{s_act} and a pressure source for the nozzle to detect the wafer p_{s_noz}. The nozzle has two restrictions, R_{sup} is located between the supply pressure p_{s_noz} and the nozzle back pressure p_b, and the other is a restriction between the nozzle and the surface (R_{noz}).

At the edge of the wafer a boundary condition of atmospheric pressure is applied. With COMSOL a one-dimensional approach is used to simulate this situation. The governing equations that describe the air flow, are explained up next.

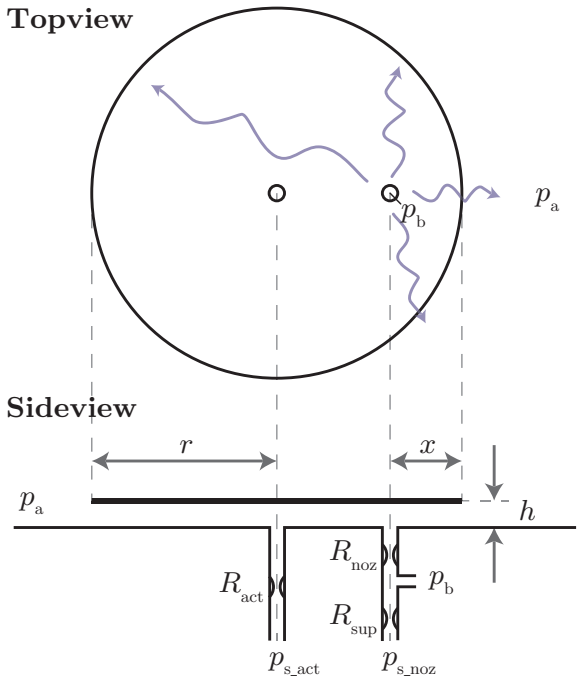

Figure 3.3: Nozzle-wafer model

The mass flow through the capillary restrictors, used for the inlets, is represented by the following equation taken from [28].

$$M = \frac{\pi d_c^4}{256 L_c} \frac{p_\mathrm{s}^2 - p_\mathrm{b}^2}{\eta R_s T} = K\left(p_\mathrm{s}^2 - p_\mathrm{b}^2\right) \tag{3.1}$$

Where d_c is the diameter of the capillary inlet, L_c is the length of the restriction, η is the dynamic viscosity of the medium, T is the temperature and R_s the specific gas constant of air. The p parameters describe the pressure before and after the restriction. This equation is applicable for a viscous flow through a long tube (Re < 1000 and $l/d > 20$).

The Reynolds equation [29] for the one dimensional approach is used to simulate the thin air film underneath the wafer:

$$\frac{\partial}{\partial x}\left(\frac{\rho h^3}{12\eta}\frac{\partial p}{\partial x}\right) = 0 \tag{3.2}$$

Where ρ is the density of the air, h is the fly height of the wafer and p is the pressure at a position x under the wafer. Using this equation assumes that the wafer and the surface are not moving and it is a static problem.

In this situation air is used as a medium, in order to solve this, the equation has to be altered. The reason being that gas in compressible, so the density will change along with the pressure. The ideal gas law eq. (3.3) is used to write the density as a function of pressure.

Assumptions of ideal gas law (1) the gas consists of a large number of molecules, which are in random motion and obey Newton's laws of motion; (2) the volume of the molecules is negligibly small compared to the volume occupied by the gas; and (3) no forces act on the molecules except during elastic collisions of negligible duration.

$$pV = mR_{\mathrm{s}}T \tag{3.3}$$

$$\rho = \frac{p}{R_{\mathrm{s}}T} \tag{3.4}$$

Substituting this in the Reynolds equation gives:

$$\frac{\partial}{\partial x}\left(\frac{p}{R_{\mathrm{s}}T}\frac{h^3}{12\eta}\frac{\partial p}{\partial x}\right) = 0 \tag{3.5}$$

In fig. 3.4 the one-dimensional COMSOL model is shown. On the two outer points a boundary conditions holds the pressure at atmosphere. The point in the middle represents the pressure source for the actuator. Right of the actuator the pressure source of the nozzle located. In the COMSOL simulation the two restrictions of the nozzle are taken together as R_{tot}. When the pressure under the wafer is calculated, the back pressure can be obtained using equation 3.1.

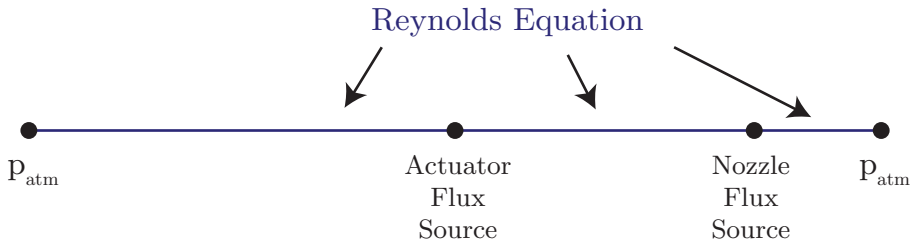

Figure 3.4: Comsol Nozzle-wafer model

3.4.3 Results

A parametric sweep is performed on the total restriction of the nozzle. This restriction needs to be as high as possible, because this will lower the mass flow of the nozzle, as the purpose of this system is to limit air use. However, the nozzle back pressure must be high enough to switch a relay, thus the mass flow cannot be too low. In the equations here below show how the restrictions are calculated. It also adds that the restriction of the nozzle should be lower than that from the nozzle to the supply. Otherwise the back pressure would not drop to atmospheric pressure if no wafer is present.

$$R = \frac{1}{K} \tag{3.6}$$

$$R_{noz} < R_{sup} \tag{3.7}$$

In table 3.1 the values of the parameters are listed that are used in the simulations. In table 3.2 the properties of dry air are listed.

Table 3.1: Parameter values for different simulations.

Parameter	Value	Unit	Description
x	10	mm	Position of nozzle from edge
h	20	µm	Flyheight of wafer
D	10	cm	Diameter wafer
$p_{\text{s\_act}}$	1.2	bar	Source pressure actuator
$p_{\text{s\_noz}}$	1.2	bar	Source pressure nozzle
$d_{\text{c\_act}}$	1	mm	Diameter capillary restrictor actuator
$L_{\text{c\_act}}$	20	mm	Length capillary restrictor actuator
$d_{\text{c\_noz}}$	0.5	mm	Diameter capillary restrictor nozzle
$L_{\text{c\_noz}}$	10	mm	Length capillary restrictor nozzle
K_{act}	4.05×10^{-18}	$\text{m}^2\,\text{s}^3\,\text{kg}^{-1}$	Restriction actuator
K_{tot}	$5.82 \cdot 10^{-19}$	$\text{m}^2\,\text{s}^3\,\text{kg}^{-1}$	Restriction nozzle

Table 3.2: Properties of air

Property	Value
$R_{\text{s\_air}}$	$286.98\ \text{J}\,\text{kg}^{-1}\,\text{K}^{-1}$
η	$1.8 \times 10^{-6}\ \text{Pa}\,\text{s}$
T	293 K

In figure 3.5 a pressure distribution is given under the wafer for different nozzle restrictions (R_{tot}). The actuator pressure source is disabled to investigate the situation when no actuator has been opened. The pressure decreases under the wafer as the restriction becomes higher. This would suggest to keep the restriction low to get a high back pressure.

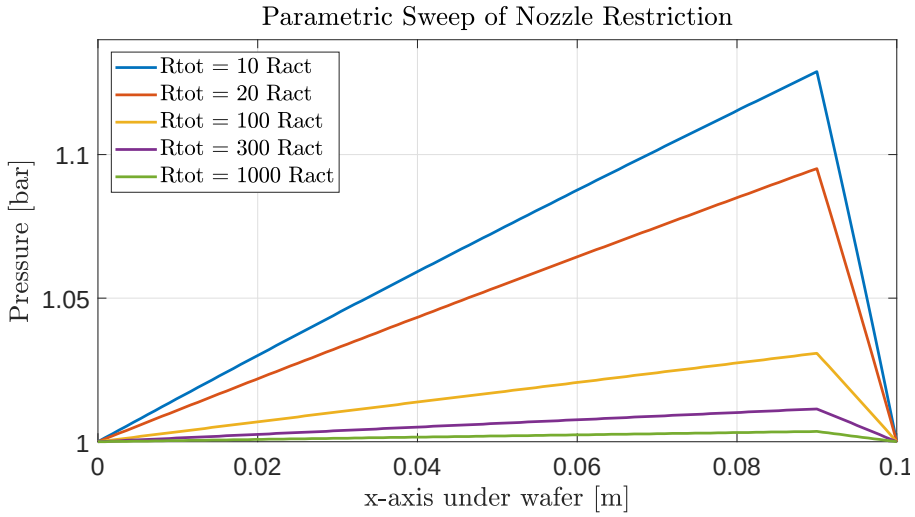

Figure 3.5: Case I: Parametric sweep of nozzle position

When the actuator is activated the pressure distribution changes (fig. 3.6). It is examined that lower restrictions have a higher impact on the pressure distribution. To keep this to a minimum the restriction should be on the high side. This would result in no disturbances in flying behaviour of the wafer and lower air use.

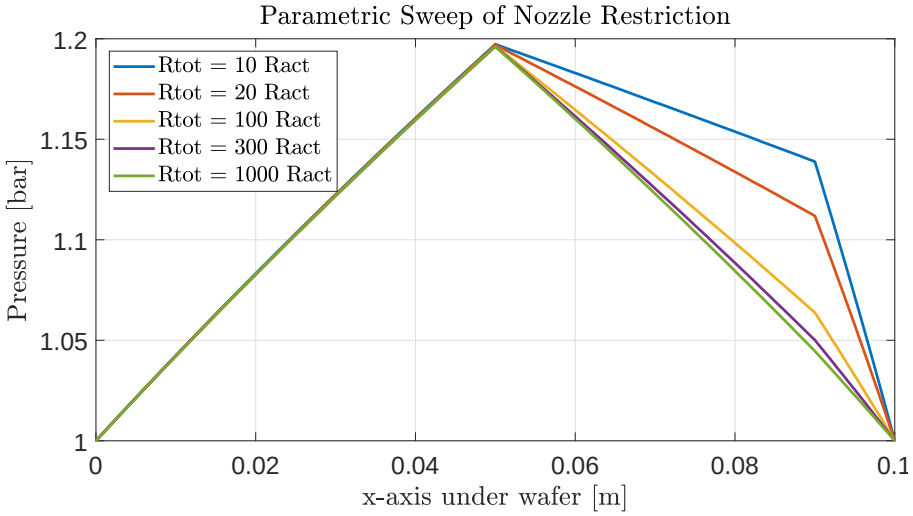

Figure 3.6: Case I: Parametric sweep of nozzle position

To calculate the nozzle back pressure the ratio between the two restrictions in the nozzle must be chosen. In the equation below the ratio of the restrictions is given. In table 3.3 The back pressures are given for two different actuator and nozzle combinations and multiple α-ratios.

$$\alpha = \frac{R_{sup}}{R_{tot}} \tag{3.8}$$

Table 3.3: Nozzle Back Pressures for Different Restriction Ratios

$\frac{R_{tot}}{R_{act}}$	$\alpha = 0.9$	$\alpha = 0.8$	$\alpha = 0.7$	$\alpha = 0.6$	$\alpha = 0.5$	Unit
20	1.110	1.128	1.137	1.147	1.156	bar
100	1.032	1.067	1.084	1.102	1.119	bar

This table would suggest that an α-ratio as low as possible would be beneficial as the back pressure increases. However, this will also influence the back pressures capability to reach atmospheric pressure. In table 3.4 the lowest pressures are listed that can be reached for each restriction ratio. As α increases, so does the minimal attainable value for the pressure.

Table 3.4: Minimal Nozzle Back Pressures

$\alpha = 0.9$	$\alpha = 0.8$	$\alpha = 0.7$	$\alpha = 0.6$	$\alpha = 0.5$	Unit
1.002	1.043	1.064	1.084	1.105	bar

Because of these conflicting objectives an ideal ratio has to be found somewhere in between.

Depending on how far the nozzle is placed from the actuator it switches, the pressure in the nozzle can be increased by the pressure from an active actuator. This means the nozzle is placed closer to an active actuator (moving the nozzle to the left in fig. 3.6).

3.5 Discussion

By altering the value of nozzle source pressure and nozzle restriction every desired nozzle back pressure can be achieved. However, this must not influence and disturb the flyheight and use flow is to be minimized.

It is assumed that the nozzle-wafer concept can provide a suitable back pressure for switching a valve. The remainder of the research focusses on the development of the valve itself.

In the next chapter different valve concepts are investigated and one is chosen to be expanded upon. Also the connecting logic of a whole table is examined.

4

Conceptual Design of a Switching Air Conveyor

This chapter focuses on the implementation of a pneumatic relay and nozzle-wafer in a larger system. Different configurations are investigated and explained.

Apart from the valve design concept that will be fabricated, the application of the valve in a larger system can be worked out. In this section the pneumatic relay will be treated like a black box. So no inner workings are explained, this is done in order for different designs to be applicable.

In the next subsections various connection schemes are discussed. First 1 dimensional configurations are looked at, to keep it simple. Then 2 dimensional schemes are examined that cover the surface on which the wafer floats. But first the black box that is used in these arrangements is explained as a finite state machine.

4.1 The Black Box

The valve has the following operation. When a wafer travels over a surface, covered with measuring points, the air supply must turn on at the position of the wafer. This will happen when it floats above over a measuring (pilot) point. The valve must deactivate if the wafer has passed. To do this a similar pressure signal is needed.

This means that the black box has two input (pressure) values and one output value. The inputs can be high (1) or low (0) and with different combinations the output will change to a high or low value. Input 1 activates the black box and input 2 deactivates it. When both inputs are high or low the output does not change, the previous combination of inputs will continue to determine the output. The finite-state theory is used to describe the different states the valve can have. In the table below the different possibilities are listed (table 4.1), the figure illustrates this same situation (fig. 4.1).

Table 4.1: Sets of Inputs and Outputs of the Black Box

Initial State	Input 1	Input 2	Next State
On	1	0	On
On	1	1	On
On	0	1	Off
On	0	0	On
Off	1	0	On
Off	1	1	Off
Off	0	1	Off
Off	0	0	Off

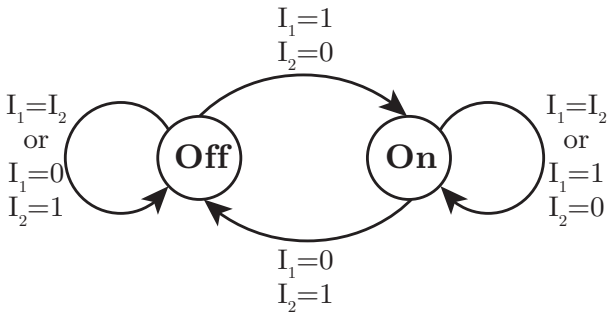

Figure 4.1: Finite State Machine of the Valve

4.2 1 Dimensional Connecting Schemes

One of the simplest one dimensional connections possible is illustrated here below (fig. 4.2). Basically each valve is connected to the surface with its own input and output channels. The wafer can move from the left to right. Each valve will switch on when input 1 becomes high as the wafer floats over the channel. As the wafer passes over input 2 and no longer covers input 1 the output will become 0.

If the wafer moved from right to left, nothing would happen because input 2 cannot activate the valve.

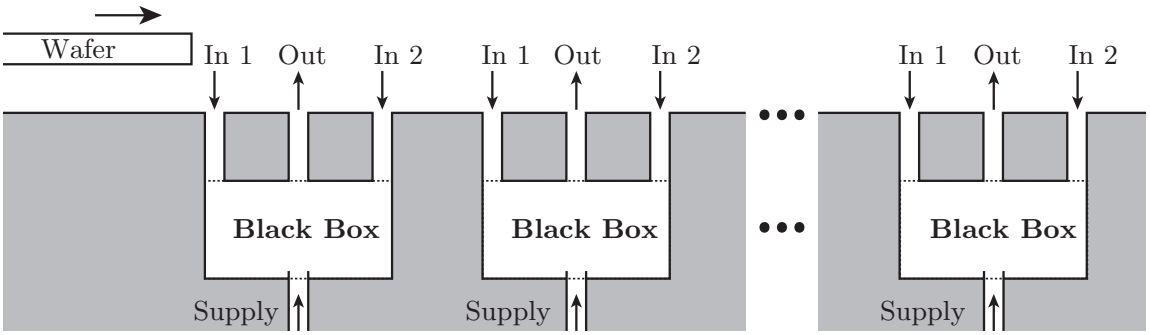

Figure 4.2: 1 Dimensional Pattern of Black Boxes

An alternative is, that black boxes share input channels with each other. In figure 4.3 such a pattern is displayed. This has as result that there are less channels connected to the surface. An output is alternated with an input when looked at the surface.

Still the wafer can only move from right to left. However there is a difference in operation compared to the previous pattern. When a valve is activated by its input 1, simultaneously the previous valve gets a high value for its input 2. The former valve will switch off if its input 1 has a low value.

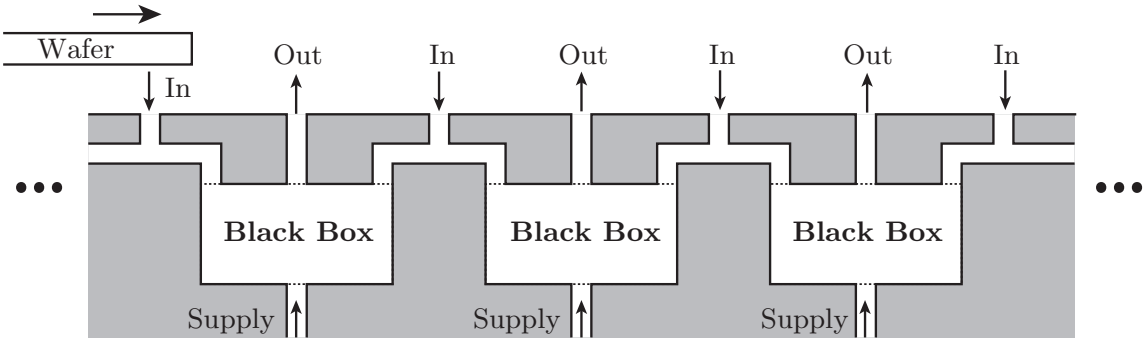

Figure 4.3: 1 Dimensional Connection where input channels are shared between valves

The nozzles for each relay can be placed farther apart from each other so the relay will turn on earlier and turn off later. In this way the sudden flow of air ,at activation of a valve, will disturb the wafer less.

As the arrangements can become more complex it can be difficult to imagine their function. Therefore simulations in MATLAB are created to visualise its working.

In figure 4.4 frame captures of two simulations are shown. The red and green circles represent the closed or open outlets and the blue asterisks are the pilot points. The simulations have the shared pilot point configuration from previous figure 4.3.

In the top simulation (#2) the nozzles are connected further apart from the outlet to provide a bigger buffer of air supply around the wafer.

In simulation 3 the relays are placed in different directions alternately. As a result half of the relays are opened when the wafer has passed and do not close any more.

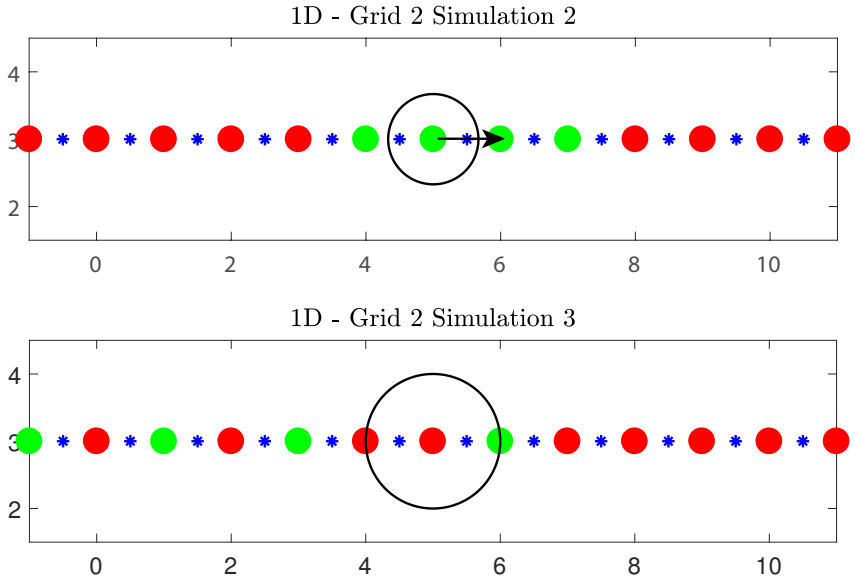

Figure 4.4: Different Connecting Schemes on Grid 2, nozzles (blue) closed oulet (red) and open outlets (green). Arrow for Wafer Direction.

4.3 2 Dimensional Connecting Schemes

Using the gathered knowledge of the 1 dimensional connecting patterns, now 2 dimensional variants are investigated. The different grids that are used in the simulations are shown in the figure here below (fig. 4.5).

In grid 1 the 1 dimensional array is basically extended and in grid 2 the rows are shifted with respect to each other. In grid 3 the pilot points lay on another row and in grid 4 the pilot points are put under an angle for each outlet.

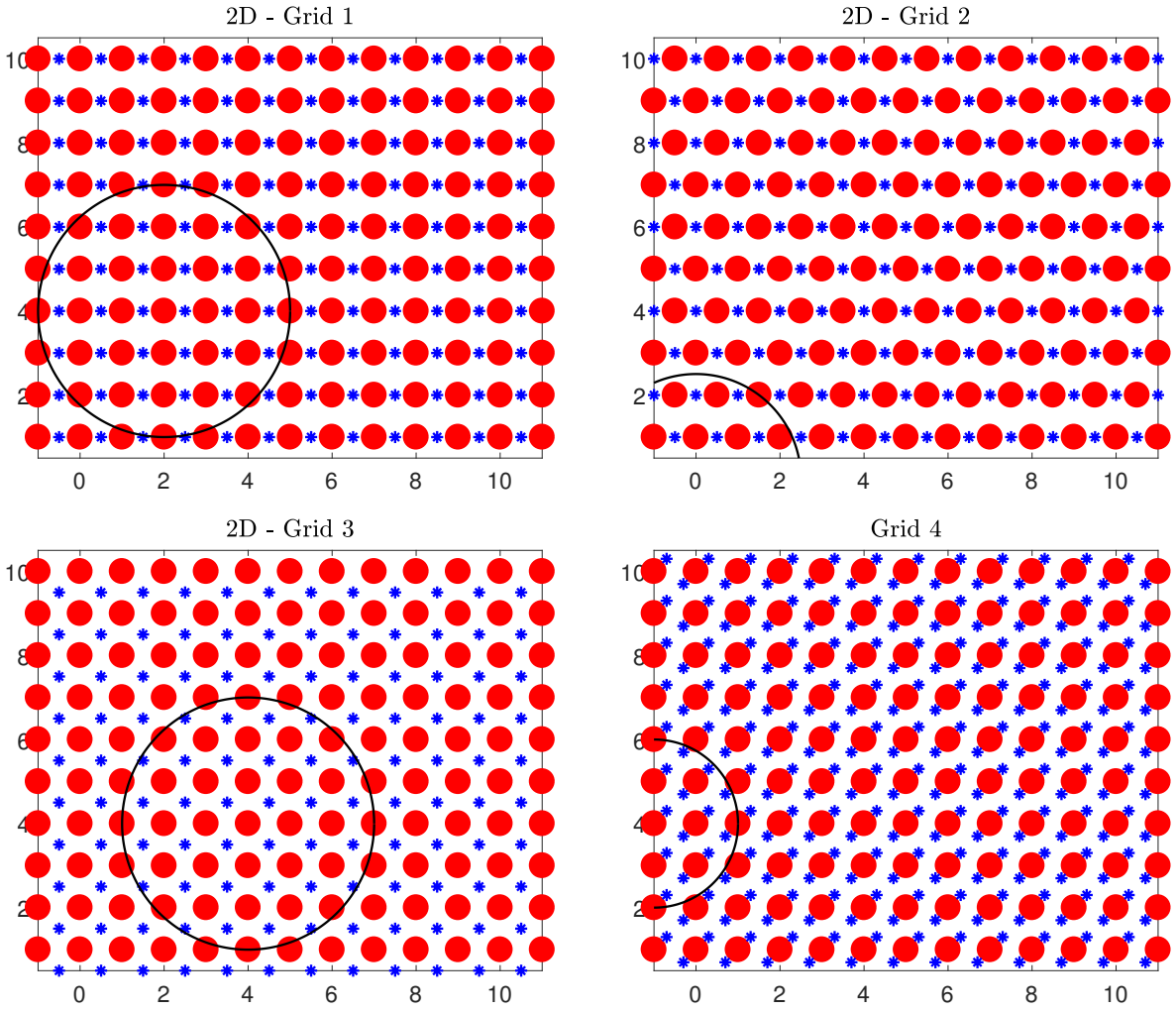

Figure 4.5: Different Grids with Nozzles (blue) and Outlets (red)

With the simulations it is examined if connection schemes can be made, where a functioning surface can move a wafer in different directions. Because one direction is already possible.

In figure 4.6 a two simulations are shown. For the left model, the arrangement manages to move a wafer from left to right and close all relays again. If this path deviates less than 45 degrees the wafer will still have an air film under it. Only now some relays remain open after passage because the wafer never moved over the nozzle that closes the relay.

In the right simulation on grid 4 the grid can move the wafer from bottom left to top right. If the wafer deviates slightly from this path some relays remain open. The more it deviates the more relays stay open.

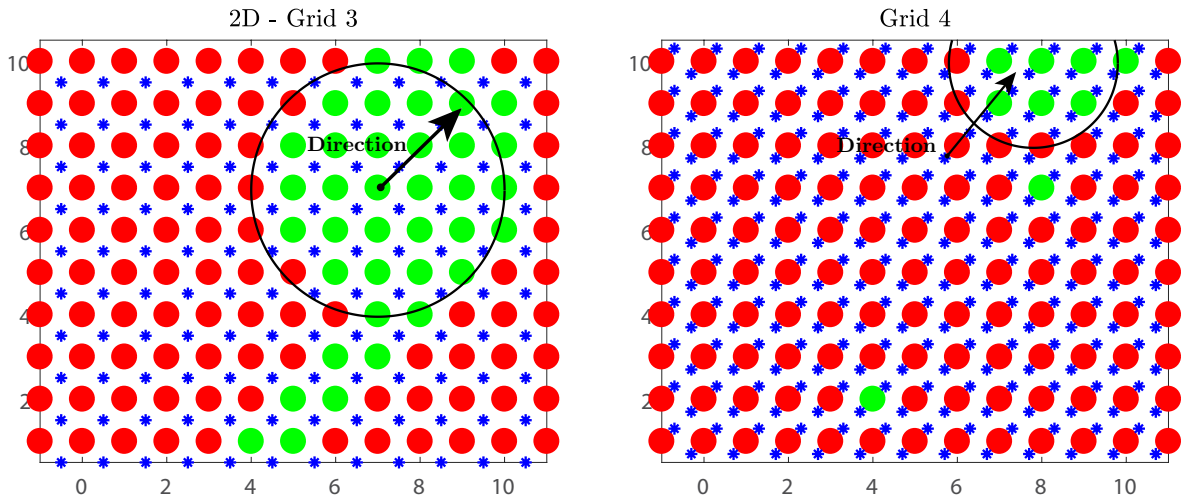

Figure 4.6: Different Grids with Nozzles (blue) and Outlets (red)

4.4 Network of Nozzles

Because the two dimensional grids, that have been researched, can only function accordingly in one direction another approach is used. A grid of nozzles is suggested where all the nozzles are connected to each other with a resistor network beneath the surface (fig. 4.7). The maximum number of nozzles per relays still cannot be larger than two.

The working principle is as such. Under the wafer a high pressure (1) is generated and elsewhere an atmospheric pressure (0) is present at the surface. These values are passed down through the nozzles (vertical resistors) to the relays (the points on the layer below the surface), and next divided over the other nozzles via the resistor network. By tweaking the resistances and supply pressures the activation border of the relays around the wafer can be affected. The vertical resistors are denoted by R_1 and the horizontal ones connecting the nozzles with each other by R_2.

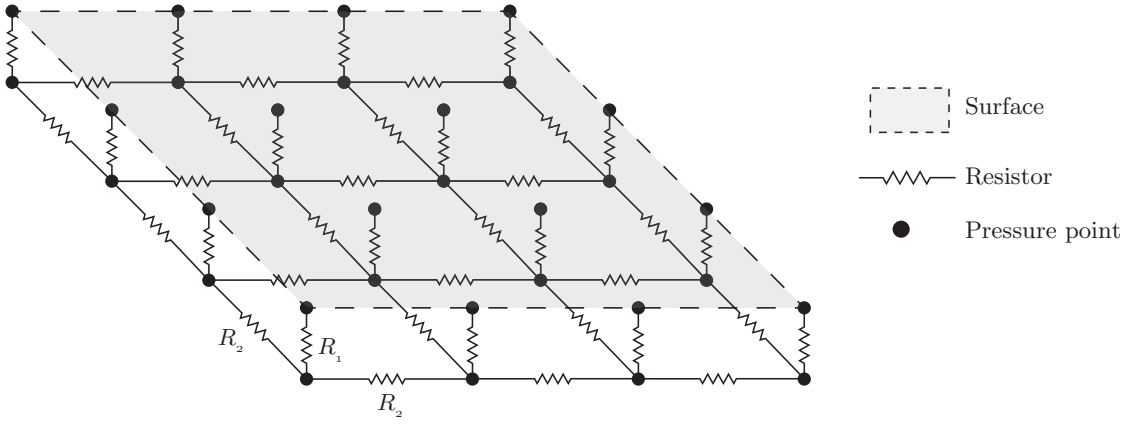

Figure 4.7: Repeatability of Measurements

This is also put into a model using a electric-pneumatic analogy. Kirchoff's circuit laws can be used to determine the pressures in each point that leads to the relays. At the surface an input is given of a high or low pressure. In Matlab a model is constructed as in the previous sections to see which relays will open in what situation.

In the figures here below, three different situations are plotted (fig. 4.8). The wafer is placed at the same position each time. The only thing that is changed is the ratio of the two different resistors. Here the pressure distribution is represented with values between a high and low pressure (1 and 0). No real values are introduced. If the resistance to the surface becomes relatively higher the pressure will divide itself more over the relays.

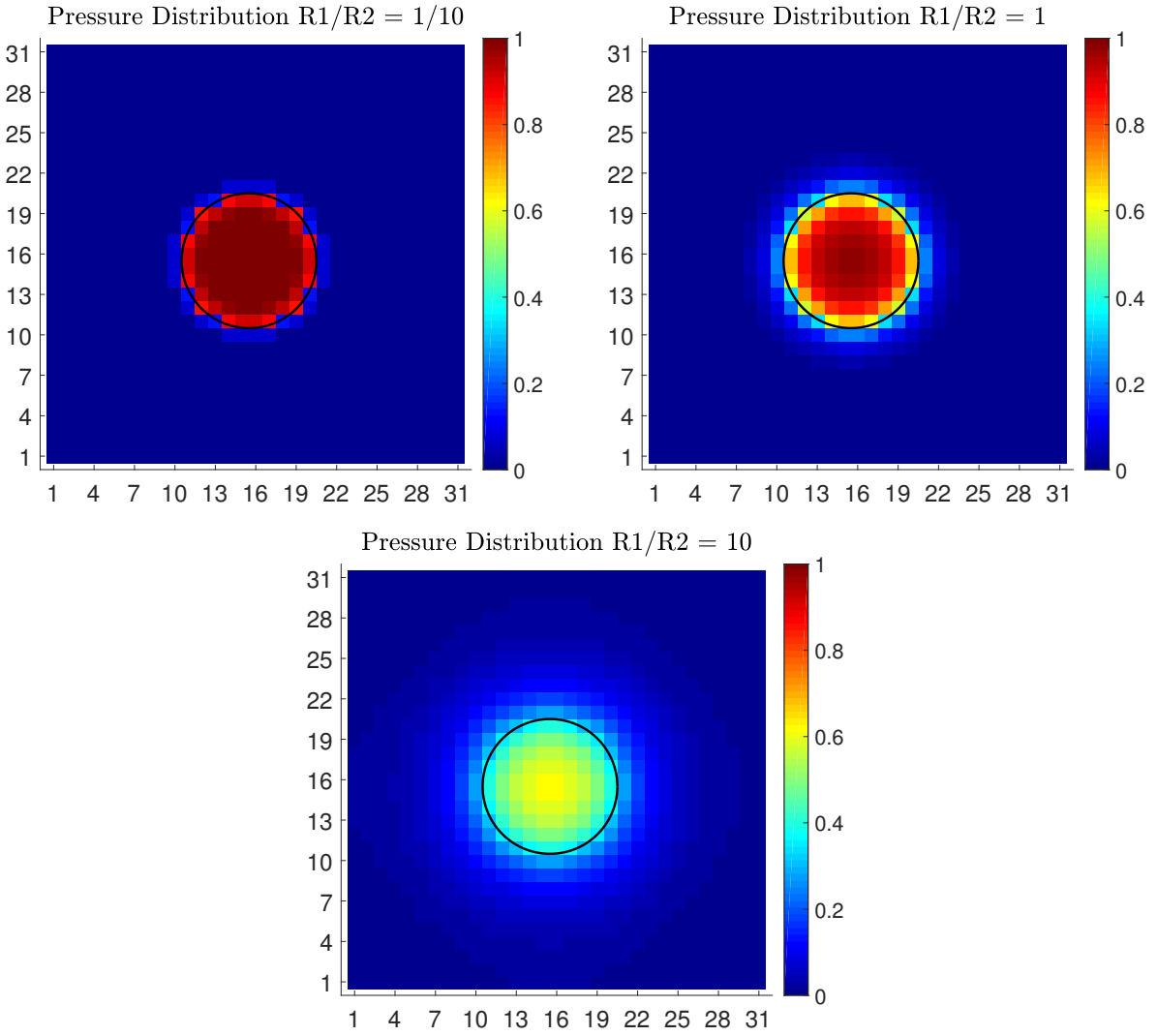

Figure 4.8: Surface plots of three different resistor ratios

Now different functions can be modelled. For instance a design where the grid will open an extra array of relays around the wafer. To choose which ratio to utilize, a plot is made of the pressure just outside the wafer for different ratios (fig. 4.9.a). Here it is clearly seen that around a ratio of $R_1/R_2 = 4$ the pressure in this relay will be the highest, around 0.29 of the high inlet pressure.

Using this ratio, a grid can be made where the switching pressure of relays is 0.28. In figure 4.9.b the model shows that indeed an array of open valves is present around the wafer.

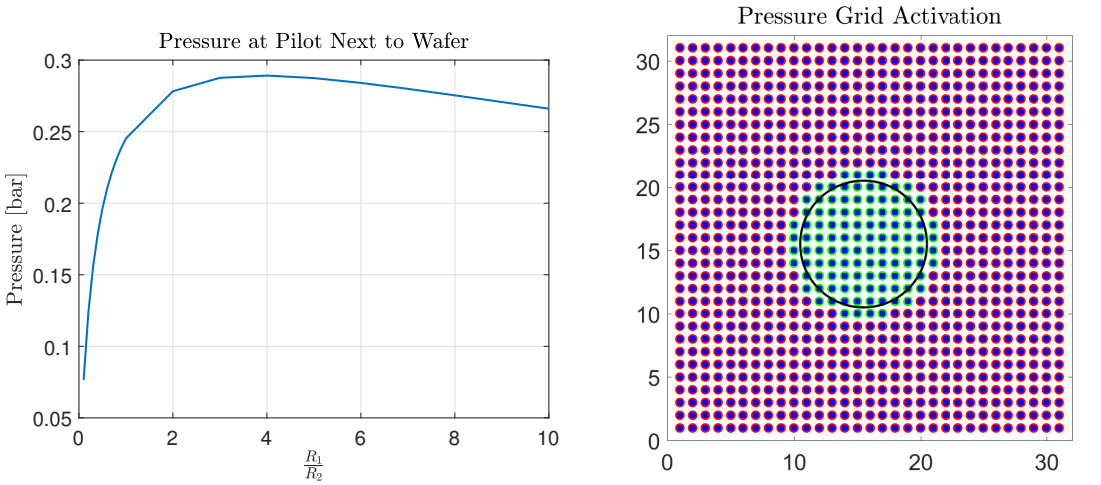

(a) Plot of Pressure Next of Wafer against Resistor Ratios

(b) Grid with Open Outputs in green and Closed in Red

Figure 4.9: Models of a Grid with Extra Array of Active Relays around the Wafer

This R network has one disadvantage and that is that it cannot be used with the chosen relay concept. This is because in the resistor network only pilot points are used to provide a pressure to open the valve. It closes when the wafer has passed and the high pressure disappears. The chosen relay concept needs another nozzle back pressure to close the valve.

However with different concepts like the one described in section 6.4.3 a system can be made that would work. This is beyond the scope of this research though.

5

Analysis of Concept and Prototype Design

In this chapter the chosen concept is analysed using different COMSOL models. First a simplified membrane is modelled of a disc, curved in a single direction. Subsequently, this model is expanded using the concepts waved membrane geometry. Because the results were unsatisfactory, an alternative concept is proposed that mimics the original function.

5.1 Simplified Model of Single-Curve Membrane

The snap acting relay concept (fig. 5.1) that was chosen in chapter 3, is simulated in a model to get a feel of how the dimensions affect behaviour of the concept. In this model the air flowing through the channels is not included. It is quite difficult and time consuming to model the fluid flow and the bi-stable membrane mechanics. Section 3.4 has shown that any desired back pressure can be obtained, so the focus lies on investigating the membrane snap acting ability.

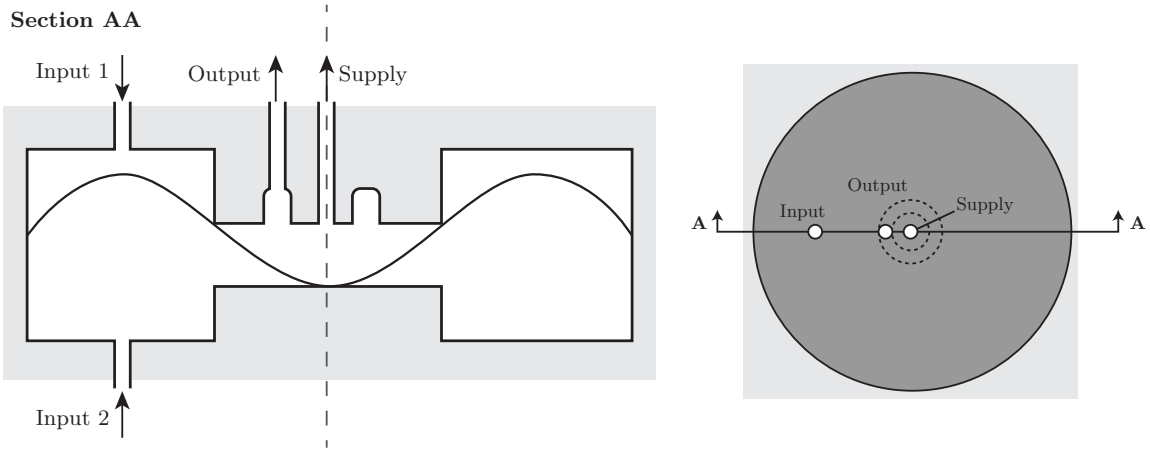

Figure 5.1: Snap Acting Relay with an Extra Input, in open Position

There are relevant examples provided by COMSOL called the *Scordelis-Lo Roof Shell Benchmark* and the *Postbuckling Analysis of a Hinged Cylindrical Shell*. In the first example a roof is modelled as a bent plate. The outer edge is free and the curved edge is constrained in y and z translations. Here the edge will deform and the middle of the roof will mostly stay at the same position.

The second example takes a slightly curved plate and puts a load at the middle of the plate. This plate will then deform and buckle at a certain point. Because of a snap-back effect at the moment of buckling, the displacement cannot be increased to see what the corresponding

force will be. An increasing parameter has to be used (in this case the average displacement of the whole plate) to make sure an solution follows. This results in a graph that shows the corresponding force to the displacement of the plate.

Both of these examples do not describe exactly the problem that has to be modelled for the relay. They give however an insight in what physics to use and how such a problem can be tackled. The basic concept for the model is described here below. The geometry, material and boundary conditions are explained. Next the implementation in COMSOL is discussed and then the results and conclusions are reported.

5.1.1 Model Approach

A pressure distribution load is applied on the membrane to represent an air pressure difference on two sides of the membrane. A shell module is used in COMSOL to represent the thin membrane as the thickness is an order two smaller than the other two dimensions.

Geometry and Boundary Conditions

A number of boundary conditions are used to define and limit the simulation. The boundary conditions that are needed to model the system, are listed below and shown in fig. 5.2.

1. **Pinned** The membrane has to be deformed by the difference in air pressure between the two sides of the chamber. The connection of the membrane and wall is represented by a fixed constraint. These two sides cannot move or deform because of these constraints.

2. **Symmetry** axis. The diaphragm is sometimes modelled by using only a quarter of the whole membrane. A symmetry constraint is then used on the edges of the quarter model. This applies reaction terms symmetrically to the dependent variables in the model. In this case displacements.

3. **Face Load** The air at both sides of the membrane have a pressure difference. This is realised by a face load on the membrane, which is a pressure distribution on the top surface of the membrane.

In fig. 5.2, the locations of the different boundary conditions are illustrated.

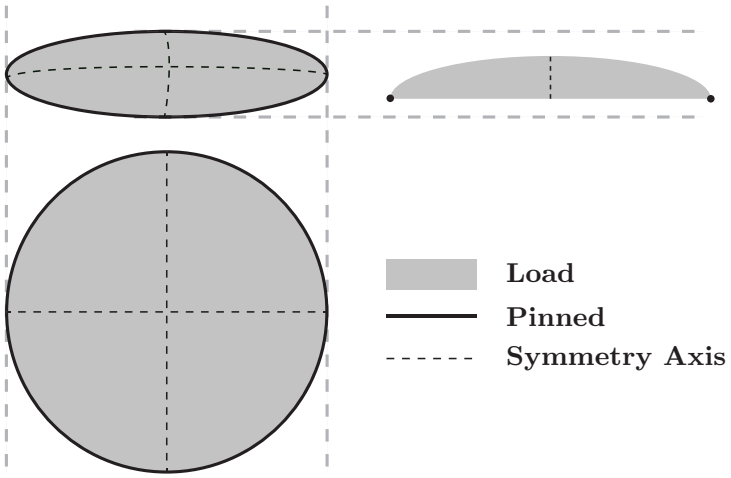

Figure 5.2: The Boundary conditions locations on the geometries

In the table below the dimensions are given of these geometries. These geometries are chosen to make them as small as possible while retaining a simple fabrication process and function accordingly.

Table 5.1: Dimensions of the Model

Symbol	Parameter	Value
R	Radius	10 mm
H	Curvature	2 mm
t	Thickness	0.2 mm

Material

Different kind of materials can be used to manufacture the membrane. Springsteel and PET are considered. In table 5.2 the relevant material properties are given.

Table 5.2: Material Properties used in modelling

	Parameter	Value	Unit
Spring Steel			
	Density	7600	$\mathrm{kg\,m^{-3}}$
	Young's Modulus	210	GPa
	Shear modulus	81.5	GPa
PET-G			
	Density	1270	$\mathrm{kg\,m^{-3}}$
	Young's Modulus	2.2	GPa
	Poisson's ratio	0.2	-

5.1.2 Results and Discussion

The results of the PET model are shown in the graphs below (fig. 5.3). In the left figure a section view of the membrane is illustrated for different applied pressures. There it clear that the membrane snaps at a certain pressure and does adopt the inverse shape.

In the right graph the absolute displacement of the middle point of the membrane is plotted against the applied pressure. The large step is the snapping occurring at a pressure of 0.81 bar above atmosphere.

A similar simulation is performed where steel is used as the membrane material. This showed a similar snapping behaviour, with a snap-pressure of 2.59 bar for a thickness of 0.1 mm and a curve height of 1 mm.

These initial result gives the impression that a single curve membrane does indeed act as suspected. This model is now extended to investigate the concepts waved membrane.

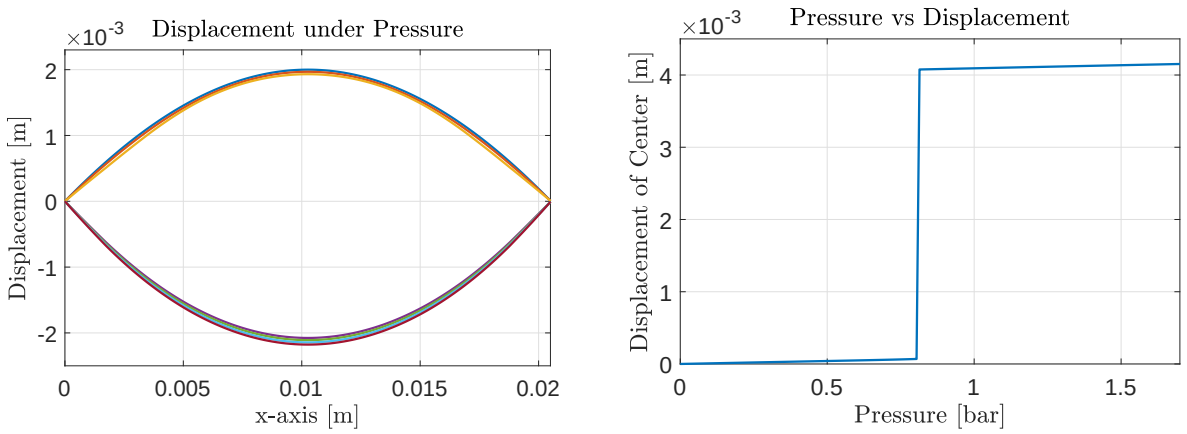

Figure 5.3: Simulation Results of Snapping PET Disc

5.2 Final Model of Membrane Concept

To simulate the concept found in the patent the following model is made. It has a different geometry and to model this some extra steps are made to solve this, compared to the previous models.

5.2.1 Geometry

In figure 5.4, the geometry of the final model is shown with a top view and a side view. This geometry compared to the simpler model, has an extra ring with a curve in the opposite direction compared to the centre disc. From here on out these two sections of the geometry will be called the inner disc and outer ring.

The equation of the curve is listed below. To get a continuous curve a 4th order polynomial is used. Four points are specified where the curve goes through x-axis. This two dimensional curve is revolved around the z-axis to form a disc.

$$z = (x^2 - Ri^2)(x^2 - Ro^2)\frac{H}{Ri^2 Ro^2} \tag{5.1}$$

Here R_i stands for the radius of the inner disc and R_o stands for the radius of the outer disc. H is the height of the centre point.

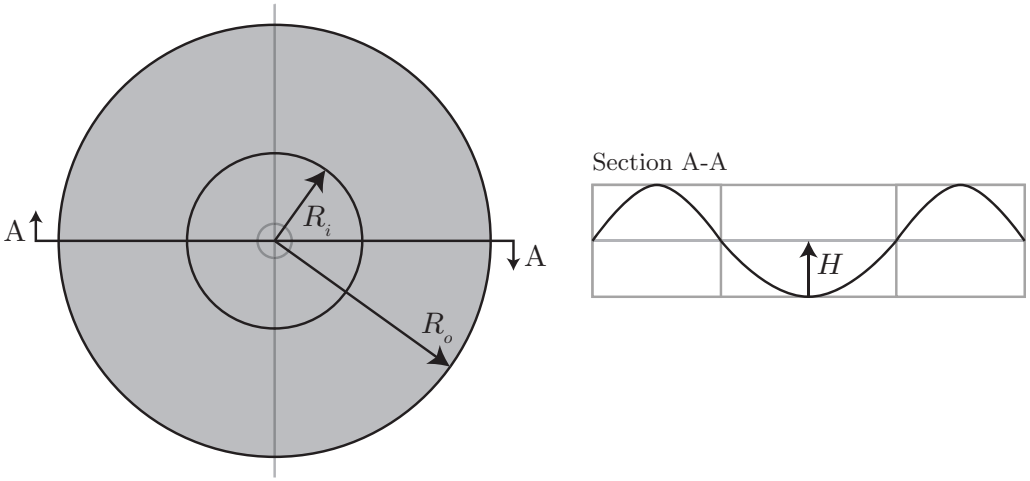

Figure 5.4: Geometry

Parabolic factor

Because the 4th order polynomial gives a somewhat peculiar curve an attempt is made to fit it to a more desirable form. This is done by multiplying the geometry with an parabolic form. In this way the middle portion can be increased by a larger factor than the outside of the geometry. In the figure below (fig. 5.5) it is illustrated how this parabolic factor changes the geometry. The key is to create a factor-parabola that has values between 1 and 0 for the width of the geometry. On the widest part, the parabola has the lowest height. Thus decreasing the values of the original geometry. The equation of this parabolic factor is described here below:

$$y = \frac{factor - 1}{R_o^2} x^2 + H \tag{5.2}$$

The $factor - 1$ describes the value of the parabola on the edge of the membrane at $x = R_o$ and $y = H$ when the parabola crosses the $y-$axis.

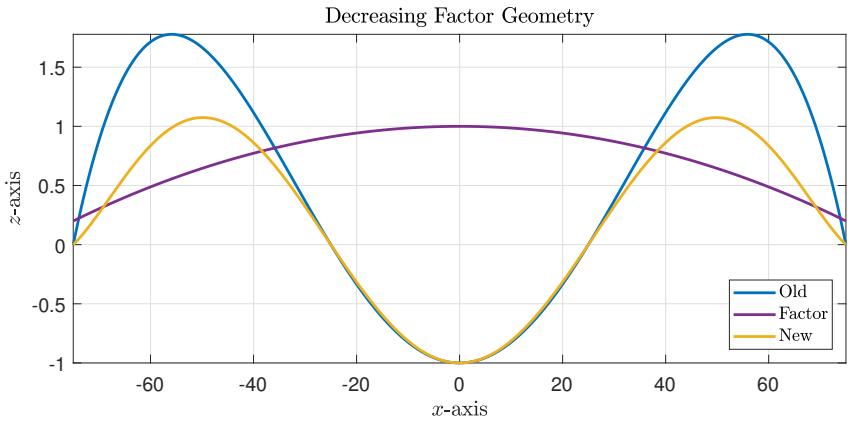

Figure 5.5: Geometry with Parabolic Factor

It is also possible to make a increasing factor in the middle. But the parabola cannot become negative in the window of the geometry. Otherwise the whole geometry will also change its sign.

5.2.2 Boundary Conditions

The boundary conditions are shown in the illustration below (fig. 5.6). The outer boundary is pinned down and can only rotate, not translate. The blue domain will have a prescribed force or displacement on it. And the red boundary is pinned or has a prescribed stiffness. In some simulations it has no condition at all.

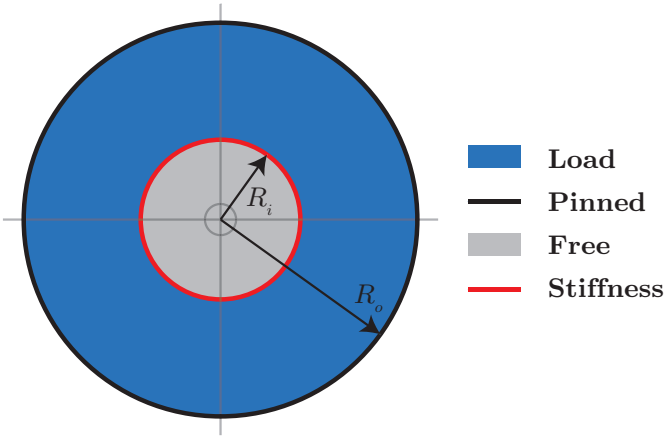

Figure 5.6: Boundary Conditions

5.2.3 Modelling approach

A force prescribed based simulation is performed. This is the same principle used in section 5.1. A parametric sweep is performed to increase the force on the outer ring. The post-snap behaviour will probably not be simulated well. But an indication of the disc characteristics are formed. In the following section the results are discussed of this approach.

5.2.4 Results

The results of the discussed simulations are given here. Different dimensions are used in the simulations to see its effect. This section will not elaborate on all the different cases, but will focus on the general outcomes that different approaches have.

Force prescribed

The boundary between the inner and outer disc can have several conditions. The different options that are applied to this "joint" are: The boundary can be free to move, be pinned down or have a spring joint, where the point can move but it will require a force.

In figure 5.7 the results of a simulation with a free to move boundary is shown. It is clear that this does not work. Instead of snapping the whole membrane just moves downward. This means that at least a boundary condition has to be present.

It should be noted that also the parabolic factor is used to change the geometry a bit. This yields the same results for this simulation.

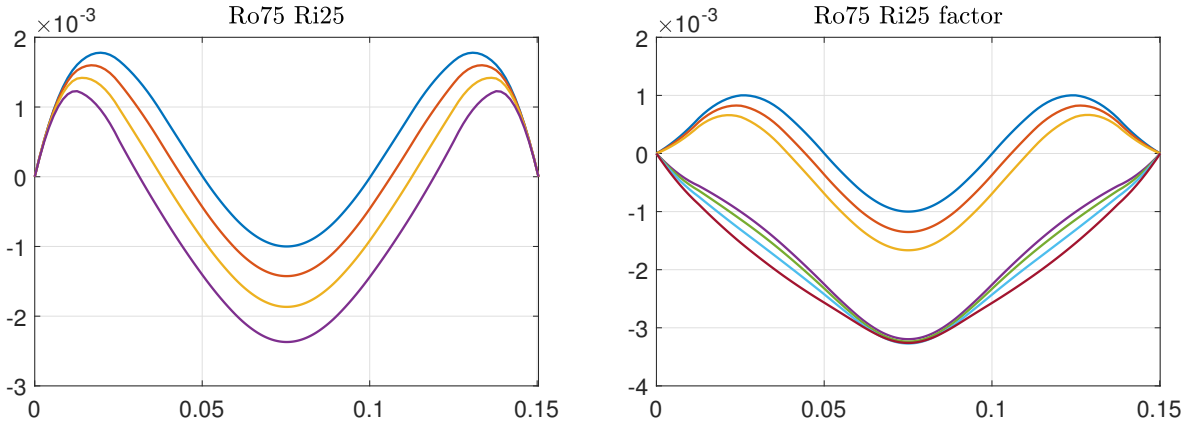

Figure 5.7: Force prescribed, free joint

When the ring between the inner and outer disc has a no displacement condition on it. For an outer radius of 50, 75 and 125 mm the snap in the inner disc does not occur (fig. 5.8). However, for an outer radius of 100 mm it does. Still the simulation seems unstable, as the solvability is dependent on small dimension changes.

All these simulations assume there is no pre-stress at the beginning of the simulation. The fabrications process will probably add pre-stress to the membrane, because a flat material will be deformed in the membrane shape.

If pre-stress is added to the models, the results will differ and the simulation might show a desired snapping behaviour. This is however not researched properly, because the amount of pre-stress added by the production of such snapping discs is not investigated.

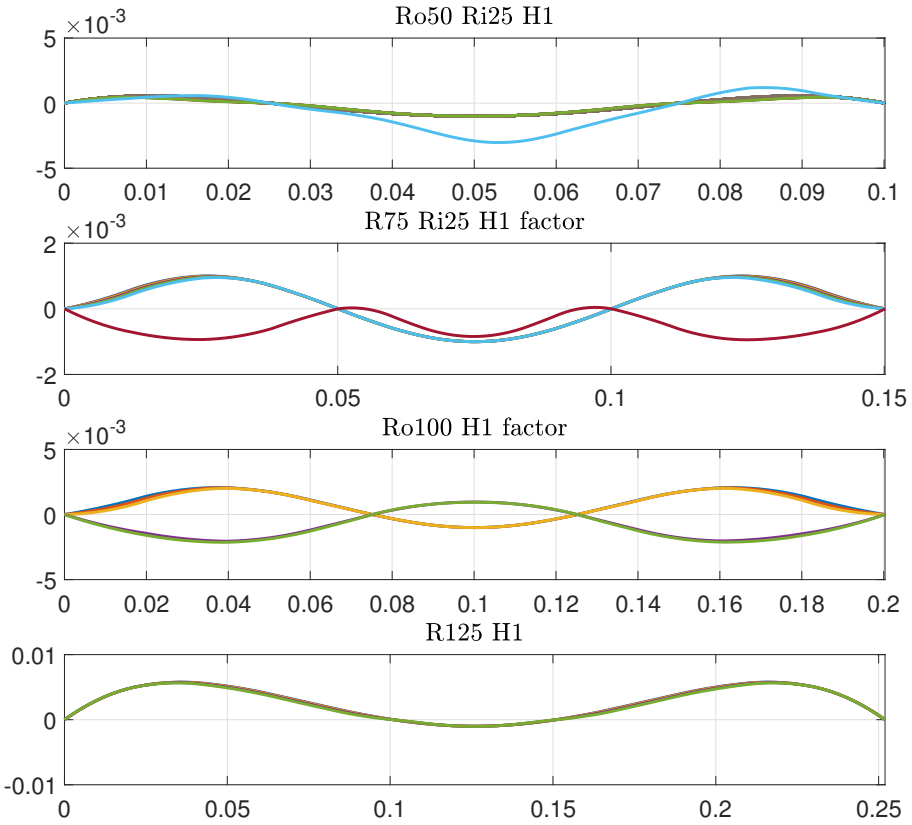

Figure 5.8: Force prescribed, pinned joint

The last contact method that is simulated is the spring imposition. This means the joint can move but it requires a force. Different spring constants are used in the model. The dimensions are changed as well like in the precious simulations. In figure 5.9 some of the results are shown.

If the spring constant is too low the membrane will behave more like a free moving joint. Only the outer ring will snap and the whole membrane will keep moving downward. For a higher stiffness the membrane will snap accordingly.

For a stiffness of 2e6 N/m (a compression of 1 mm for a force of 2000 N) the joint can move somewhat but the membrane still snaps as intended.

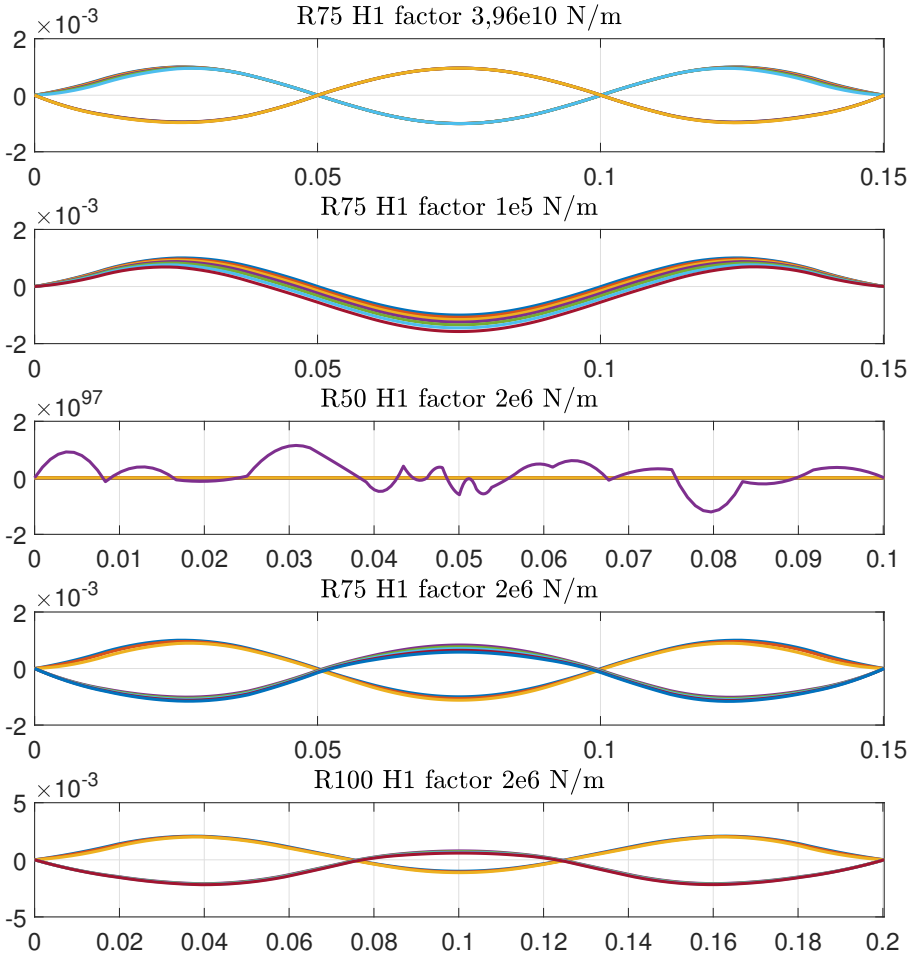

Figure 5.9: Force prescribed, spring joint

5.2.5 Conclusion

As can be seen by the previous models it is not trivial to arrive at a membrane that snaps like it is intended. Some of the models give a result while others do not, even though the differences in design are quite small.

These results evoke doubt about the implementation of this design in real life. The next step is to make a demonstrator to see how easy or difficult the fabrication of such a valve is.

It appears the successful functioning of such a membrane can be quit difficult. It can therefore be beneficial to start thinking about alternatives. The single curve shell simulations gave functioning results. The next section will focus on the design of a single curve with the same function as the intended double curve shell.

5.3 Alternative Designs using a Single Curve Membrane

In the previous section it was concluded that an double curve membrane can give difficulties with its snapping behaviour. An alternative solution is investigated using a single curve shell, because the use of a single curve shell looks more promising according to the simulations from section 5.1.

Among other things an idea is searched where a combination of several single curve membranes function as a double curved valve. In figure 5.10 a concept is illustrated that provides

the same function as the original idea.

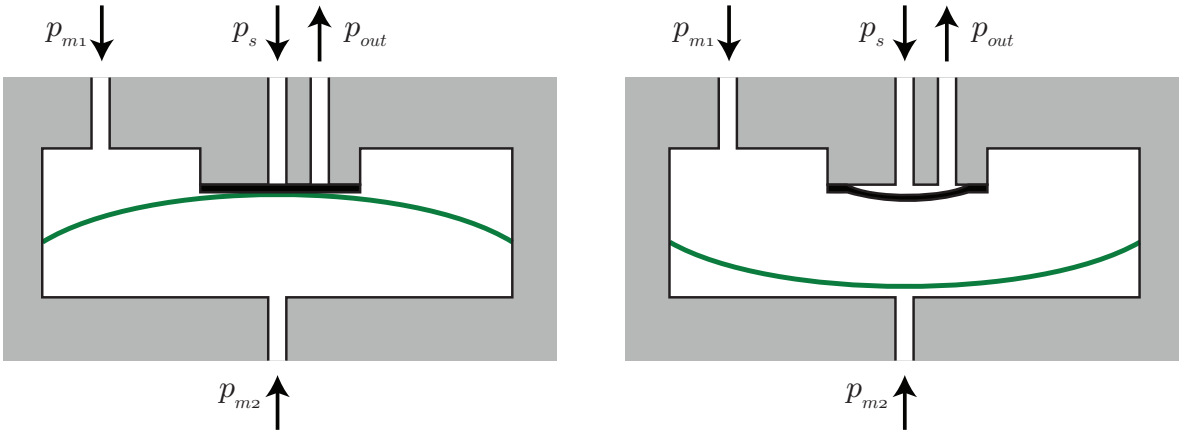

Figure 5.10: Single Membrane Valve in Closed and Open position

The valve has the same number of inlets and outlets. An air supply channel and an outlet that leads to the surface. Along with two measurement pressures that originate from the nozzle wafer system.

Because the supply pressure is generally higher than the two measurement pressures, a seal is placed between the upper chamber and the supply and outlet channels. In the open position of the valve this prevents the upper chamber being pressurized to the supply pressure. Otherwise the lower chamber would be unable to close with p_{m2}.

The seal also has a smaller circumference than the membrane so the force that is generated in the seal curve can be less than the force generated by the membrane and p_{m2}.

5.3.1 Seal Model

A simple seal model is made using the same PET membrane that was modelled in section 5.1. Now only a pressure is applied to the centre of the membrane. This represents the valve in a closed position, where the membrane pushes against the flexible seal. With the use of COMSOL it is investigated how much the membrane would deform under only a supply pressure under the seal.

A uniform pressure is applied on a circular area with a diameter of 4 mm. This area is placed at the centre of the membrane. It is assumed that the seal is made of a material that is flexible enough to shape itself around the shape of the diaphragm. Thus, establishing contact with the membrane over the circular area where pressure is applied.

In figure 5.11.a the stress distribution is seen on the membrane when a pressure of 1 bar is applied to the centre ring. Next to it the displacement of the centre is plotted against the applied pressure (fig. 5.11.b).

As expected the centre displaces as the supply pressure rises. If the membrane is placed closer to the seal at manufacturing, pushing the membrane against the seal. It will be able to keep the relay closed for a higher supply pressure, due to the pre-stress introduced by the placement.

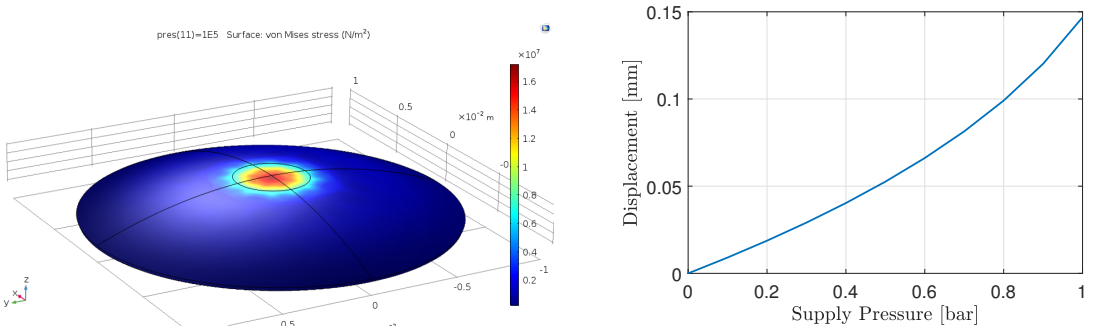

(a) Plot of Von Mises Stress at applied Pressure of 1 bar

(b) Displacement of Centre versus Applied Supply Pressure

Figure 5.11: Results of Parametric Sweep of Pressure on Centre of Membrane

6

Prototype Fabrication and Testing

In this chapter the proposed snap acting relay design is fabricated and tested. First the fabrication method is briefly explained. How the membrane is manufactured along with the housing and which materials could be used.

As the creation of reliable membranes proved difficult, the use and failing of membranes is investigated further. Next the prototype relay is introduced. It is supplied with pressurized air in a test setup and the results are discussed

Lastly an alternative design is introduced using an elastic membrane where different size surfaces are used to use smaller pressures to close off air channels with a higher pressure.

6.1 Fabrication and Materials

In this section different possibilities for the fabrication and materials are investigated for the prototype. First the manifold is examined. After that the options for the membrane materials and seal are discussed. The requirements for the materials and method in short are:

1. Non-leaking.
2. Simple to fabricate a prototype, in 1 week time.
3. The materials should be readily available for purchase or in stock.
4. The cost should not be above the range of hundreds of Euro's.

In Appendix D the methods used and tried out are described in more detail.

6.1.1 Manifold

In the research of E. Vagher [27], several small air conveyor prototypes, the same requirements were important for his design. Several methods are described, where the most successful method, is composing a design in layers. Next they are laser-cut out of perspex (PMMA) slabs and glued together using an adhesive transfer tape. An advantage of this method is that a type of glue is used that can also attach metal layers.

An other method is to make the manifold out of metal and assemble the different parts with bolts and screws. This is probably more time consuming as metal is harder and more difficult to work with. As more than one prototype is needed, the quicker method of gluing and laser-cutting perspex is chosen. In appendix D.1 a more detailed explanation about how to assemble such a manifold along with failed attempts.

6.1.2 Membrane

The required membrane can be made form different materials. A thin metal plate or plastic sheets are considered. To create the right curvature, several methods have been explored. The custom vacuum form technique is chosen as the main method because it works easy efficient and quick. In appendix D.2 all the investigated methods to create a membrane are described in more detail.

The working principle is as follows. Clamp a sheet of plastic above a closed crevice that is linked to a vacuum source. In this chamber a mould with the desired curvature is placed. Heat the plastic with for instance a heat gun until it becomes soft (hangs down). Then open the channel to the vacuum source. Let the membrane cool and the shape will remain in the plastic.

Using this method a number of spheres are formed in a PVC sheet with a thickness of 0.3 mm.
Initial tests are performed using a spring-steel membrane along with several vacuum formed PVC membranes placed in a manifold. and pressurized. The diameter of each PVC membrane is 20 mm and has a thickness of 0.3 mm. the spring-steel curve created with a dapping punch set has a thickness of is 0.1 mm and a diameter of 10 mm.

It is observed that the steel membrane did not flip as expected. The PVC membranes did flip when the maximum curve height is larger than 0.75 mm (table 6.1). Also the pressure to switch the membrane back to its original position is less. This suggest that the vacuum-formed process plastic foil can create the curved membranes.

Table 6.1: Initial Test Results of PVC Membranes Switching Behaviour

Sphere	Switching P	Switch back P	Model P_{switch}
H = 0.75	0.35 bar	0.2 bar	0.303 ba
H = 1.25	0.80 bar	0.25 bar	0.954 bar
H = 2	0.80 bar	0.55 bar	2.31 bar

Heating PVC can be dangerous because chloride fumes can be formed. Therefore a different plastic is chosen to manufacture for the later designs. The following readily available plastic sheets have been found: polycarbonate (PC), PolyPropyleen (PP) and (PET-G). Because of its widespread use in food industry as a flexible non-leaking container and it can be manufactured and shaped with more techniques than PP, PET-G is chosen. Also the Young's Modulus of these plastics lie in the same order of magnitude. This material property along with the membrane curvature are largely responsible for its behaviour.

6.1.3 Seal

To separate the supply and outlet channel from the upper membrane chamber a seal is necessary. This is achieved by placing a flexible rubber plate against the two channels. To keep this plate in place a layer of the manifold is pressed against it to function as a flange. In the figure below an exploded view of these parts are illustrated (fig. 6.1).

The membrane has to push against the seal through the opening in the flange. A thin layer of 0.5 mm thick is used because otherwise the membrane would not reach the seal. The flange is made from a steel plate instead of PMMA, because the available minimum thickness of PMMA is 2 mm.

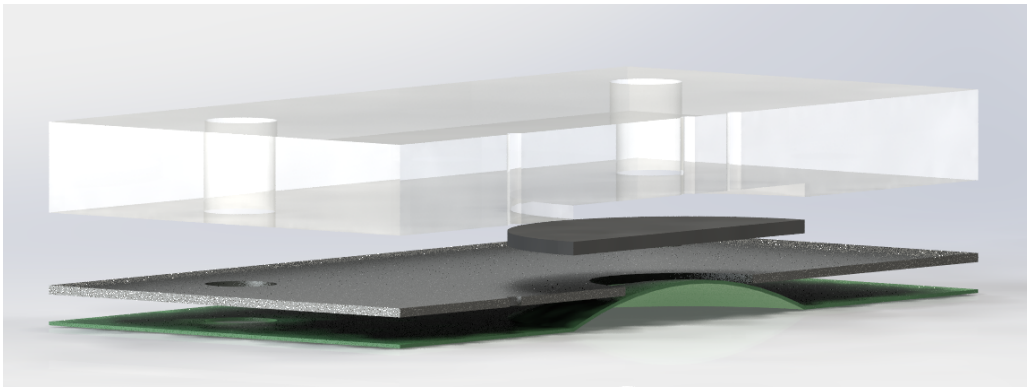

Figure 6.1: Exploded view of Flange Layer, Rubber Seal and Green Membrane

The seal is tested and failed at 5.56 bar. The rubber seal has a small tear near the middle of the seal. The seal does not leak air at lower pressures.

It is not expected that a supply pressure near 5.56 bar is needed, because the membrane will not be able to close off a supply pressure that high. To investigate what the characteristics are of manufactured membranes some tests are performed in the next section.

6.2 Membrane Failure Examination

To examine membrane behaviour more thoroughly, different shapes and sizes are made and tested. Using PET sheets of 200 and 300 µm thick membranes are manufactured with a diameter of 20mm. Curvatures with a maximum height of 2 and 3 mm are made.

These membranes are placed and bolted in a manifold, so it can be reused for each test. The pressure is slowly increased inside the chamber to flip the membrane. At the same time a camera is pointed at the membrane to examine the snap through. This process is repeated for 10 times flipping both ways.

6.2.1 Results

During the tests a few things are noteworthy. In figure 6.2 the starting position for each test is shown. Ideally this shape is similar in its flipped position. This is only observed in the membrane with a H = 2 mm and a thickness of 200 µm.

All the other membranes showed a inverse shape that had folded lines in its surface (fig. 6.3). The points where these lines meet are still visible when the membrane snaps back to its original shape (This was difficult to see on the photos, therefore the observations are described.).

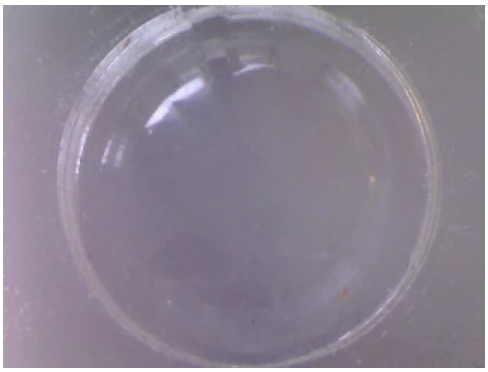

Figure 6.2: Starting Position of Membrane Snap Experiment

The membrane with the largest thickness and curvature (fig. 6.3) failed when pressurized. This happened twice in a similar manner. When closely examined there two pieces are completely blown off. There are cracks that run in radial and tangential direction.

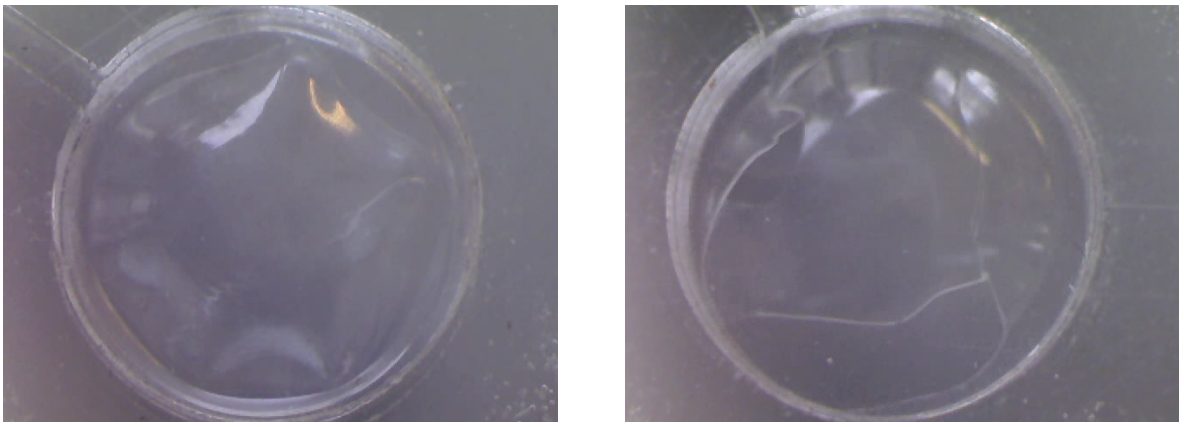

Figure 6.3: Switching Pressures for Different Memebranes with the Dashed Line the Calculated Switching Pressure

In table 6.2 the switching pressures are compared with calculated values from the COMSOL model. The simulated membranes generally have a higher switching pressure than measured of about 20 %. Also the pressure needed to snap the curve back from its flipped to the starting position is lower than the initial snap. This is about 16 % lower than the initial snap for the first two membranes, but for the third the difference goes to 35%.

Table 6.2: Overview of the Calculated and Measured Switching Pressures

Curve Height [mm]	Thickness [µm]	Model [bar]	Measurement [bar]	Inv Measurement [bar]
2.0	200	1.81	1.45 ± 0.01	1.18 ± 0.03
2.5	200	2.18	1.55 ± 0.03	1.33 ± 0.02
2.0	300	2.78	2.26 ± 0.12	1.48 ± 0.04
2.5	300	3.61	3.11	-

When the all the measured flipping attempts of the working membranes are plotted, it is seen that the switching pressures decrease after the number of attempts for the starting displacement (fig. 6.4). After three tries this pressure stabilises for the 200 µm sheets. For the thicker sheet this downward trend is present in all attempts. This suggest that the award shape to which the membrane flips, effects its performance.

Looking at the inverse switching pressures an upward slope is noticed. This means that the band between flipping in both directions becomes smaller after more use.

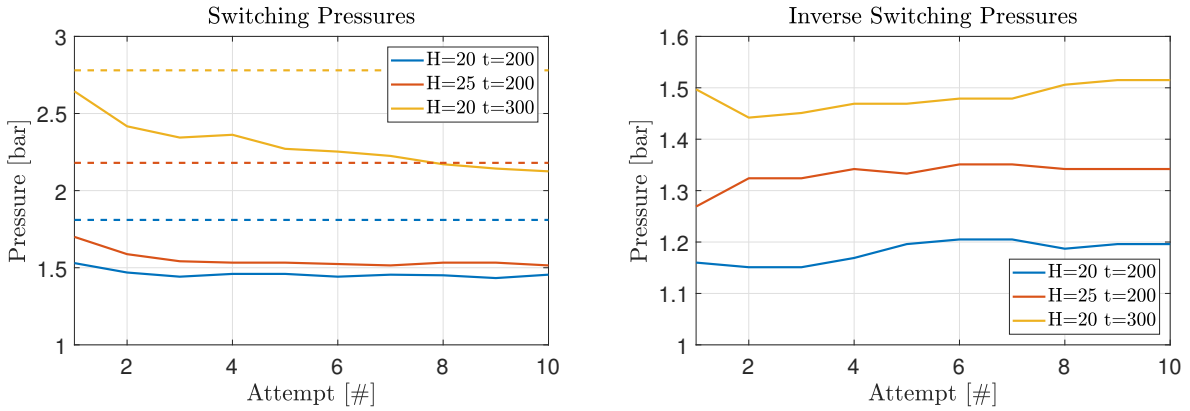

Figure 6.4: Switching Pressures for Different Membranes with the Dashed Line as Calculated Switching Pressure

In the COMSOL model the thinning of the plastic sheet due expansion is not taken into account. Therefore as a quick improvement the thickness of each membrane is measured with a micrometer and changed in the model. In table 6.3 the measurement show indeed a decrease in thickness and simulated switching pressure.

However, this does not consider the difference in flipping pressures for different directions. This could be dealt with by simulating the manufacturing process. So heating a membrane and deforming it in a curved position and cooling it back to room temperature. The stresses resulting from this model can then be implemented in the current model as pre-stress. This modelling step exceeds the scope of this thesis and is left for further research.

Table 6.3: Overview of the Corrected Thickness Calculated and Measured Switching Pressures

Curve Height [mm]	t [µm]	Measured t [µm]	Model [bar]	Measurement [bar]
2.0	200	190	1.73	1.45 ± 0.01
2.5	200	180	1.96	1.55 ± 0.03
2.0	300	280	2.55	2.26 ± 0.12
2.5	300	270	3.12	-

6.3 Prototype

To prove the relay concept introduced in section 5.3, a prototype is developed. In this section the prototype is briefly described along with some design choises.

Because it proved difficult to predict the characteristics of a manufactured plastic membrane, a membrane that is already tested is chosen. A 200 µm PET-G with a maximum curve height of 2 mm displayed the most consistent switching pressures, as well as a flipped shape that resembled the starting position.

In figure 6.5 a section view of a CAD drawing is illustrated along with annotations of some parts. In appendix E the prototype along with its dimensions is illustrated in more detail.

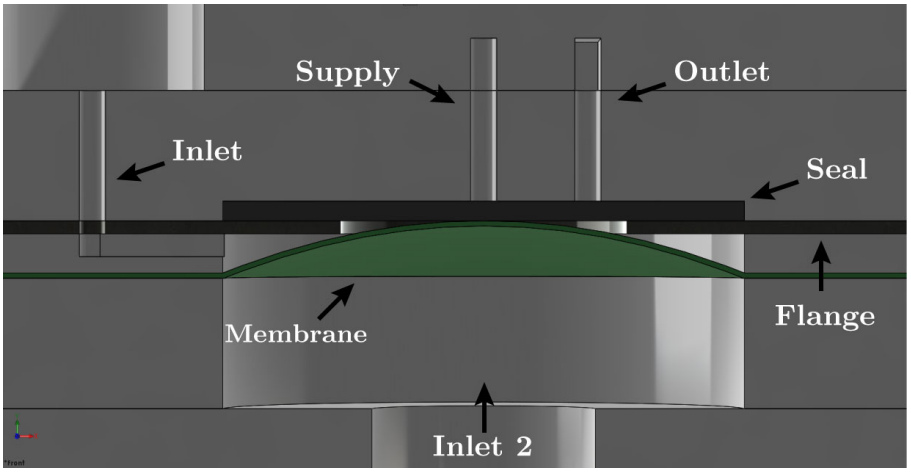

Figure 6.5: CAD Drawing of Prototype

6.4 Prototype Static Test

In this section the working principle of the prototype is investigated. Applying increasing pressures at the inputs it is tested when the prototype switches to the different states, earlier described in section 4.1.

In short the different states how the relay is intended to be used are:

State 1. No inputs and valve stays closed.

State 2. Input 1 becomes high and the valve opens.

State 3. Input 1 and 2 high and valve stays open.

State 4. Input 1 becomes low and valve closes.

In the experiments input pressures are slowly increased by a hand operated pressure regulator. With a digital pressure sensor and a DAQ system the pressures are measured.

6.4.1 Results

In table 6.4 the results of the tests are listed. In the first State test it is found that the valve begins to leak from the supply to outlet channel at 1.72 bar. This is because the supply pressure will press the seal and membrane enough to form a channel to the outlet.

For the remaining states a supply pressure just below this leaking occurs is used.

Table 6.4: Overview of the Corrected Thickness Calculated and Measured Switching Pressures

State [-]	p_{m1} [bar]	p_{m2} [bar]	p_s [bar]	Output
State 1	-	-	1.70	off
State 2	1.47	-	1.70	on
State 3	1.47	1.47	1.70	on
State 4	-	1.47	1.70	off

State 3 is tested with a the same high pressure on the input and output, to see if the valve still stays open. This is the case for a pressure of 1.47 bar. This means that the same nozzle back

pressures can be used for opening and closing.

Because the snapping behaviour of the valve is not identical in both directions, the pressure of the second input p_{m2} can be lower than that of p_{m1}. The membrane snaps back at a minimum pressure of 1.18 bar. With this lower pressure the valve still functions.

6.4.2 Discussion

The initial switching pressure is 13.5 % lower than the absolute supply pressure it switches. This proves the concept that a pneumatic relay with a snap acting membrane can work where a higher supply channel can shut on or off depending on a lower input pressure.

To reach a higher pressure difference more of these relays can be joined together. Each relay increasing the pressure incrementally.

6.4.3 Alternative Rubber Design

The tests proved that the prototype functions as was originally intended
. However, the manufacture of membranes turned out to be more difficult than expected. This concludes the first iteration of the design process. As a proposal for the next step an alternative concept is introduced in this section. It has a similar function, only with this concept a single curve plastic membrane is avoided. Instead the use of a rubber membrane is proposed.

In figure 6.6 a concept is illustrated using such a rubber membrane. The neutral position is shown in this image, which means that all the pressures are set at the same level. The principle behind this, is that no longer a membrane will have to snap. It provides a stiffness by having a difference in chamber pressures.

At the supply and outlet channels a rubber seal membrane is placed so the upper chamber will only depend on the measured signal (p_m). This seal can be attached by glue or a type of clamping mechanism that was used in the prototype.

The rubber membrane consist of two thin rubber sheets. In between a rigid part, which has the same size as the seal, is glued in the centre. This is to provide enough stiffness to close the supply off, as this has a larger pressure than the lower chamber pressure. If this rigid component is excluded the working area of p_m would be the same size as the seal. And thus the path to the output would remain open as the supply pressure is the systems largest.

The lower chamber will be pressurized by connecting it to an outside pressure source (p_b). This value does not change for the different states of the valve or the position of the wafer floating on top. Thus it functions as a sort of spring element.

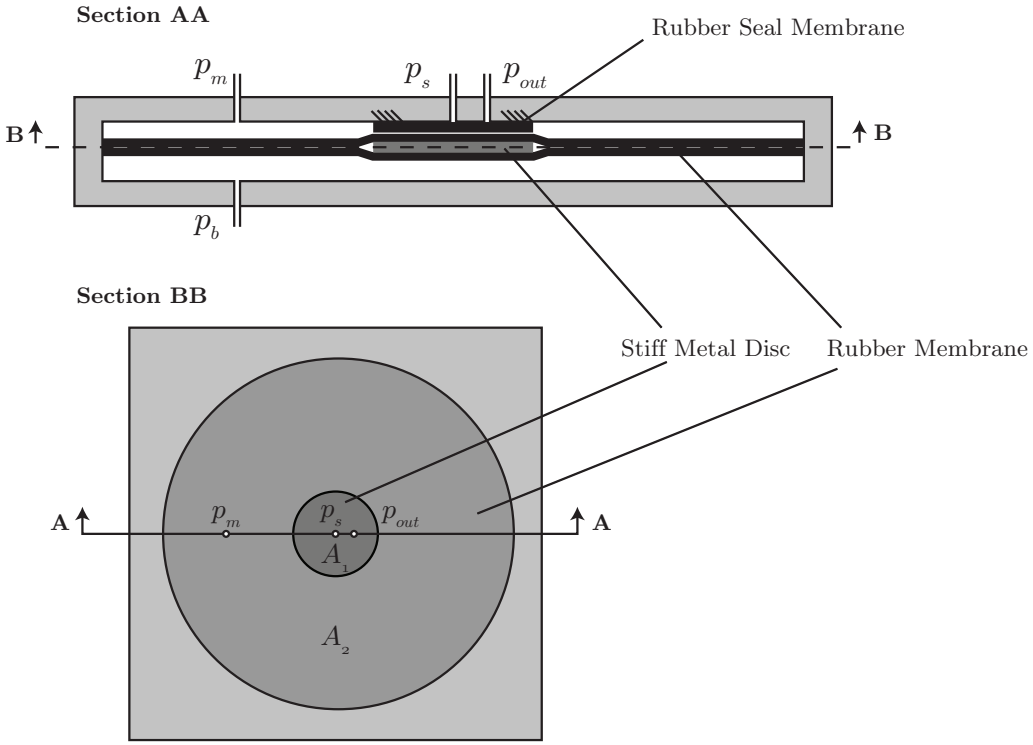

Figure 6.6: Two Section Views of a Rubber Alternative Concept

This concept uses different areas for pressures chambers, and thus a larger force can be generated by a smaller pressure exciting a larger area. The seal area is denoted by A_1 and the area of the outer rubber ring by A_2 (eq. (6.1)).

The closed and open positions are illustrated here below (fig. 6.7). For the valve to close the force generated by the total area and the lower chamber pressure must be higher than the force generated in the seal and upper chamber (eq. (6.2)). p_m is equal to atmospheric pressure in this case.

$$A = A_1 + A_2 \tag{6.1}$$

$$A \cdot p_b > A_1 \cdot p_s + A_2 \cdot p_{atm} \tag{6.2}$$

To open the valve the nozzle back pressure increases and the force above will be larger than the force generated on the bottom of the membrane (eq. (6.3)).

$$A \cdot p_b < A_1 \cdot p_s + A_2 \cdot p_m \tag{6.3}$$

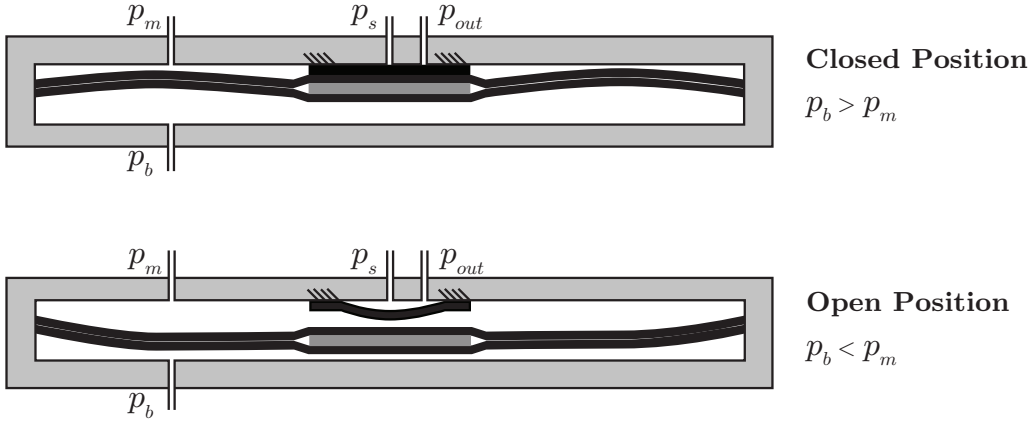

Figure 6.7: Closed and Open Position of the Alternative Concept

An open position where the rubber membrane still touches the rubber seal can be operational. As long as the seal displaces enough to form a channel to the output. This means that the pure open and closed operation of the original snap concept valve is not exactly mimicked, as the restriction changes depending on how much the seal has displaced.

This effect could be minimized by making the gap under the seal between the supply and output channel as small as possible, or reducing the restriction by rounding the edges. An example is shown in figure 6.8).

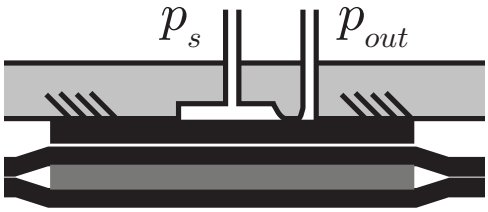

Figure 6.8: Closed and Open Position of the Alternative Concept

7

Conclusions and Recommendations

After investigating the development of an pneumatic relay for a nozzle-wafer system to implement in a floating wafer design, the following conclusions and recommendations can be made.

7.1 Conclusions

1. It is found by simulation that a desired nozzle back pressure can be achieved by setting the appropriate nozzle diameter and supply pressure. Also nozzle-flapper systems have been around and used for a long time. Therefore it is concluded that a nozzle-wafer design can provide any necessary pressure to switch a pneumatic relay. However, at higher pressures the fly-height will be influenced by the nozzles. Therefore it is desired for the relay to have an minimal switching pressure.

2. The way in which the nozzles and pneumatic relays can be arranged in a grid of an conveyor is examined. In this research a black box is used for the valve, in order for multiple relay concepts to be applicable. With the current function two inputs are needed to fully operate the relay. It is possible to make a grid where substrates move in one direction and an extra array of outlets are active around it to make a smoother air film. No arrangement is found that can be used in different directions without leaving a single relay open when the substrate has passed.

3. A pneumatic relay concept is investigated where a curved membrane snaps to its inverse shape to open or close a channel. The original concept with a circular waved membrane is simulated using a force prescribed method. The results from these models are not consistent. Most of the time these numerical models do not converge. If they do come to a solution the shape of the snapped membrane would not always be its inverse. Therefore this concepts is discarded and an alternative is sought out.

4. A design using a circular single curved membrane is introduced. The models are consistent in converging to a solution of its snapping behaviour.

5. Plastic membranes are created with a vacuum form method. Initial testing of these membranes showed unexpected behaviour (flipping in other shapes and breaking). Also the switching pressure to snap back to the initial shape is considerable lower. This can be attributed to the manufacturing method where pre-stress are introduced as the membrane is curved in one direction.

6. A prototype is built using the only properly functioning snapping membrane that was constructed. In a static experiment it proved that the relay functions as is intended.

However it is not dynamically tested so nothing can be said about the switching bandwidth or the longevity of the membrane. Because of the behaviour of the previously tested membranes it is taken into account that this prototype might not have a lifespan higher than switching a hundreds of times.

7.2 Recommendations

It is not possible to investigate everything without unlimited time and effort. The following suggestions are made to further investigate in future projects:

1. **Investigate the Alternative Rubber Design** The concept of the relay is proven in the experiments. An alternative rubber design is introduced as an improvement (section 6.4.3). This rubber concept works with different areas and pressures to open and close a channel. It no longer uses a snapping membrane and thus will probably be more reliable. In combination with the following point it would be a promising concept for a second iteration of the design process.

2. **Research Resistance Network** The resistor network that is considered in the section 4.4 shows potential for working with single input functioning relays (for instance the proposed rubber alternative design). Further development of a network combined with such a relay can lead to an omnidirectional working floating air film conveyor.

3. **Demonstrator Nozzle-Wafer Conveyor** Create a nozzle-wafer demonstrator along with a multiple pneumatic relays. As a proof of concept for the whole system integrated in a conveyor type configuration.

4. **Elaborate on Model** Expand the membrane simulation by taking the manufacturing process into account. Include an initial step where a flat sheet of plastic is heated and deformed in the desired curvature. This will result in stresses in the membrane. Use these as pre-stress in the original model.

5. **Dynamic Experiment** Dynamically test a snapping pneumatic valve to see what its bandwidth and reliability is after extended use.

Bibliography

[1] A. Alvarez Aguirre, "Overview of commercial valves."

[2] J. Wesselingh, *Contactless Positioning using an Active Air Film*. PhD thesis, Delft University of Technology, 2011.

[3] R. van Ostayen, "Apparatus for carrying and transporting a product," Mar. 6 2008. WO Patent App. PCT/NL2007/050,424.

[4] P. Vuong, *Air-based contactless actuation system for thin substrates: The concept of using a controlled deformable surface*. PhD thesis, Delft University of Technology, 2016.

[5] K. Ogata, *Modern Control Engineering*. One Lake Street, Upper Saddle Riber, New Jersey, USA: Prentice Hall, 5th ed., 2010.

[6] A. Dunning, N. Tolou, and J. Herder, "Review article: Inventory of platforms towards the design of a statically balanced six degrees of freedom compliant precision stage," *Mechanical Sciences*, 2011.

[7] H. Murrenhoff, "Trends in valve development," *Olhydraulik und Pneumatik*, vol. 47, no. 4, pp. 226–241, 2003.

[8] J. E. Lindler and E. H. Anderson, "Piezoelectric direct drive servovalve," vol. 4698, pp. 488–496, 2002.

[9] E. Purwanto and S. Toyama, "Development of an ultrasonic motor as a fine-orienting stage," *Robotics and Automation, IEEE Transactions on*, vol. 17, pp. 464–471, Aug 2001.

[10] B. Gang, C. Tinghai, H. Yao, G. Xiangdong, and H. Gao, "A nozzle flapper electro-pneumatic proportional pressure valve driven by piezoelectric motor," School of Mechatronics engineering, Harbin Institute of Technology, Researchgate, 2011.

[11] M. Avram, C. Bucsan, D. Duminica, L. Bogatu, and A. Spanu, "Pneumatic proportional valve with piezoelectric actuator," in *Annals of DAAAM and Proceedings of the International DAAAM Symposium*, pp. 971–972.

[12] R. Le Letty, N. Lhermet, G. Patient, F. Claeyssen, and M. Lang, "Valves based on amplified piezoelectric actuators," in *NanoTech 2002 - "At the Edge of Revolution"*.

[13] M. Groen, D. Brouwer, R. Wiegerink, and J. Lötters, "Design considerations for a micromachined proportional control valve," *Micromachines*, 2012.

[14] M. Groen, K. Wu, R. Brookhuis, M. van Houwelingen, D. Brouwer, J. Lötters, and R. Wiegerink, "A piezoelectric micro control valve with integrated capacitive sensing for ambulant blood pressure waveform monitoring," *Journal of Micromechanics and Microengineering*, 2014.

[15] D. Irimia, D. Dobrikov, R. Kortekaas, H. Voet, D. Van Den Ende, W. Groen, and M. Janssen, "A short pulse (7 μs fwhm) and high repetition rate (dc-5khz) cantilever piezo-valve for pulsed atomic and molecular beams," *Review of Scientific Instruments*, vol. 80, no. 11, 2009.

[16] A. Allen *et al.*, "Pneumatic relay," Oct. 1 1963. US Patent 3,105,508.

[17] R. W. Haines and D. C. Hittle, *Control systems for heating, ventilating, and air conditioning.* Springer Science & Business Media, 2006.

[18] S. Besch, T. Suchyna, and F. Sachs, "High-speed pressure clamp," *Pflugers Archiv European Journal of Physiology*, vol. 445, no. 1, pp. 161–166, 2002.

[19] J. Phillips, "Snap acting pneumatic diverting relay," Nov. 21 1967. US Patent 3,353,559.

[20] K. G. Kreuter and K. P. Mueller, "Pneumatic selector relay," Apr. 12 1966. US Patent 3,245,426.

[21] J. Hogel, "Snap action pneumatic relay," Jan. 2 1973. US Patent 3,707,982.

[22] K. L. Tate, "Switching and timing unit for pneumatic relays," May 4 1948. US Patent 2,441,044.

[23] M. Sorli, G. Figliolini, and S. Pastorelli, "Dynamic model and experimental investigation of a pneumatic proportional pressure valve," *IEEE/ASME Transactions on Mechatronics*, vol. 9, no. 1, pp. 78–86, 2004.

[24] R. Trentini, A. Campos, G. Espindola, and A. Silveira, "Parameter identification of a pneumatic proportional pressure valve," *Journal of the Brazilian Society of Mechanical Sciences and Engineering*, vol. 37, no. 1, pp. 69–77, 2014.

[25] J. Jeon and S. Choi, "Pressure tracking control of vehicle abs using piezo valve modulator," in *Proceedings of SPIE - The International Society for Optical Engineering*, vol. 7977.

[26] J. Mueller, I. Chakraborty, S. Vargo, C. Marrese, V. White, D. Bame, R. Reinicke, and J. Holzinger, "Towards micropropulsion systems on-a-chip: Initial results of component feasibility studies," in *IEEE Aerospace Conference Proceedings*, vol. 4, pp. 149–168.

[27] E. Vagher, "Contactless passive transport of thin solar cells," Master's thesis, Delft University of Technology, 2016.

[28] A. van Beek, *Advanced engineering design - Lifetime performance and reliability.* TU Delft, 2009.

[29] K. Hamrock, *Bearing.* One Lake Street, Upper Saddle Riber, New Jersey, USA: Prentice Hall, 5th ed., 2010.

Appendix A

Table of Commercial Valves [1]

Valve	Brand	Valve type	Pressure range	Flow rate	Dynamics	Operating Voltage	Remarks
LFPA8000120H	The Lee Company	Proportional flow piezo	?	6 [l/min] (used)?	0.5 [ms]	160 [Vdc] (bias) 0-160 [Vdc] (control)	Discontinued product
Piezotronic	Asco	Proportional flow piezo	0-4 [bar]	0.12 [l/min]?	8-15 [ms]	0-40 [Vdc]	
Preciflow	Asco	Proportional flow solenoid	-0.9-6[bar]	1.6 [l/min]?	?[1]	0-14 [Vdc]	
Posiflow	Asco	Proportional flow solenoid	0-8 [bar] 0-2.5 [bar]	0.7 [l/min]? 2.9 [l/min]?	?[1]	0-24 [Vdc]	
VSO Low Flow	Parker	Proportional flow	0-10 [bar]	0-500 [sccm][2]	?	8-24 [Vdc]	
VSO Miniature Proportional	Parker	Proportional flow	1-10 [bar]	0-56 [slpm][3]	?	8-41 [Vdc]	
Lone Wolf	Parker	Proportional flow	0-1.72 [bar]	0-14 [slpm]	?	8-56 [Vdc]	Purportedly highest performance of any NO proportional valve on the market.
MD Pro	Parker	Proportional flow	0-6.89 [bar]	0-56 [slpm]	?	8-29 [Vdc]	
HF Pro	Parker	Proportional flow	0-3.45 [bar]	0-60 [slpm]	?	5-24 [Vdc]	
VSO High Flow	Parker	Proportional flow	0.35-4.14 [bar]	0-240 [slpm]	?	5-25 [Vdc]	
VSO-MI	Parker	Proportional flow	0-10 [bar]	40 [slpm]	?	5.5-29 [Vdc]	
Viva	Viking	Flow control flow	?	?	?	?	Seem to be in research stage
Tecno Easy	Hoerbiger	Proportional 3-way piezo pilot	0-8 [bar]	200 [l/min] (nom) 350 [l/min] (max)	<20 [ms]	24 [Vdc]	Acts as pressure regulator
Tecno Basic	Hoerbiger	Proportional 3-way piezo pilot	0-8 [bar]	200 [l/min] (nom) 350 [l/min] (max)	<7 [ms]	24 [Vdc]	Acts as pressure regulator
Tecno Plus	Hoerbiger	Proportional 3-way piezo pilot	0-10 [bar] 2 [bar] differential?	600 [l/min] (nom) 1600 [l/min] (max)	<10 [ms]	24 [Vdc]	Acts as pressure regulator
PSV	Aalborg	Proportional electromagnetic solenoid	3.45 [bar] (differential)	3.5 – 100 [l/min]	?	0-30 [Vdc]	No mention of dynamic characteristics
VEMR	Festo	Proportional flow control piezo	2 [bar]	17 [l/min]	~1 [ms]?	0-250 [Vdc]	VEMA valve terminal with 8 valves uses 3-way valves Not commercially available?
PPV200M	Cedrat Technologies	Proportional piezo	2 [bar]	250 [sccm]	200 [Hz]	-20-150 [Vdc]	
FQPV	Proportion-Air	Proportional flow	0-10 [bar]	0.47 [l/s]	<10-20 [ms]	10-24 [Vdc]	Used in combination with F-series flow monitor
PV630	AirCom	Proportional flow	4 [bar] (max)	0-7 [l/min]	<50 [ms]	0-40 [Vdc]	
PV202	AirCom	Proportional flow	12 [bar] (max)	0-22 [l/min]	0.1-3 [s]?	24 [Vdc]	
PV-1000/ PV-2000	Horiba	Piezo (proportional?)	300 [kPa] (differential)	25 [l/min]	<0.5 [s]	0-5 [Vdc]	
Advanced Piezo	Marotta	Piezo proportional	>100 [bar]	?	<0.5 [ms]	?	
Solenoid control	Burkert	Solenoid proportional	0-25 [bar]	?	180 [Hz]?	24 [Vdc]	

1. Considering that the Flowtronic valves are purported to be for extreme dynamic demands on flow control and their response time is < 200 [ms], a better dynamic performance of the Preciflow and Posiflow valves should not be expected.
2. Standard Cubic Centimetres per Minute [sccm] (considers standardized temperature and pressure conditions)
3. Standard Liters Per Minute [slpm] (considers standardized temperature and pressure conditions)

Notes:
Hargraves – Is now a part of Parker
LAM Technologies 250 [Vdc] power supply
More power supplies at Farnell Electronics

B

Festo Valve Experiment

B.1 Competing Systems

A concept is formed of the future pneumatic system. A comparison can me made with a different system that has the same function. However, different components will be used to achieve the same function (e.g. electrical actuators and sensors). The comparison looks at dynamical behaviour, complexity of the system among other things.

B.1.1 Type of System

There are a lot of pneumatic components available that can mimic the same function as the proposed valve. These components are usually somewhat bulkier because of their housing and often use electrical signals to operate. The company Festo has a prototype for a proportional valve, where a piëzo-electric beam is used to open or close a pneumatic channel. The prototype (VEMR) is illustrated in the figure below.

There are two air connection points. In the figure the right connector is designated as an inlet and the other as an outlet. According to the specifications of Festo, these connectors are interchangeable. Under the piëzo-beam a seal is placed to prevent leaking. The known specifications are listed in table B.2.

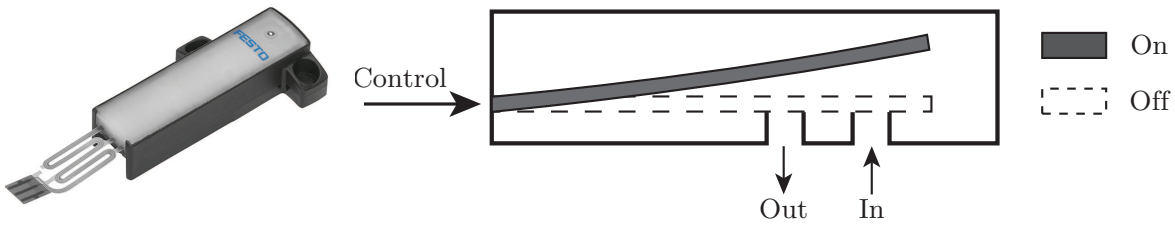

Figure B.1: Festo prototype: VEMR valve

If an electrical proportional valve is used instead of the proposed purely mechanical system, the complexity will increase. Firstly because an extra domain is used in this proportional valve, the electrical domain. This means that an additional step has to be taken to convert a pneumatic signal through the mechanical domain to an electrical signal.

This signal conversion will be present at both the sensing and actuation parts of the system. Because the actuator is operated with an electrical signal, the sensing output has to be in the same domain in order to communicate with each other. Especially if signal processing is necessary.

Next to the valve also a measuring system is needed to detect the wafer. This can still be done with the pilot points in the surface. Instead of going to the proposed design, it will lead to a pressure sensor. The sensor will probably also use some kind of mechanical deformation that is converted to an electrical signal. However, this system is not limited to the pilot points. For instance an optical sensors that use light to get the wafer position can also be used. The need for separate sensors increases the complexity of this design.

Because this Festo valve is still a prototype, not all specifications are known. An experiment is conducted to characterize the valve further. These experiments are focused on investigating the restriction of the valve at different voltages and source pressures.

General technical data	
Valve function	2/2-way valve (normally closed)
Type of connection	Flange
Ambient temperature	5 °C ... 40 °C (41 °F ... 104 °F)
Response time	< 10 ms with 10% pressure rise
BAM test*	With oxygen
Product size	42.9 mm x 10.7 mm x 12.2 mm

* BAM test = Federal Institute for Materials Research and Testing

Technical data – Pneumatic components	
Operating medium	Air, oxygen, inert gases
Operating pressure at the inlet	10 psig, 30 psig, 50 psig 0.7 bar, 2 bar, 3.5 bar
Orifice size	1.3 mm
Flow rate	17 lpm at 30 psi (2 bar)
Leakage	< 0.6 l/h

Figure B.2: Specifications of Festo VEMR piezo proportional Vavle

The capacitance of the valve is 13 nF

B.1.2 Experiment

This experiment is only designed to test the time it takes to fully open or close a channel. Because this is the function the proposed solution has. The sensing part of this alternative system is beyond the scope of this experiment. It is assumed that the measuring of the wafer position along with sending a signal to the proportional valve takes no time. In the next section the test setup is further explained.

Test-Setup

To test the Festo VEMR valve a signal is send to the valve to open and close at a certain interval. To see how long it takes for the pressure to actually rise and fall, a pressure sensor is added. In fig. B.3 it is illustrated how the airflow runs through the different components.

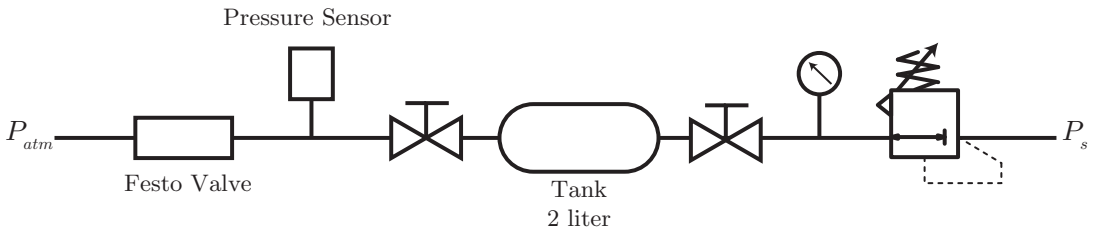

Figure B.3: Schemetic of Airflow in First Setup

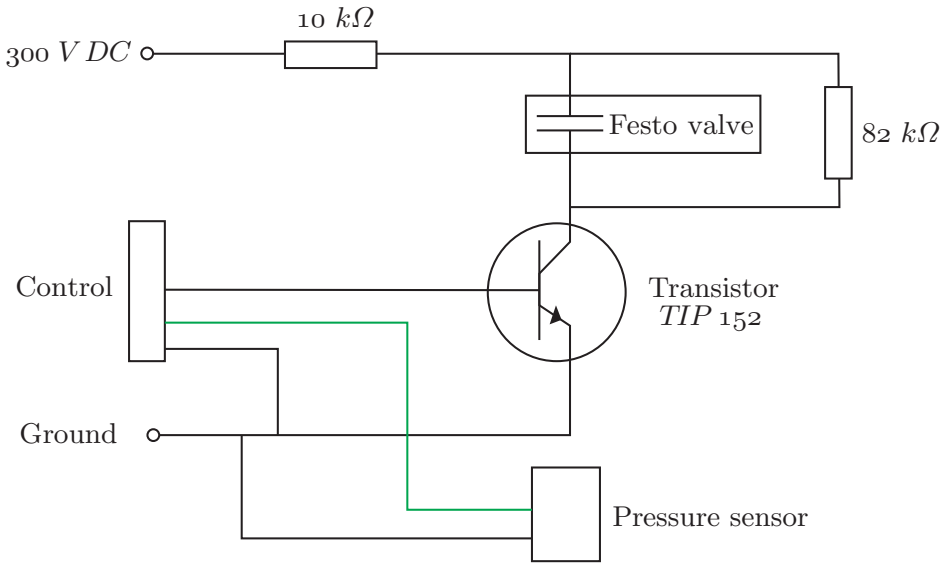

Figure B.5: Festo test setup electrical scheme

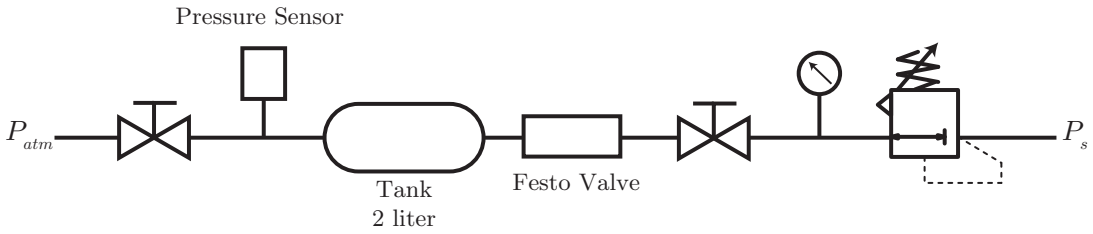

Figure B.4: Schemetic of Airflow in Second Setup

In figure B.5 the electrical scheme for the setup is shown. The valve is connected to a 300 V direct current source. With a voltage divider and a transistor the path to the ground can be closed or opened. The transistor and pressure sensor are controlled/read out by an National Instruments USB-6211 DAQ module operated with LABVIEW.

In this setup the valve is connected in a *RC*-circuit. The time constant of a *RC*-circuit is given by the equation below. Here R is the resistance b and C the capacitance. A capacitor is fully charged at 5 times the time constant.

$$\tau = R \times C \tag{B.1}$$

Festo did an initial test were a resistance of 47 kΩ was used to charge and discharge the valve. Using eq. (B.1) the capacitor would (dis)charge in 31 ms.

In the current setup a resistance of 10 kΩ is used to charge and 82 kΩ to discharge the valve. This voltage divider is chosen as such, so that a larger voltage will be formed over the valve, opening it further. Computing the rise times with the same equation it is calculated that the valve will open in 0,65 ms and close in 53 ms.
In figure B.6 the actual setup is shown. A custom manifold was manufactured because the prototype does not have standard connection ports.

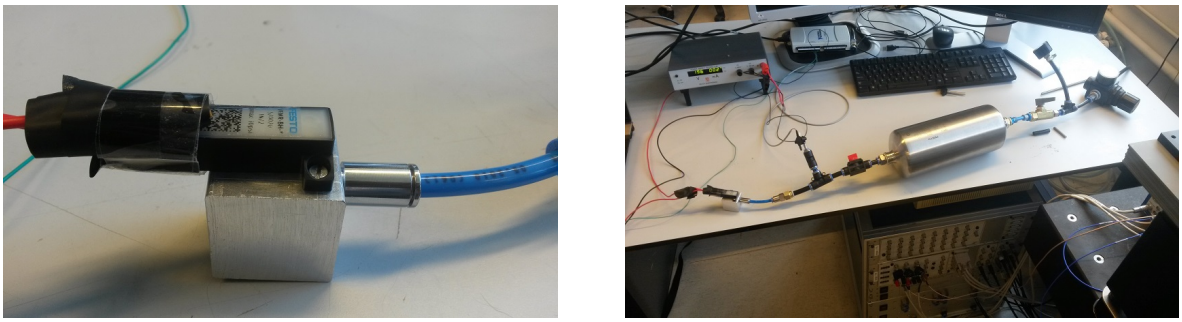

Figure B.6: On the left the custom made manifold and on the right side the other pneumatic parts.

Tests

For each of the two setups, different voltages were used to open the valve for each test. Starting at 100 Volts, increments of 25 Volts are made until the maximum voltage is reached. In this case that is 273 V due to the voltage divider and power source.

B.1.3 Results

The results of each experiment are plotted in figure B.7. Here the pressure drop is plot against time for both setups. Next the data is processed to get the mass flow and conductivity for each voltage. After that the results are compared between the two setups and repeatability is discussed.

For the first setup, as expected the higher the voltages the faster the tank de-pressurizes. The tank is empty within 90 seconds for 225 V and above. At 175 V it takes almost 12 minutes longer for the tank to fully return to atmospheric pressure.

At voltages of 150 V and lower something different happens. The de-pressurization halts at around 110 kPa. There is still a slight decrease visible in pressure. However, this has probably more to do with the leaking of some of the connectors than with the actual piezo valve.

This effect could be the result of a leaf spring that is attached to the end of the bending actuator (see fig. B.1). As the pressure underneath the seal is dropping the spring will close off the opening, stopping the airflow.

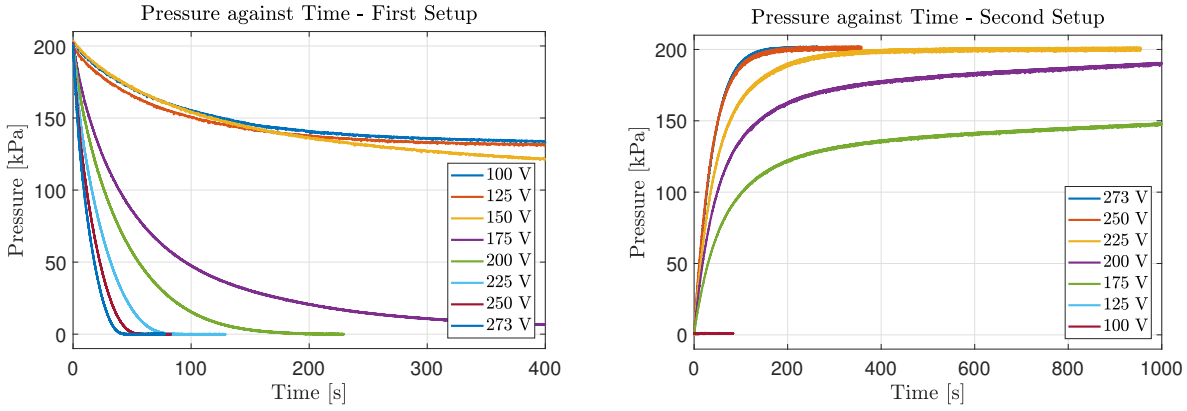

Figure B.7: Pressure vs Time for Differing Voltages

When the tank is pressurized in the second setup, no airflow is present when the lowest two voltages are applied. The pressure stays at atmospheric level.

As the voltage increases, the valve opens and the tank will begin to pressurize. If the valve is further open the tank will fill quicker with air as expected. However, if these results are compared to the de-pressurization of a tank at 273 V, it is clearly seen that it takes approximately twice as long to bring the tank up to an overpressure of 2 bar, than for the same tank too de-pressurize from 2 bar overpressure to atmospheric level.

With the data gathered from the tests, the mass flow can be calculated (eq. (B.2)). Here V is the volume of the tank, R_{air} is the specific gas constant for air (286,9 J/(K kg)), T is the temperature of the air assumed to be constant (293,15 K) and $\frac{\partial p}{\partial t}$ is the pressure gradient per time.

$$\dot{m} = \frac{\partial p}{\partial t} \frac{V}{R_{air} T} \tag{B.2}$$

The conductivity of the valve restriction, for the first setup, can be described equation B.3. The mass flow ($\dot{m}$) is divided by the quadratic difference in pressure.

In figure B.8 the mass flows and conductivity are plot for different applied voltages.

$$G = \frac{\dot{m}}{p^2 - p_{atm}^2} \tag{B.3}$$

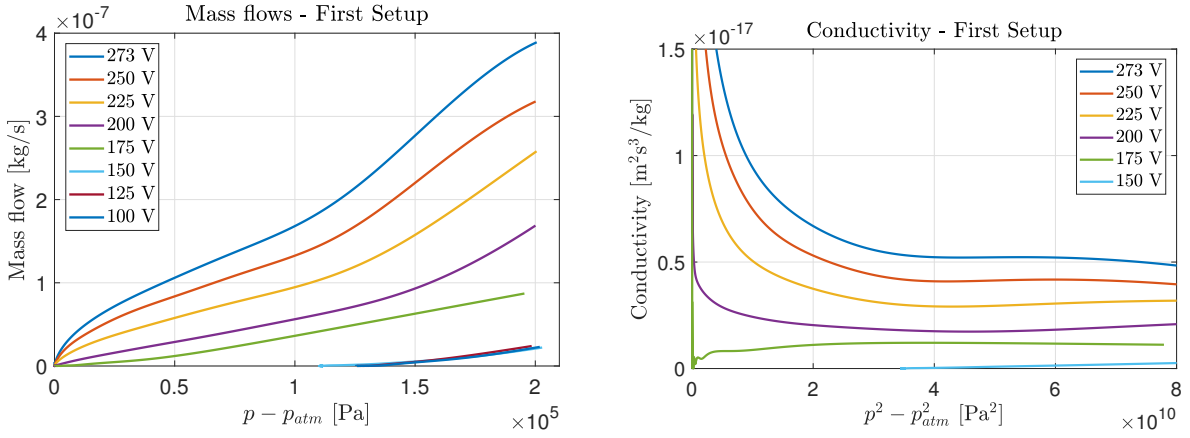

Figure B.8: Massflows and Conductivity Plotted for Varied Voltages

The mass flows of the 250 V and 273 V are very similar and even at higher pressure differences the mass flow of the lower voltage is higher.

At smaller pressure differences the conductivity increases. Around zero the conductivity rapidly changes due to noise and dividing by zero pressure difference.

To compare the results when different boundary conditions are applied on the valve, the mass flow and conductivity for of second setup are also computed. Because the boundary conditions are now a supply pressure outside the tank, equation B.4 describes the conductivity for this situation.

$$G = \frac{\dot{m}}{p_s^2 - p^2} \tag{B.4}$$

Figure B.9 illustrates the differences in mass flow and conductivity for different boundary conditions. The applied voltage is in both cases 200 V.

The mass flow for emptying the container is at the largest pressure difference 1 $\frac{\text{kg}}{\text{s}}$ higher than filling the tank. As lowers, this mass flow difference lowers to 0,5 $\frac{\text{kg}}{\text{s}}$.

This behaviour is also detected in the conductivity plots, where air discharges out off the tank has less resistance than air flowing in. These results are comparable with other applied voltages, except for the lower range of voltages when the valve did not open.

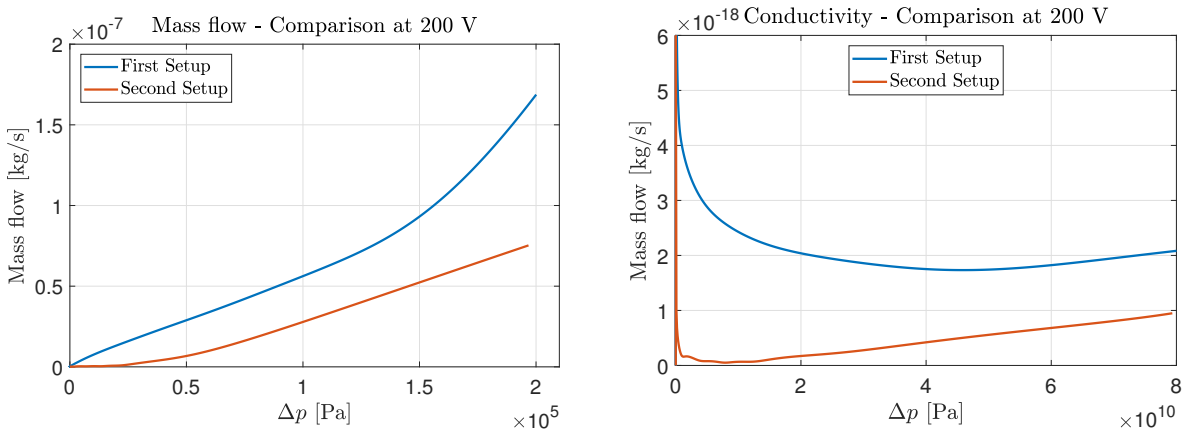

Figure B.9: Comparison for different Boundary Conditions at 200 V

The same test is repeated to investigate its behaviour. In figure B.10 the pressure drop is plotted against time for five test at an applied voltage of 273 V. It is clearly evident that the valve behaves quite differently.

Test 1 and 2 lie on the same line. However the other test do not compare well. It should be noted that in between test 2 and 3, a voltage of 150 V was applied to the valve. This can imply that this valve is influenced by hysteresis in a significant manner.

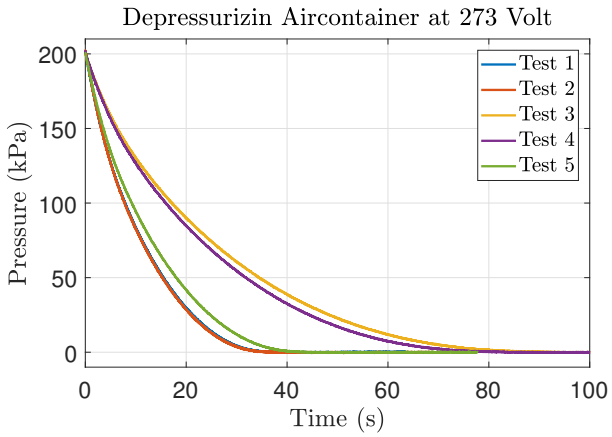

Figure B.10: Repeatability of Measurements

B.1.4 Discussion

During the investigation and testing of the Festo valve, the following points are observed:

1. Festo characterizes the valve as a 2/2 way valve. Which means that the air can flow through in both directions, depending where the supply line is attached. Unfortunately, this behaviour is not observed, as the valve remained shut when an supply line is attached to the output from fig. B.1.

2. When no voltage is applied the valve does not let airflow through, it is normally closed.

3. When different boundary conditions are applied the characteristics also change. A higher conductivity is observed when the pressure at both sides of the valve is lower. The maximum mass flow measured is 1,67 $\frac{\text{kg}}{\text{s}}$ at a pressure difference of .....

4. The valve did not open (completely) for voltages < 150 V. At a constant atmospheric pressure on the oulet, the valve closed around 110 kPa. For a constant pressure at the inlet, the valve did not open at all. This could have something to do with the next point.

5. It seems that historic actions have effect on the use of the valve. This does not ensure repeatable behaviour during operation and would exclude feed forward use.

The valve cannot be used in feed forward situations. The repeatability of the valve is not good enough to know exactly at what voltage an amount of air flows through. It would need feedback to be used effectively, making the system more complex.

It is recommended that the hysteresis characteristics are examined in future studies, to fully make understand the operation of this valve.

C

Pneumatic Relay Configuarations

C.1 One Dimensional

Here the output of the Matlab models used for the configuration are illustrated.

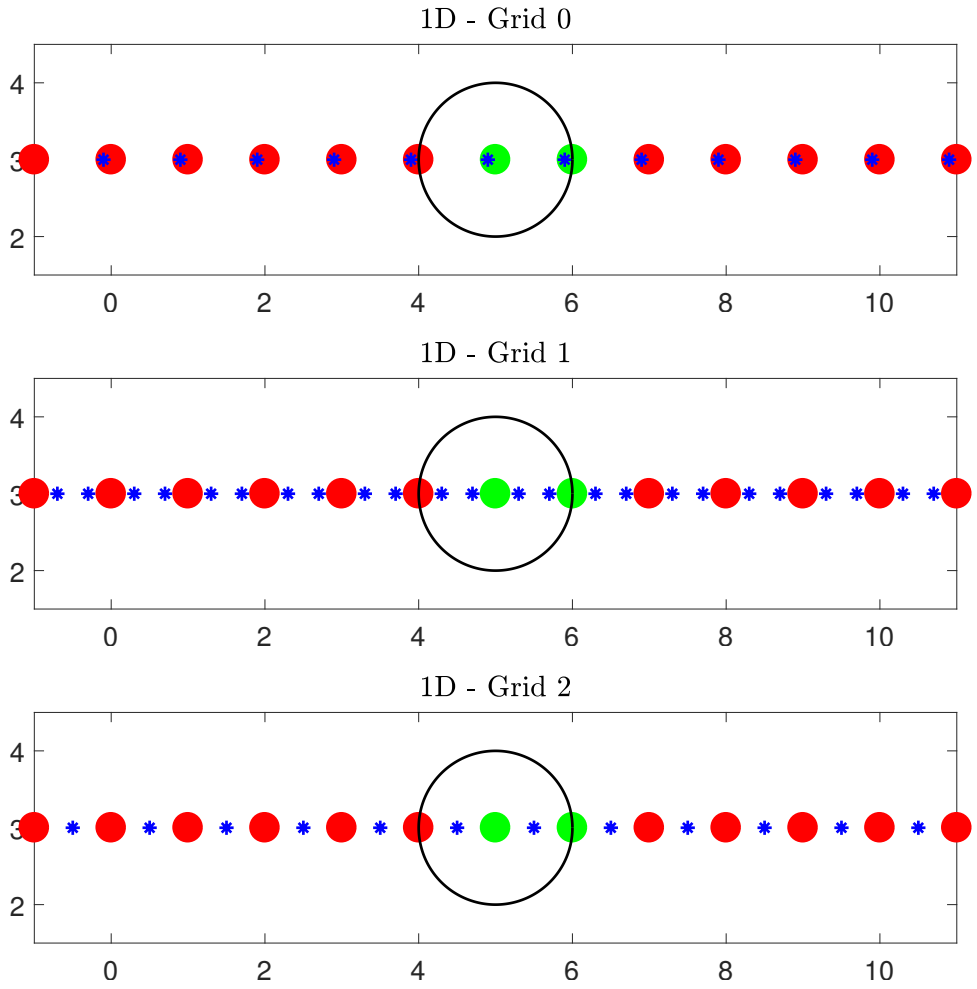

Figure C.1: Several 1 Dimensional Configurations, nozzles (blue) closed oulet (red) and open outlets (green)

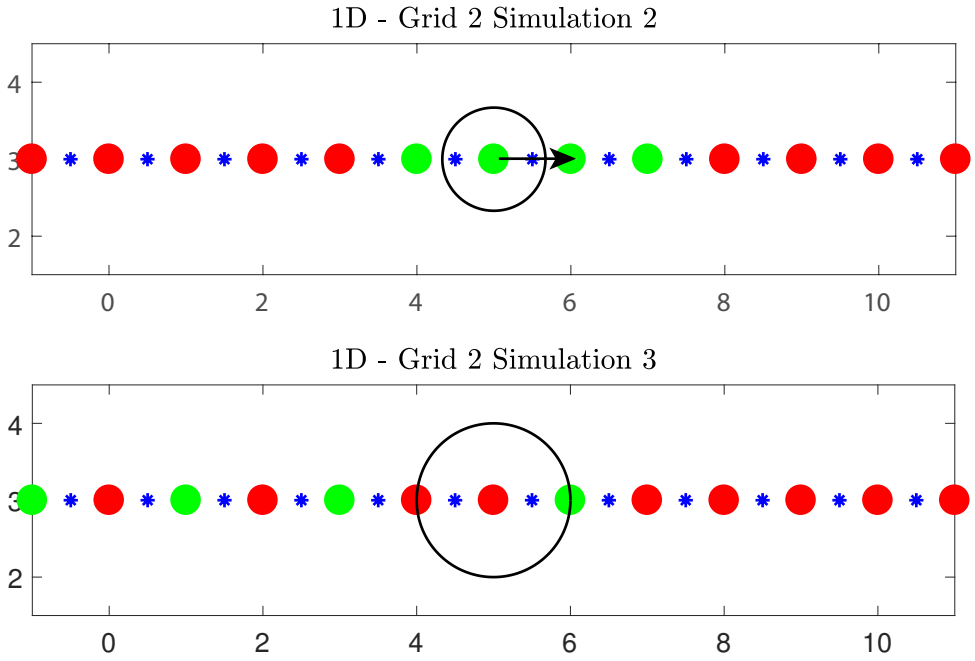

Figure C.2: Different Connecting Schemes on Grid 2, nozzles (blue) closed oulet (red) and open outlets (green)

C.2 Two Dimensional

C.2.1 Grids

The different grids that are used in the simulations are shown in the figure here below.

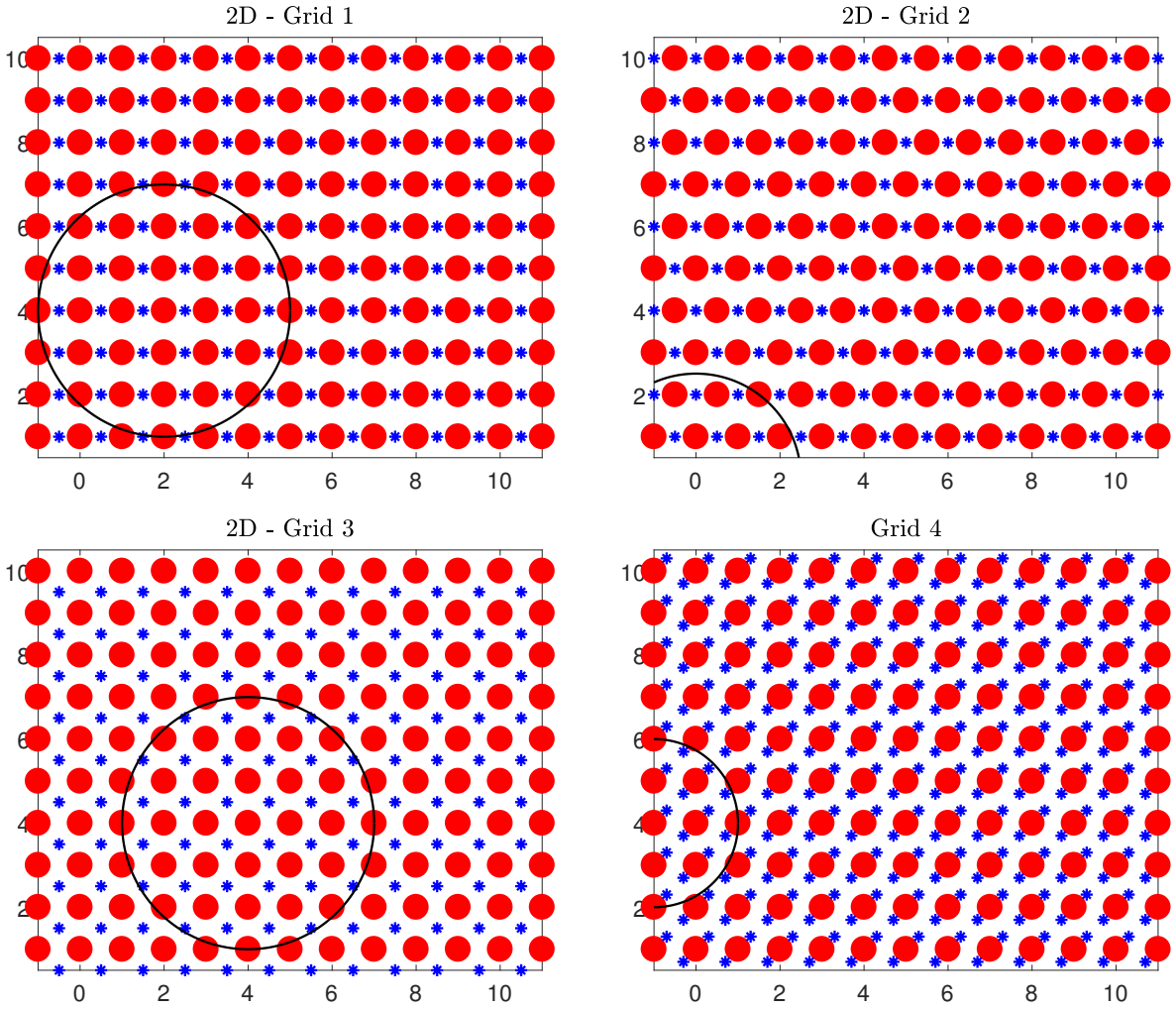

Figure C.3: Different Grids with Nozzles (blue) and Outlets (red)

Laten zien dat dit vrij moeilijk is onder een hoek of wat dan ook.

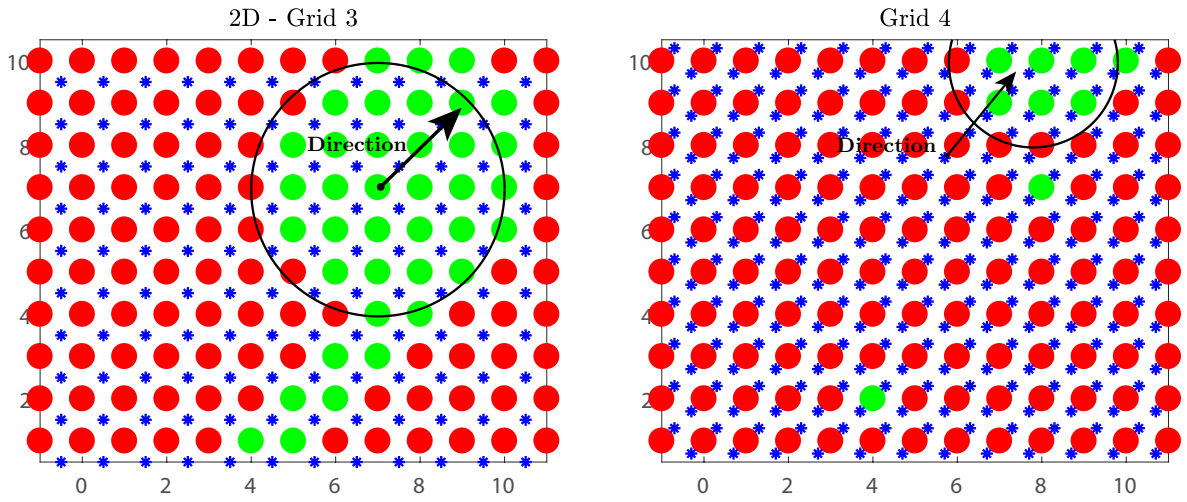

Figure C.4: Different Grids with Nozzles (blue) and Outlets (red)

Connecting Nozzles to Multiple Relays

The first 1 dimensional pattern can be placed next to each other (fig. C.5). The wafer can only move from left to right, but if the rows are inverted the wafer can translate from right to left. If the rows are alternated a wafer could move in both directions.

This can also be done for the other previously discussed one dimensional pattern. The 2D result is depicted in figure C.6.

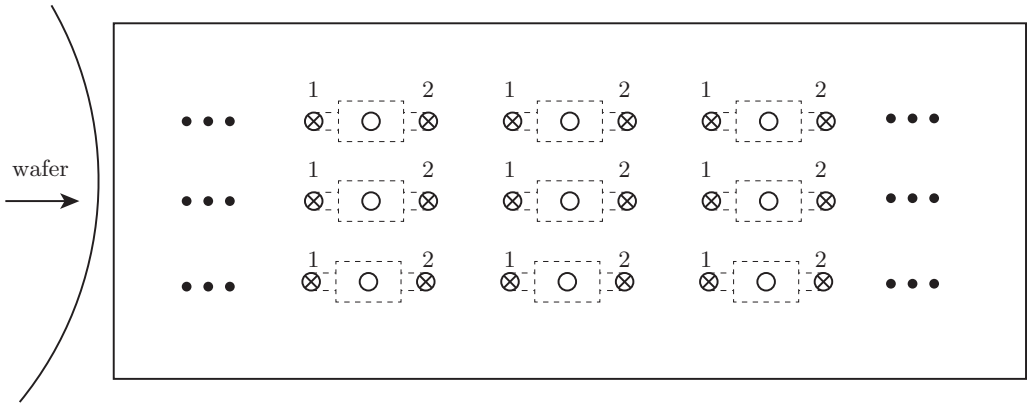

Figure C.5: 2 Dimensional Connection Pattern

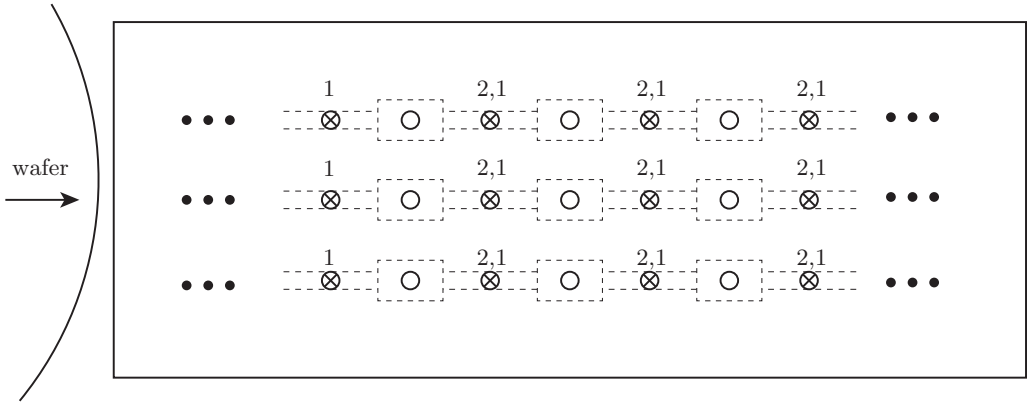

Figure C.6: 2 Dimensional Connection Pattern with shared input channels

In figure C.7 a connection scheme is shown where a single input is used for 4 valves. Twice to activate the valve as input 1 and twice to deactivate it (input 2). In this way a high input has a an increased effect over pressure distribution under the wafer. This can used if it is needed to have a little buffer of air film for the wafer to travel over.

In this configuration there are two distinct rows visible. One of these rows could be inverted to create a bi-directional conveyor. However a larger gap will be formed in the air film.

A variant of this pattern (fig. C.8) is when the inputs are placed between the black boxes. This creates a continuous field of valves. This can however not be alternated because ti is all connected to each other and no separate rows exist.

In the next pattern (fig. C.9) the inputs are in line with the outputs. However they are linked with the valves that are above and below the row of the input. The air film gap that when alternating the direction of the rows becomes smaller than in pattern **??**.

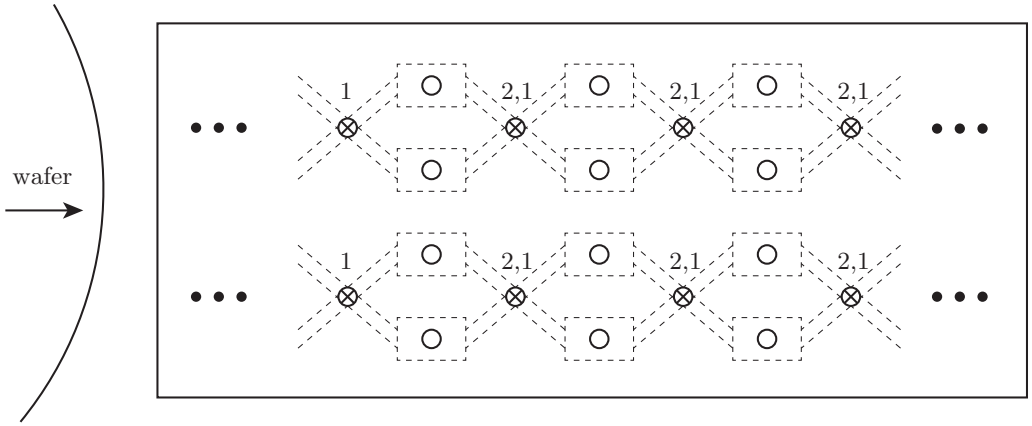

Figure C.7: 2D Connection where input channels are shared between valves

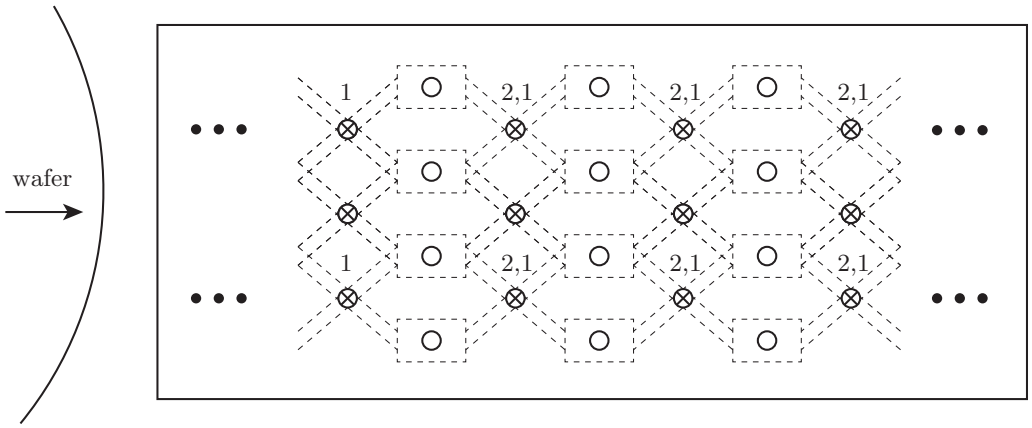

Figure C.8: 2D Connection where input channels are shared between valves

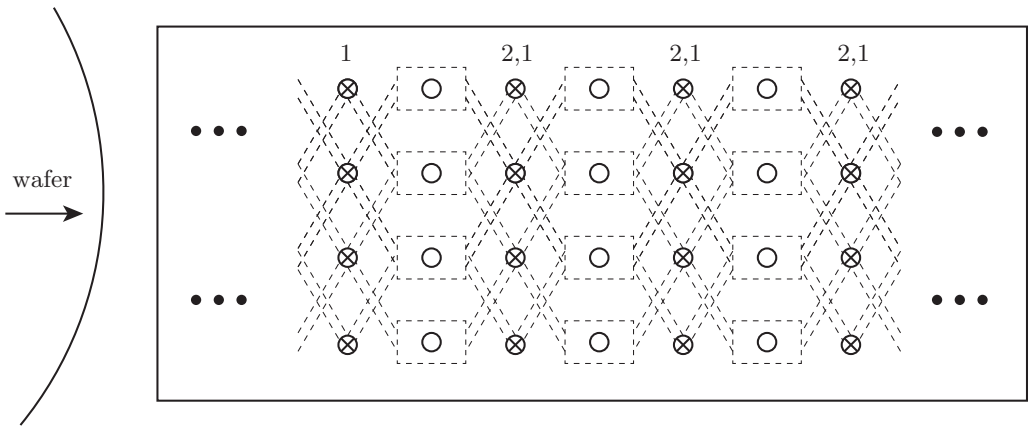

Figure C.9: 2D Connection where input channels are shared between valves

If the pattern of figure C.6 is tilted by 45 degrees, a pattern follows that can move wafers in two directions (fig. C.10). From left to right and also from the top to the bottom.

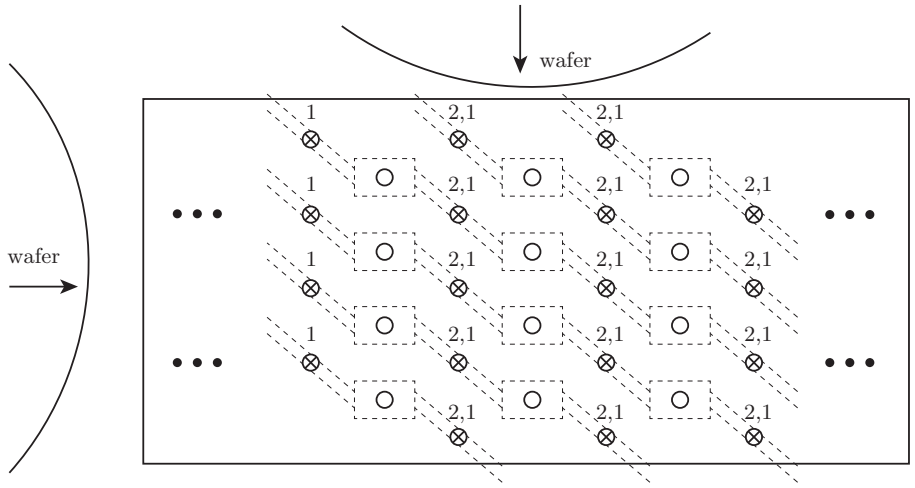

Figure C.10: 2D Connection where input channels are shared between valves

C.2.2 Resistance Network

To calculate the pressures in a resistance network shown in figure C.11, MATLAB is used. In figure C.12 the symbols are shown that are used for each flow (I_{nm}) in the channels.The restrictions are denoted by R_{nm} and the pressures at the surface by E_{nm}. The n and m symbols depict the position of each parameter in the network.

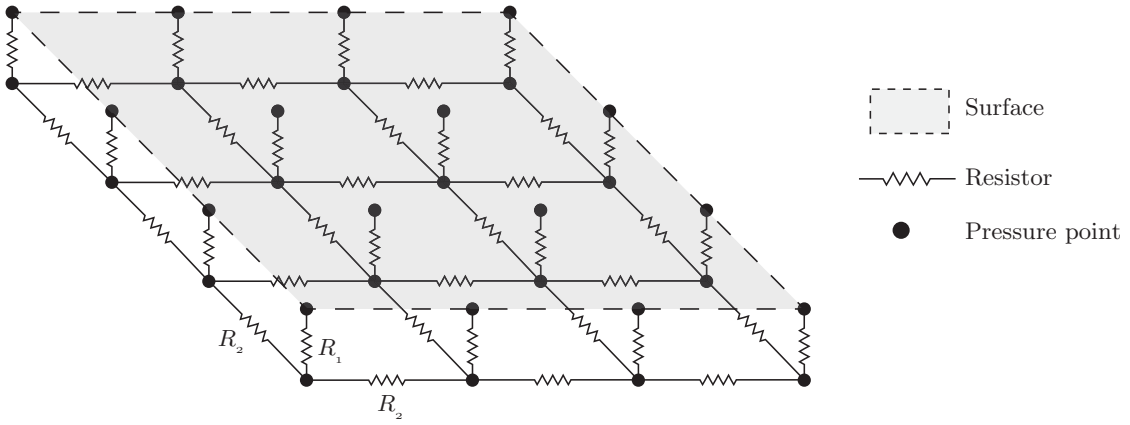

Figure C.11: Repeatability of Measurements

Kirchoff's voltage and current laws can be applied by the electrical pneumatic analogy. Where voltage is equal to a pressure, current to an airflow and resistance to a flow restriction. Kirchoff's current law states that on each junction of channels, all the airflows sum up to zero. The voltage law states that in each loop of channels the voltage will sum up to zero.

Using Kirchoff's voltage and current laws, a matrix R is constructed that contains the equations of each vertical voltage loop and each junction. In general for each nozzle three equations are solved. The voltage loop that moves to column to the right (eq. (C.1)), the voltage loop that goes down a row (eq. (C.2)) and the sum of the flows at each junction (eq. (C.3)). The equations below are valid for the upper right point.

$$R_1 I_{11} + R_2 I_{21} + R_1 I_{12} = E_{11} - E_{12} \tag{C.1}$$
$$R_1 I_{11} + R_2 I_{31} + R_1 I_{41} = E_{11} - E_{21} \tag{C.2}$$
$$I11 - I21 - I31 = 0 \tag{C.3}$$

The columns vector V represents the terms after the equal signs. With the matrix and vector constructed the air flows in each channel can be calculated (vector I).

$$V = RI \tag{C.4}$$
$$I = R^{-1}V \tag{C.5}$$

Now all the airflows are known the pressure distribution can be calculated using equation C.6. Where k stands for each row of nozzles and m for the columns of nozzles.

$$E_{km} - R_1 I_{km} = p_{km} \tag{C.6}$$

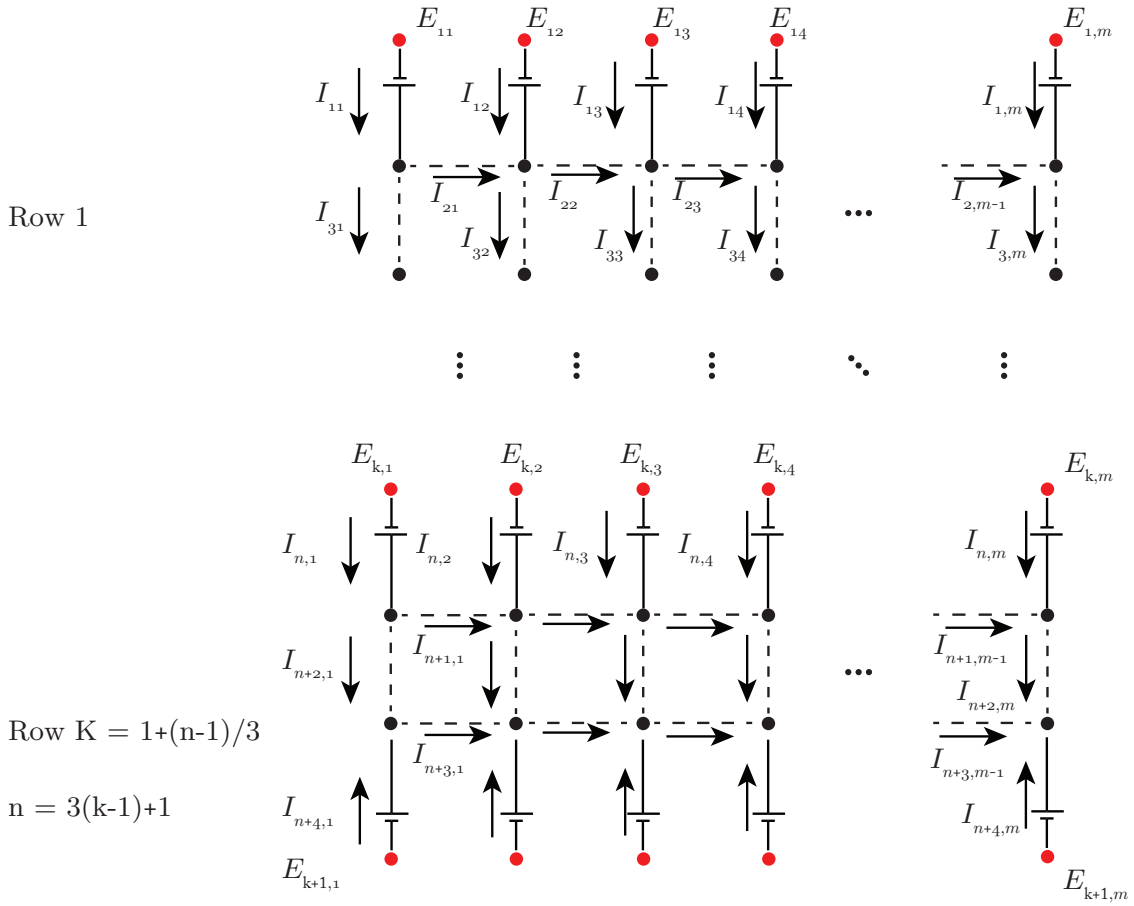

Figure C.12: Logic of making R Network in Matlab

D

Manufacturing Techniques for Rapid Prototyping

In this appendix the different methods used to build a valve are indicated and described. First methods that are used to make the manifold are explained. Next the different techniques to create the membranes are listed and finally the assembling of a valve is presented.

D.1 Creating the Manifold

The manifold is made with a technique that is inspired by E. Vagher thesis [27]. In that project, manifolds are manufactured to redirect pressurized air. A method is described that uses a rapid approach of lasercutting PMMA sheets and gluing them together. Using that method as inspiration, the process used in to make the pneumatic relays can be described in the following steps:

1. Make a layered design in a CAD programm (export to an .DXF file).
2. Glue 3M 468MP adhesive transfertape on top of one side of a PMMA plate.
3. Lasercutt the features along with alignment holes of each layer in PMMA plates.
4. Clean each layer that does not have 3M tape on it with water and a little soap.
5. Glue the PMMA sheets together. The plates are aligned by bolts that are inserted in alignment holes.
6. Press the plates together to ensure most of the air bubbles are removed in between the layers.
7. Let the glue settle for a day before pressurizing the manifold.

In figure D.1 laser-cut parts (layers) are shown next to each other. The right photo shows the channels that were milled after the laser-cutting process.

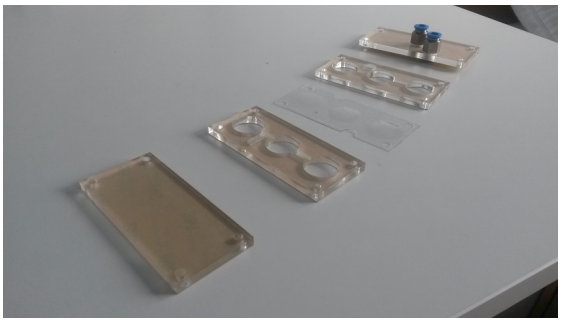

Figure D.1: Different Lasecut Parts of the layered Design

D.2 Creating the Membrane

Creating the membrane proved to be a more difficult process. In this section different methods of fabricating a membrane with a curve in it are described. Vacuum-pressing, dapping, 3D printing, Casting and hot pressing are all considered. Though not all thoroughly investigated. Because snapping membranes are formed succesfully with the custom vacuum-press, the casting or Spincoating polyurethaan and 3D printing of thin design have not been looked into.

Hot-pressing plastic sheets between two moulds can make other more elaborate forms possible. This has however also not been put to the test.

D.2.1 Vaccuum-pressing Plastic

Vacuum-pressing is a method of forming plastic. Below two different machines/methods are used. First a conventional larger vacuum press machine. Because the results were not satisfactory a smaller custom vacuum-press machine was manufactured.

Large vacuum-press machine

In the workshop at TU Delft a vacuum-press is used at the faculty for Industrial Design for rapid prototyping. Its working process is as follows.

A sheet of plastic is stretched out over a gap. Underneath the sheet a mould of the desired form is placed, that can move up and down. At the start this is in the downward position.

A heating element is placed over the plastic sheet until it begins to cave in a bit. Now it can be easily shaped. This machine is typically used for thicker sheets of plastic (> 1 mm so it is key to move this element away in time. Otherwise the plastic can melt and render the material useless.

Next the mould is pressed up in the plastic and air is sucked out of the chamber, creating a vacuum. In the mould small channels can be made to let the air escape between the sheet and mould for a better fit.

Different types of moulds can be used. In figure D.2 a CNC milled foam mould is illustrated along with its resulting plastic membrane. Here the mould has already been used and as can be seen the features are not that defined. This is because the process has plastically deformed the mould, and cannot be used a second time

Also the Features in the membrane are barely visible and do have the desired snapping behaviour. Therefore a different mould is used that is 3D printed, using a thermosetting polymer [fig. D.3].

Figure D.2: The CNC'd Foam moulds (left) and finished product (right)

Some of these membranes do in fact snap through. The lower curves do not posses a snapping characteristic. However, there are several disadvantages to this machine that make this method awkward.

Material is not efficiently used. The machine and products it usually makes is far larger than the relatively small membranes that are manufactured. This results in spending a lot of material for simply securing a plastic sheet in the device. Also the because this device is normally used for thicker plates the amount of generated heat is difficult to control for thinner materials.

This is why an alternative method is sought out in the form of a smaller custom made vacuum-press.

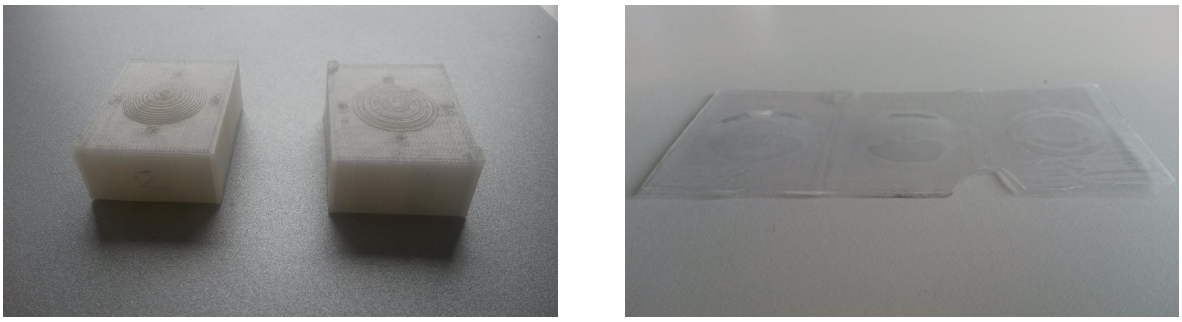

Figure D.3: The 3D printed moulds (left) and finished product (right)

Custom made vacuum-press machine

In figures D.4 a small scale vacuum form device is shown. Basically it consists of an aluminium block with a milled pocket on the top, an opening on the side to provide a vacuum channel to the pocket and a plate that is placed on the top to secure a plastic sheet. In the vacuum chamber a 3D printed mould can be placed to create specific membranes.

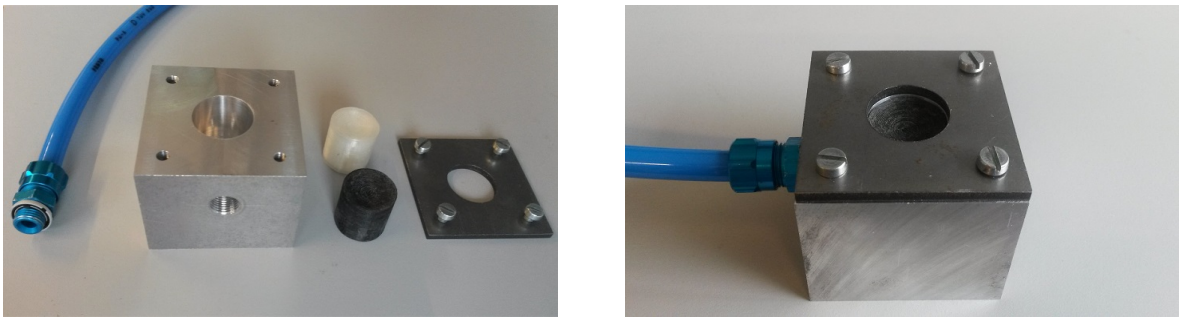

Figure D.4: The custom made vacuum-press

A heat gun pointed at the membrane blowing air at 150 °C [D.5]. After a few seconds the plastic has become soft enough to deform and air is sucked out the chamber via the vacuum channel. As the membrane curves to its desired form, the heat gun is turned off and the vacuum is released when the plastic cooled off.

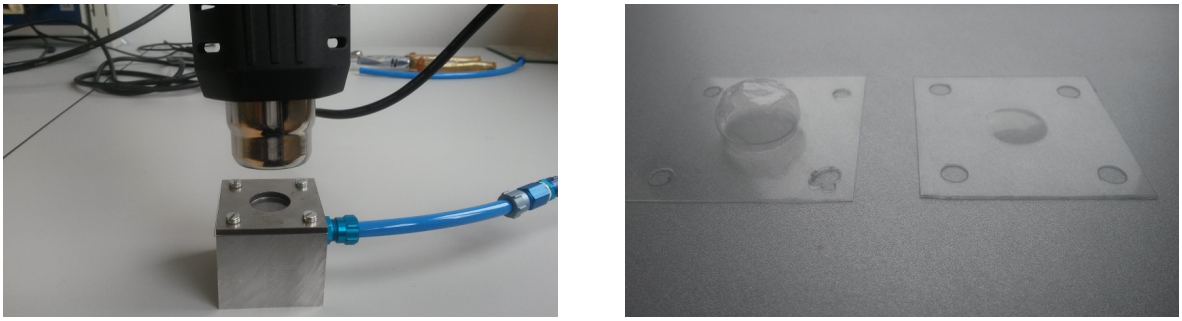

Figure D.5: Manufacturing Process and Resulting Membranes

Test are preformed where no mould is used in the chamber, to see if a more natural curve could be established that would always snap. However, this proved difficult as a little too much vacuum sucks the membrane in making it useless [D.5]. More constant results are obtained using a 3D printed mould, which has been sanded down to create a smoother surface.

D.2.2 Dapping Steel

If a different material is used to manufacture a spherical membrane, other techniques have to be considered. In this section spring steel of 0.1 mm is used.

To create a sphere in a sheet of this material a dapping block is used. This required a delicate touch because if too much force is used, the whole sheet is deformed. Experience found out that rubbing the sheet slowly in the dapping die with the punch, a spherical form is created in the sheet without inducing unwanted deformations.

In figure D.6 the result of a successful attempt is illustrated. This curve can snap through when force is applied. However, a slight curve of the sheet is noticeable. This proved to be too much of a deformation in order for the membrane to work accordingly when placed in a manifold and put under pressure. Therefore the manufacturing of steel membranes is abandoned.

Failed Attempt

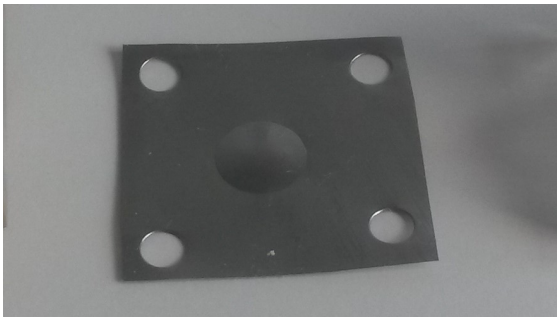

Tested Membrane

Figure D.6: Results of Dapping Springsteel

D.3 Creating a Rubber Seal

The rubber seal that separates different channels inside a air chamber is made by using a circular punch cutter on a rubber sheet. In the manifold a compartment is milled for the seal to be placed in. A second layer of the manifold will keep clamp seal and keep it in its place.

Punchcutting Circular Rubber Slabs

Milling a Pocket in the Manifold

Figure D.7: Creating the Rubber Seal Membrane

D.4 Assembling the Valve

When the manifold parts, the rubber seal and membrane are successfully manufactured they can be put together. Before they can be glued, the surfaces have to be cleaned. Preferabbly this is done with water and a little soap. Alcohol is not preferred to degrease the surface, there is a chance that the PMMA will crack [fig. D.8] because alcohol acts as a solvent for polymers.

Figure D.8: Cracked PMMA Layer after Cleaning with Alcohol

Using the alignment holes on the sides of each part, the layers can be glued together. In figure D.9 the alignment holes are shown with bolts through them. Next the liner of the transfer tape can be removed and the layers can be glued.

Figure D.9: Assembling the different parts using the alignment holes.

To remove any air bubbles in between the glued layers, they are placed in a large press. Two pieces of wood are situated on both sides to protect the valve its surface. The press is operated by hand to carefully apply a pressure. When most of the bubbles are gone the manifold is finished and can be used the next day.

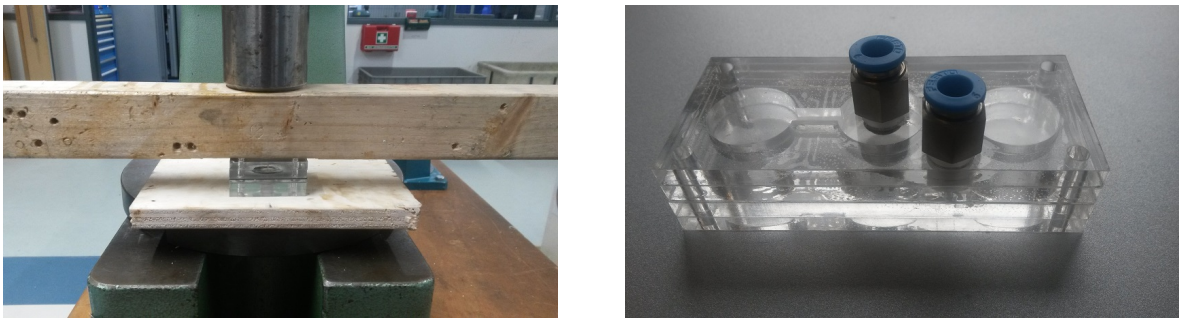

Figure D.10: Pressing the Layers Together and the Final Product

E

Prototype in Detail

The prototype is shown here in more detail (fig. E.1).

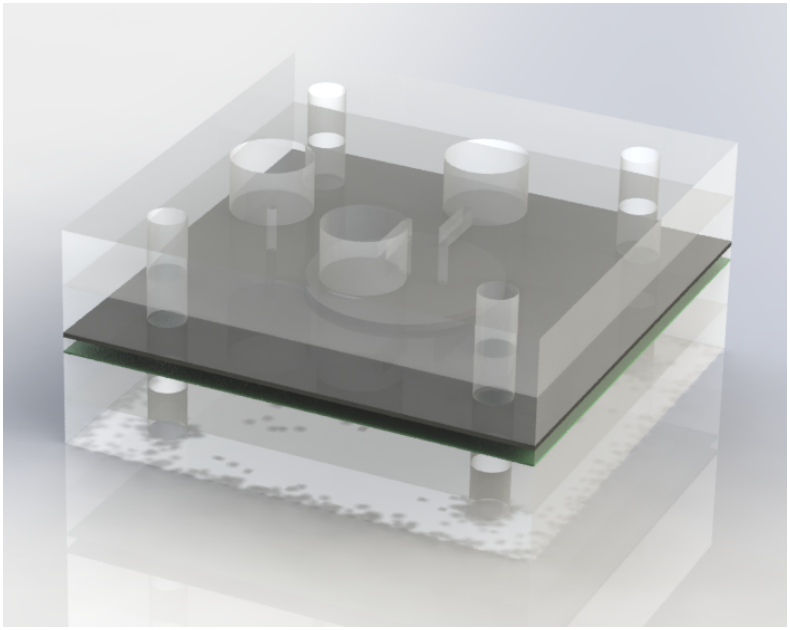

Figure E.1: Rendered CAD-model of Prototype

In figure E.2 an exploded view of the prototype is illustrated. Each layer is numbered and in the table below some properties of each layer is listed. The width and length is 50 mm for each sheet.

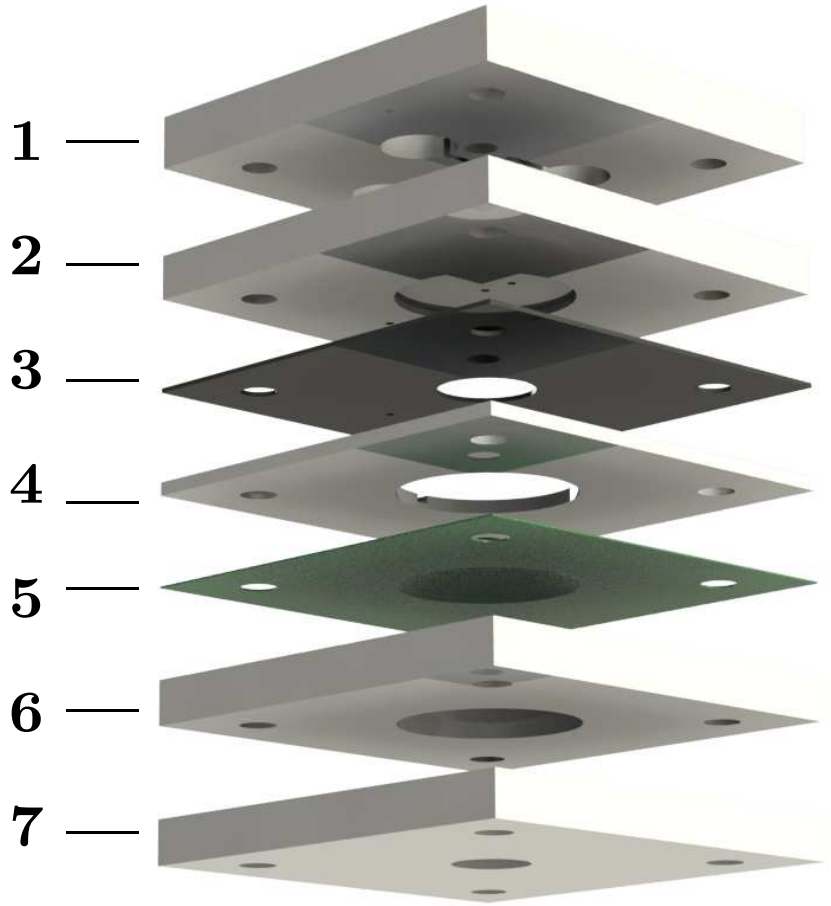

Figure E.2: Exploded View of Prototype

Table E.1: Properties of the Prototypes Layers

Layer	Thickness [mm]	Material	Description
Layer 1	6.0	PMMA	Top with Screw connection for outlet and inlets
Layer 2	5.0	PMMA	Layer with rubber seal cavity
Layer 3	5.0	Steel	Flange plate to keep the seal in place
Layer 4	2.0	PMMA	Spacer plate
Layer 5	0.2	PET-G	Membrane
Layer 6	4.0	PMMA	Spacer plate
Layer 7	5.0	PMMA	Bottom with screw connection for inlet